

PB85247716



Research, Development,
and Technology

Turner-Fairbank Highway
Research Center
6300 Georgetown Pike
McLean, Virginia 22101

CENTRIFUGAL TESTING OF MODEL PILES AND PILE GROUPS



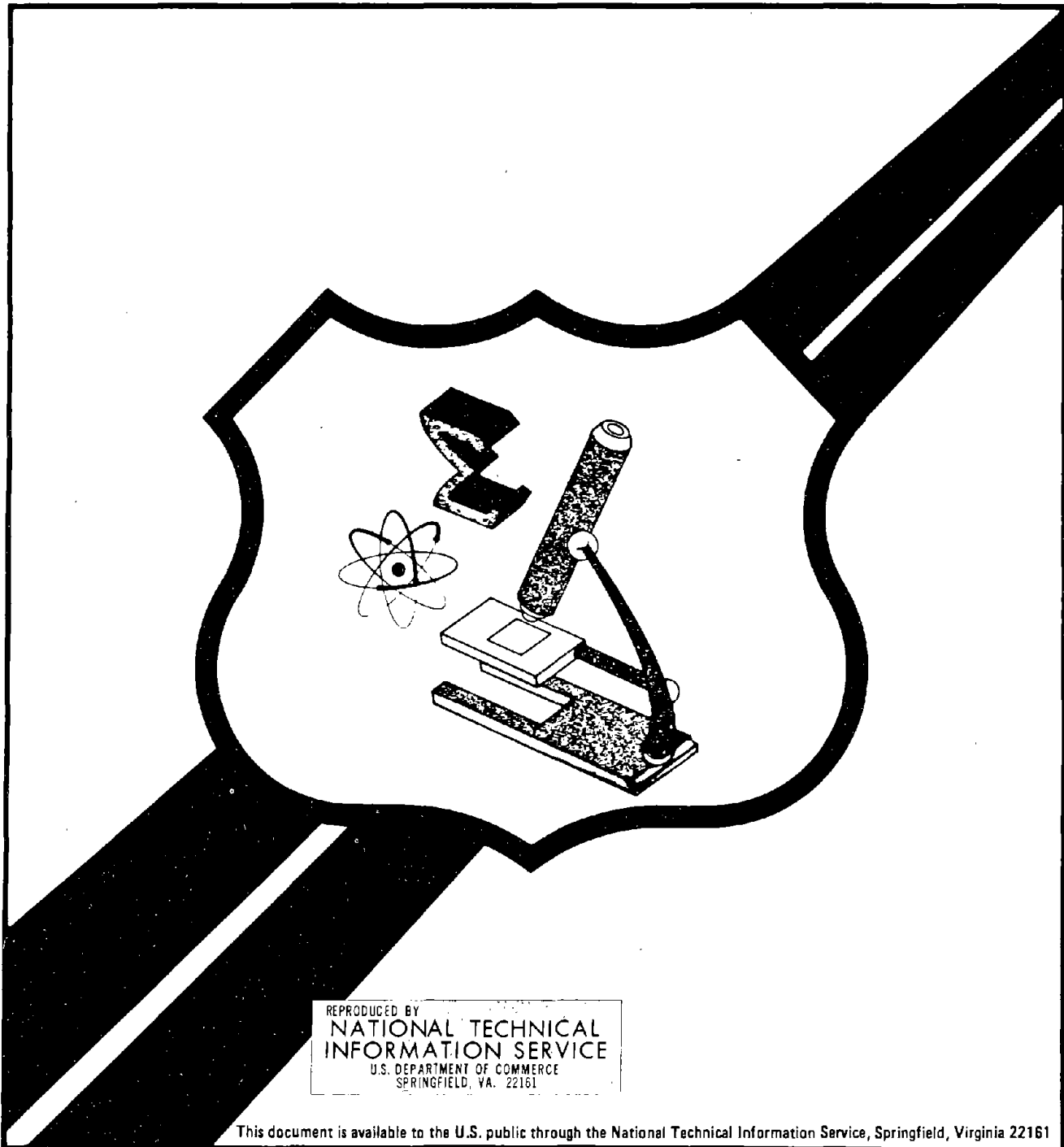
VOL. II CENTRIFUGE TESTS IN SAND

U.S. Department
of Transportation

**Federal Highway
Administration**

Report No.
FHWA/RD-84/003

Final Report
November 1984



REPRODUCED BY
NATIONAL TECHNICAL
INFORMATION SERVICE
U.S. DEPARTMENT OF COMMERCE
SPRINGFIELD, VA. 22161

This document is available to the U.S. public through the National Technical Information Service, Springfield, Virginia 22161

FOREWORD

This report presents a detailed description of a research study on the use of geotechnical centrifuge to test model piles and pile groups in sand. Information presented will be of use to other investigators using the centrifuge as a research or engineering design tool. Results presented will be of interest to engineers designing pile foundations in sand.

The project was conducted for the Federal Highway Administration, Office of Engineering and Highway Operations Research and Development, Washington, D.C., under contract DTFH61-81-R-00034, "Centrifuge Testing of Model Piles and Pile Groups."



Richard E. Hay, Director
Office of Engineering
and Highway Operations
Research and Development

NOTICE

This document is disseminated under the sponsorship of the Department of Transportation in the interest of information exchange. The United States Government assumes no liability for its contents or use thereof. The contents of this report reflect the views of the contractor, who is responsible for the accuracy of the data presented herein. The contents do not necessarily reflect the official policy of the Department of Transportation. This report does not constitute a standard, specification, or regulation.

1. Report No. FHWA/RD-84/003		2. Government Accession No. PB85 247716/AS		3. Recipient's Catalog No.	
4. Title and Subtitle CENTRIFUGAL TESTING OF MODEL PILES AND PILE GROUPS VOL. II, CENTRIFUGE TESTS IN SAND				5. Report Date November 1984	
				6. Performing Organization Code	
7. Author(s) Monzoori, M.; Atkinson, R.H.; Ko, H-Y.; and Goble, G.G.				8. Performing Organization Report No. 8126	
9. Performing Organization Name and Address Atkinson-Noland & Associates, Inc. 2619 Spruce St. Boulder, CO 80302				10. Work Unit No. (TRAIS) FCP 35P1-132	
				11. Contract or Grant No. DTFH 61-81-R-00034	
12. Sponsoring Agency Name and Address Offices of Research & Development Federal Highway Administration U.S. Department of Transportation Washington, DC 20590				13. Type of Report and Period Covered Final Report June 1981 - June 1984	
				14. Sponsoring Agency Code CME/0122	
15. Supplementary Notes FHWA Contract Manager: Carl D. Ealy (HNR-30)					
16. Abstract This volume is a detailed report of a research program conducted to evaluate the feasibility of conducting tests on model piles and pile groups in sand using the geotechnical centrifuge. The report describes the preparation of the sand samples, details of the model piles, method of pile placement, description of the centrifuge and its operation and test procedures. Results are presented and analyzed. Conclusions are presented on the verification of the similitude relations, sensitivity of capacity to ϕ angle, influence of driving sequence, pile group efficiency, and load transfer relations. Other reports developed in this study are FHWA/RD-84/002, Vol. I, Executive Summary, and FHWA/RD-84/004, Vol. III, Centrifuge Tests in Clay. Dr. R. H. Atkinson, Atkinson-Noland & Associates served as Project Director. Prof. H-Y. Ko and G. G. Goble served as Principal Investigators. Mr. F. Harrison conducted the test program in clay while Mr. M. Manzoori conducted the test program in sand. All experimental work was conducted using the geotechnical centrifuge of the Department of Civil, Environmental, and Architectural Engineering, University of Colorado, Boulder, Colorado.					
17. Key Words Piles, Pile Groups, Sand, Centrifuge, Model Tests, Analysis			18. Distribution Statement No restrictions. This document is available to the public through the National Technical Information Service, Springfield, VA 22161		
19. Security Classif. (of this report) Unclassified		20. Security Classif. (of this page) Unclassified		21. No. of Pages 106	22. Price

METRIC CONVERSION FACTORS

APPROXIMATE CONVERSIONS FROM METRIC MEASURES

SYMBOL WHEN YOU KNOW MULTIPLY BY TO FIND SYMBOL

LENGTH

in	inches	2.5	centimeters	cm
ft	feet	30	centimeters	cm
yd	yards	0.9	meters	m
mi	miles	1.6	kilometers	km

AREA

in ²	square inches	6.5	square centimeters	cm ²
ft ²	square feet	0.09	square meters	m ²
yd ²	square yards	0.6	square meters	m ²
mi ²	square miles	2.6	square kilometers	km ²
	acres	0.4	hectares	ha

MASS (weight)

oz	ounces	28	grams	g
lb	pounds	0.45	kilograms	kg
	short tons (2000 lb)	0.9	tonnes	t

VOLUME

tsp	teaspoons	5	milliliters	ml
tbsp	tablespoons	15	milliliters	ml
fl oz	fluid ounces	30	milliliters	ml
c	cups	0.24	liters	l
pt	pints	0.47	liters	l
qt	quarts	0.95	liters	l
gal	gallons	3.8	liters	l
ft ³	cubic feet	0.03	cubic meters	m ³
yd ³	cubic yards	0.76	cubic meters	m ³

TEMPERATURE (exact)

°F	Fahrenheit temperature	5/9 (after subtracting 32)	Celsius temperature	°C
----	------------------------	----------------------------	---------------------	----

APPROXIMATE CONVERSIONS FROM METRIC MEASURES

SYMBOL WHEN YOU KNOW MULTIPLY BY TO FIND SYMBOL

LENGTH

mm	millimeters	0.04	inches	in
cm	centimeters	0.4	inches	in
m	meters	3.3	feet	ft
m	meters	1.1	yards	yd
km	kilometers	0.6	miles	mi

AREA

cm ²	square centimeters	0.16	square inches	in ²
m ²	square meters	1.2	square yards	yd ²
km ²	square kilometers	0.4	square miles	mi ²
ha	hectares (10,000m ²)	2.5	acres	

MASS (weight)

g	grams	0.035	ounces	oz
kg	kilograms	2.2	pounds	lb
t	tonnes (1000kg)	1.1	short tons	

VOLUME

ml	milliliters	8.03	fluid ounces	fl oz
l	liters	2.1	pints	pt
l	liters	1.06	quarts	qt
l	liters	0.26	gallons	gal
m ³	cubic meters	36	cubic feet	ft ³
m ³	cubic meters	1.3	cubic yards	yd ³

TEMPERATURE (exact)

°C	Celsius temperature	9/5 (then add 32)	Fahrenheit temperature	°F
----	---------------------	-------------------	------------------------	----

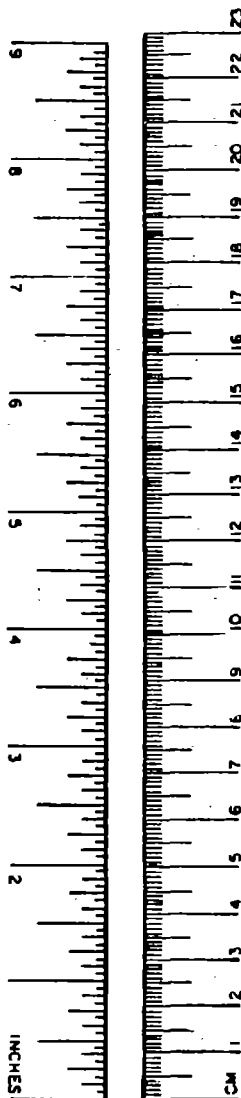


TABLE OF CONTENTS

	Page
LIST OF TABLES	v
LIST OF FIGURES	vi
CHAPTER 1. INTRODUCTION	1
1.1 Centrifugal Modeling of Geotechnical Structures	1
1.2 Similitude Theory and Centrifugal Modeling	2
CHAPTER 2. PROTOTYPE AND MODEL DESCRIPTION	7
2.1 Problem to be Modeled	7
2.2 Soil Model and Soil Sample Preparation	7
2.3 Pile Modeling	15
2.4 Modeling of Models	20
CHAPTER 3. EQUIPMENT AND PROCEDURE	21
3.1 The Centrifuge	21
3.2 The Sample Container	21
3.3 Axial Loading	24
3.4 Lateral Loading	27
3.5 Pile Instrumentation	27
3.6 Calibration Procedures	29
3.7 Test Procedure	31
3.8 Data Acquisition System	33
CHAPTER 4. PRESENTATION OF TEST DATA	35
4.1 Introduction	35
4.2 Test Plan	35
4.3 Presentation of Test Results	35
CHAPTER 5. ANALYSIS OF DATA	64
5.1 Introduction	64
5.2 Test Series 1	64
5.3 Test Series 2	64
5.4 Test Series 3	64
5.5 Test Series 4	66

TABLE OF CONTENTS (continued)

	Page
5.6 Test Series 5	66
5.7 Test Series 6	69
5.8 Test Series 7	69
5.9 Test Series 8	72
5.10 Test Series 9	72
CHAPTER 6. COMPARISON OF MODEL TEST RESULTS TO FIELD DATA AND ANALYTICAL PREDICTIONS	74
6.1 Introduction	74
6.2 Ultimate Bearing Capacity of Piles	74
6.3 Settlement of Pile Foundations	75
6.4 Computer Solutions	77
6.5 Comparison of Model Tests to Field Tests Results	84
CHAPTER 7. SUMMARY, CONCLUSIONS, RECOMMENDATIONS	94
7.1 Summary	94
7.2 Conclusions	94
7.3 Recommendations	96
REFERENCES	97

LIST OF TABLES

Table	Page
1. Scaling Factors for Various Quantities	4
2. Soil Properties	13
3. Pile Properties	19
4. Centrifuge Specifications	23
5. Summary of Testing Programs in Sand	36
6. Group Test Data, Sand	50

LIST OF FIGURES

Figure	Page
1. Site soils data, Locks and Dam No. 26, (Woodward-Clyde)	8
2. Profiles of relative density and generalized subsurface description (Woodward-Clyde)	9
3. Sieve analysis results	11
4. Friction angle versus density	12
5. Raining process	16
6. Height versus soil density	17
7. Schematic view of centrifuge	22
8. Schematic of hydraulic system	25
9. Axial and lateral load cells	26
10. Mechanism for loading model piles in the centrifuge	28
11. Strain gauge positions on one half of the aluminum pile	30
12. Model pile cap	32
13. Effect of in-flight versus 1 g installation (prototype scale), 1/70 scale	37
14. Effect of in-flight versus 1 g installation (prototype scale), 1/50 scale	38
15. Effect of centrifuge stoppage between pile installation and testing (prototype scale)	40
16. Load-settlement curves from 'modeling of models' test series	41
17. Parametric study load-settlement curves, Tests 4.1 and 4.2 (prototype scale)	42
18. Parametric study load-settlement curves, Tests 4.3, 4.4, 4.5, and 4.6, (prototype scale)	43
19. Parametric study load-settlement curves, Tests 4.7 and 4.8, (prototype scale)	44
20. Influence of driving order, Test 5.2 (model scale)	46
21. Influence of driving order, Test 5.4 (model scale)	47
22. Load-settlement curve, group Test 5.2 (prototype scale)	48
23. Load-settlement curve, group Test 5.4 (prototype scale)	49
24. Load-settlement curve, group Test 5.1 (prototype scale)	52
25. Load-settlement curve, group Test 5.3 (prototype scale)	53

LIST OF FIGURES (continued)

Figure	Page
26. Tapered versus straight pile response (prototype scale)	54
27. Saturated versus dry pile group test (prototype scale)	55
28. Saturated versus dry single pile test (prototype scale)	56
29. Lateral load Test 8.1 (prototype scale)	57
30. Lateral load Test 8.2 (prototype scale)	58
31. Lateral load Test 8.3 (prototype scale)	59
32. Lateral load Test 8.4 (prototype scale)	60
33. Load-transfer curve, aluminum pile in sand	62
34. Load-settlement curve, aluminum pile (prototype scale)	63
35. Load-settlement curves from 'modeling of models' test series (prototype scale)	65
36. Ultimate load versus friction angle, (prototype scale)	67
37. Comparison between single pile and pile group tests, Tests 4.3 and 5.1, (prototype scale)	70
38. Comparison between single pile and pile group tests, Tests 4.5 and 5.3, (prototype scale)	71
39. Axial load transfer curve	76
40. PILGPl predictions vs centrifuge results, recommended load transfer curves (prototype scale)	79
41. PILGPl predictions vs centrifuge results, adjusted load transfer curves, (prototype scale)	80
42. PILGPl predictions vs centrifuge results, adjusted load transfer curves, (prototype scale)	81
43. Schematic illustrating differences between predicted sand and clay pile response	83
44. Elasticity-based predictions vs centrifuge data, floating tip (prototype scale)	85
45. Elasticity-based predictions vs centrifuge data, end bearing (prototype scale)	86
46. Comparison of single pile field test M-6 to centrifuge results	89

LIST OF FIGURES (continued)

Figure	Page
47. Comparison field group test to scaled centrifuge test (prototype scale)	91
48. Comparison field lateral load test to centrifuge test, single pile (prototype scale)	93

CHAPTER 1. INTRODUCTION

1.1 Centrifugal Modeling of Geotechnical Structures

One of the shortcomings of geotechnical engineering is the inability to conduct adequate model tests of earth structures. Since full-scale testing of such structures is usually expensive and time-consuming it is rarely performed. Furthermore, the inability to control test conditions and soil parameters in prototype situations makes it impossible to do parametric studies for such problems. These comments particularly apply to full-size tests of piles and pile groups. On the other hand, subscale physical modeling can be invalid unless the same stress state is obtained in both the prototype and model. This means that the testing of reduced scale models in soil under normal gravity conditions will not correctly satisfy required similitude relations as discussed below.

An accepted model testing technique in geotechnical engineering will permit verification of soil behavior theories, will allow parametric studies to determine sensitivity of various factors, and will permit model studies of various types of geotechnical structures such as piles, footings, dams, etc. Because of the complexity of soil behavior, it is mandatory to provide as much verification of analytical methods as possible, so that they can be applied with confidence to prototype design.

One approach is to conduct scale-model tests under an artificial gravity induced by a geotechnical centrifuge. The centrifugal acceleration produced by the rotating centrifuge can produce the artificial gravity field necessary to reproduce the gravity-induced stress conditions of a full scale pile load test, for example. Thus, through the use of the centrifuge, numerous pile load tests can be performed under a variety of conditions at a fraction of the cost of full-scale tests. The method was first developed in the U.S. by Bucky (1931) for mining applications and in Russia by Pokrovsky (1936). Due to development of the digital computer, and the numerical modeling methods made possible by the computer, centrifugal modeling lost its appeal as a modeling tool except in the Soviet Union. However, in the past decade interest in centrifuge modeling has

revived in Europe, Japan and the U.S. There are now at least five centrifuges operating in American universities in addition to the ones in industry.

The technique has been applied to a wide range of problems in geotechnical engineering. This report describes an investigation on modeling of pile foundations in sand using the centrifuge.

The research described by this report consisted of a series of single pile and pile group axial and lateral load tests carried out in the centrifuge at the University of Colorado. These tests were scale models of a full-scale load test performed on single piles and pile groups at the site of Lock and Dam No. 26 near Alton, Illinois.

In the remainder of this chapter similitude relations as they apply to centrifugal tests are briefly reviewed. Next in Chapter 2 the problem to be modeled is outlined and the soil and pile models are described. In Chapter 3 the equipment and test procedures are described. Test data are presented in Chapter 4 and analyzed in detail in Chapter 5. In Chapter 6 model test data, prototype test data and theoretical predictions are compared. The project is summarized in Chapter 7, conclusions are drawn and suggestions for future work are presented.

1.2 Similitude Theory and Centrifugal Modeling

The objective of centrifugal modeling is to test a scaled model under an increased gravitational body force field such that the self-weight stresses and strains are equal to those in the prototype at corresponding points. In order to do this, the requirements of similitude must be satisfied. Two systems are said to be physically similar when a unique relationship between all points of the two systems can be determined and when the physical quantities have a constant relationship at corresponding points.

The basic similitude relationship is given by equation 1.1, which is derived from the Buckingham Pi theory (Rocha, 1957). Here y is the property of the prototype, y' is the corresponding model property, and Ω is a scaling factor determined from the fundamental properties of the two systems.

$$y = y' \Omega \quad (1.1)$$

For the work described by this report, the scaling relationships for three independent quantities, from which all other quantities are derived, are required. They are length, stress, and time; and their scaling factors are depicted in equation 1.2, 1.3, and 1.4. It should be noted that these scaling factors must be accurate for derived quantities.

$$L = L'\lambda \quad (1.2)$$

$$\sigma = \sigma'\epsilon \quad (1.3)$$

$$t = t'\tau \quad (1.4)$$

For example, the specific case of strains, is demonstrated by equation 1.5.

$$\frac{\epsilon}{\epsilon'} = \frac{\Delta L/L}{\Delta L'/L'} = \frac{L'\Delta L}{\Delta L'L} = \frac{L'\Delta L'\lambda}{\lambda \Delta L'L'} = 1 \quad (1.5)$$

This requirement can be met easily if the prototype material is used in the model. Two assumptions are involved here, however. The first is that the grain size of the prototype materials is small enough to be considered a continuum even at the model scale. This assumption is reasonable for clays, silts, and some sands if the geometric scaling factor, λ , is not overly large. For very large values of λ , say in the neighborhood of 200, problems may be encountered in using many sands as model materials.

The other assumption that must be considered is that body forces are insignificant enough to be negligible. This is clearly not reasonable in most geotechnical problems. If we are required to achieve similarity of body forces, then equation 1.6 must be satisfied,

$$\frac{\gamma'}{\gamma} = \lambda \quad (1.6)$$

where γ' and γ are the specific weights of the model and prototype, respectively. If the same material is to be used, this can only be accomplished by inducing a higher gravity in the model than that of the prototype. This can only be

practically achieved with the use of a centrifuge.

Since the prototype exists under earth's normal gravitational acceleration g (32 ft/sec^2 or 9.81 m/sec^2), the gravitational acceleration to which the model must be subjected to satisfy equation 1.6 is given by equation 1.7.

$$a = \lambda g \quad (1.7)$$

The centrifugal (radial) acceleration generated by a centrifuge of radius r spinning at a constant angular velocity ω is given in equation 1.8 which is a well known law of physics.

$$a = \omega^2 r \quad (1.8)$$

Hence, the angular velocity required for a model with a geometric scaling factor λ and centrifuge of radius r is given in equation 1.9, which is obtained by substituting equation 1.7 in 1.8 and solving for ω .

$$\omega = \frac{\sqrt{\lambda \cdot g}}{r} \quad (1.9)$$

The scaling relationships for the three independent quantities as well as derived quantities significant to this report are summarized in Table 1.

Table 1. Scaling Factors for Various Quantities.

Length	λ
Stress	1
Time	λ^2
Strain	1
Force	λ^2
Area	λ^2
Volume	λ^3
Specific Weight	$1/\lambda$
Gravitational Acceleration	$1/\lambda$
Mass Density	1
Mass	λ^3

A limitation of the centrifugal method that should be pointed out is that the gravity of the model is not constant with depth, but linearly increasing with radius as is apparent from equation 1.8. Hence the lower portions of the model are subjected to a higher level of gravity than are the upper portions. This effect can be minimized by performing high gravity tests on a centrifuge with a larger radius. In this manner the same average centrifugal acceleration can be achieved, with less variation over the depth of the model. Despite this limitation, centrifugal modeling is the most practical method of modeling most geotechnical problems that adhere to the principles of similitude.

The first recorded uses of the centrifuge to model geotechnical systems were in the 1930's. It was used in the U.S. to study mining structures (Bucky, 1931) and in the Soviet Union to study foundation deformations (Pokrovsky and Fedorov, 1936). The technique was not widely accepted in the U.S. or Western Europe at that time. The work by Pokrovsky and Fedorov, however, fostered widespread use of the geotechnical centrifuge in the Soviet Union, where it has remained in use up to the present time.

In the late 1960's, the centrifuge saw a resurgence in popularity with western researchers. Cambridge University completed its first centrifuge at this time and began extensive research into soil mechanics problems (Roscoe, 1968). Geotechnical centrifuges were soon in operation in Japan (Mikasa and Takada, 1973) and in the U.S. They have been employed to study a variety of geotechnical problems too numerous to mention here. An excellent discussion of centrifuge testing is provided by Schofield in his 20th Rankine Lecture (1980).

Research specifically involving behavior of pile foundations has begun fairly recently. Scott (1979) performed research on single piles in silt subjected to cyclic lateral loads at the California Institute of Technology. Scott's results were internally consistent and demonstrated the feasibility of conducting pile load tests centrifugally. The lack of good comparison with the prototype which would verify the similitude relationships is the only shortcoming.

Axially loaded piles in sand were investigated by Hougnon (1980) at the University of Colorado. Although this was largely a feasibility study, some

useful data regarding the effect of taper and soil density on bearing capacity were obtained. Problems encountered with uniform sample preparation and the loading apparatus limited the effectiveness of this program.

CHAPTER 2. PROTOTYPE AND MODEL DESCRIPTION

The objective of this research study was to test in a geotechnical centrifuge models of single pile and pile group field tests conducted at the Lock and Dam No. 26 site on the Mississippi River. The study provided information on test techniques, parametric studies at model scale, and similitude verification. In this chapter the prototype site conditions and pile test program are described. The design of the centrifuge model test program including soil preparation and model pile fabrication are also described.

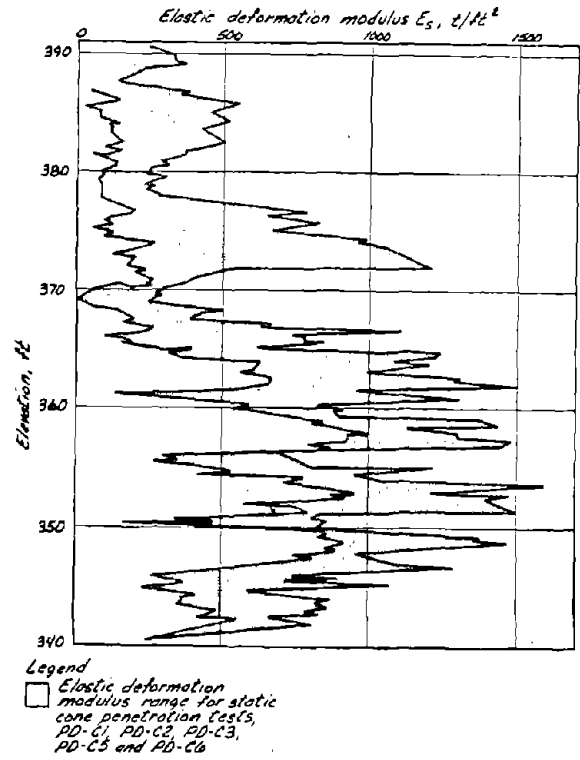
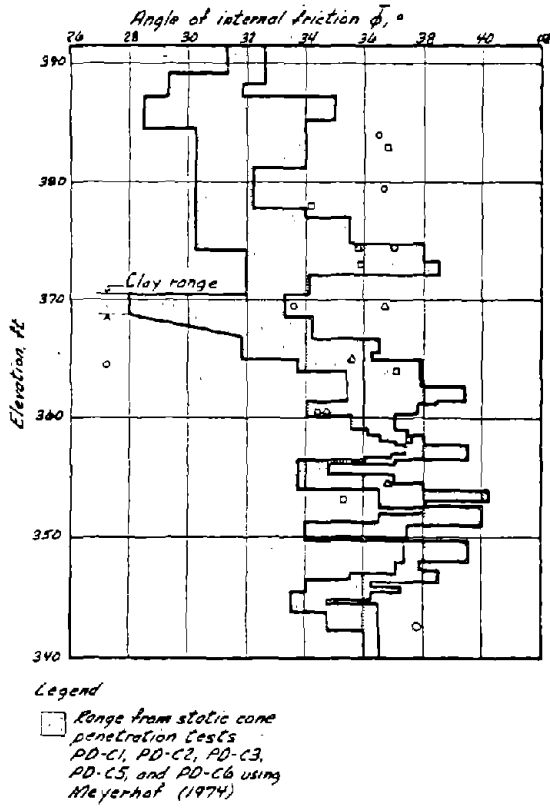
2.1 Problem to be Modeled

The test site to be modeled was located approximately 1 mile downstream of Lock and Dam No. 26, within the Mississippi River floodplain near Alton, Illinois. The test site profile consisted of approximately 112 ft (34 m) of alluvial soils overlying limestone bedrock. Five distinct soil strata were identified in descending order as: floodplain deposits, recent alluvium, outwash (reworked alluvium), Wisconsin outwash, and Illinois ice contact deposits. The cohesive floodplain deposits, approximately 24 ft (7.3 m) thick, were excavated to the surface of a recent alluvial sand stratum in the vicinity of the pile test area. The groundwater was drawn down and maintained one foot (.3 m) below foundation grade by a levee and dewatering system. Profiles of angle of internal friction, elastic deformation modulus, maximum and minimum dry unit weights, relative density, and the generalized subsurface description in the vicinity of the test are shown in Figures 1 and 2. Timber piles of 40 foot length (12.2 m), having a butt diameter of 14 inches (35.6 cm) and a tip diameter of 10 inches (25.4 cm) were installed in a 2x4 pile cluster on 3 ft (0.9 m) centers. The piles were initially jettied in place and then driven to a depth of 35 ft (10.7 m) using a Vulcan One air hammer.

2.2 Soil Model and Soil Sample Preparation

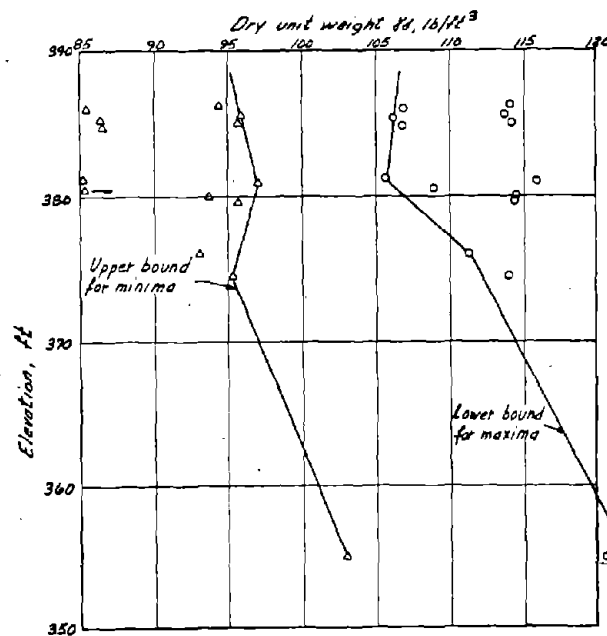
2.2.1 Soil Model Selection

From the previous centrifuge pile modeling studies done at the University of Colorado, Hougnon (1980), it was concluded that proper modeling of the soil



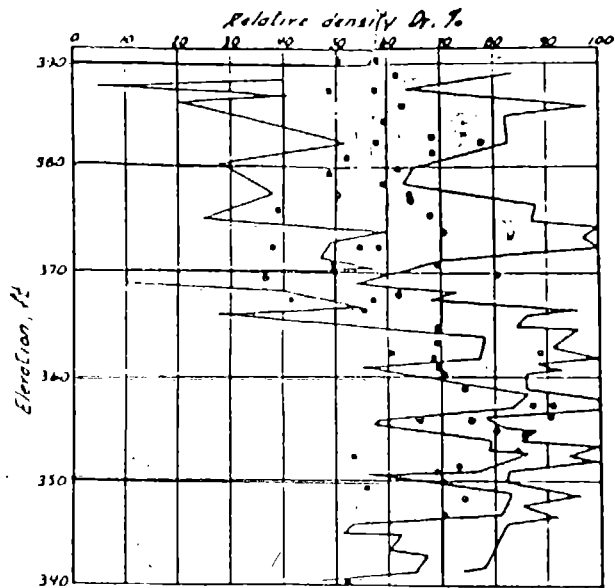
a. Angle of internal friction profile before timber pile installation.

b. Elastic deformation modulus derived from static cone penetration tests.



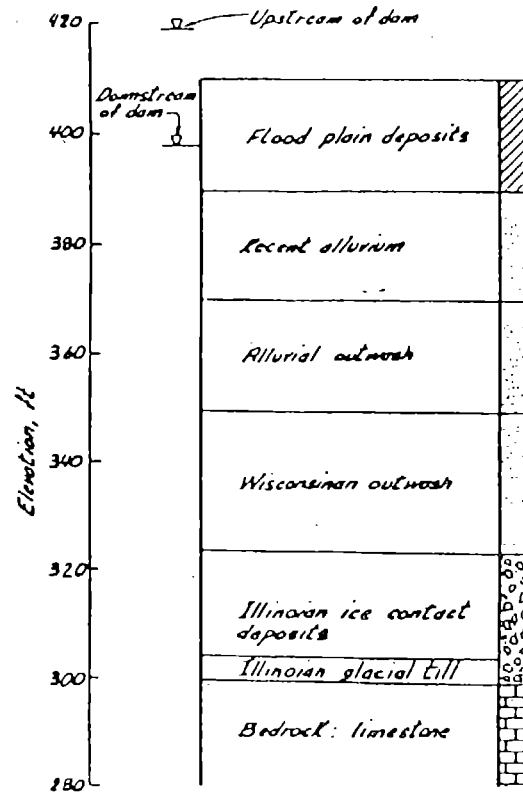
c. Laboratory maximum-minimum dry unit weights

Figure 1. Site soils data, Locks and Dam No. 26 (Woodward-Clyde)



Legend

- Range for cone sounding: PD-C1, PD-C2, PD-C3, PD-C5, and PD-C6
- From standard penetration resistance tests, borings PD-PA11, PD-PA12, PD-PA13, PD-PA14 and PDZ-371



a. Relative density profile before timber pile installation.

b. Generalized subsurface profile in vicinity of test area.

Figure 2. Profiles of relative density and generalized subsurface description (Woodward-Clyde).

conditions in a centrifuge test is of primary importance. Since the prototype soil profile contained five different layers, it was not possible to take a block sample of the insitu material. Even if the prototype soil could be obtained, it would still be necessary to remove the coarser fractions in order to permit installation of a model pile which is n times smaller than the prototype pile and to test it under n times earth's gravity.

If the strength profile and the density of a given site can be matched by using remoulded soil, it can be argued that this soil represents the site assuming density and strength are the controlling factors. After review of available soil profile data (Figures 1 and 2) and additional information received from the FHWA it was decided to fabricate a uniform test soil having a dry unit weight (γ_d) of 100 lb/ft³ (15.72 KN/m³) with an angle of internal friction (ϕ) of 40°. These characteristics can be achieved by controlling the grain size distribution of the test soil and its compaction. Since tests were to be conducted at 1/70 scale, which calls for model pile diameters to be on the order of 0.20 inch (0.51 cm) the maximum size of grains to be used in the soil model were controlled so as not to exceed about 0.04 inch (0.10 cm).

Initially, a soil available at the University of Colorado was considered because of the large amount of information that has been accumulated on it from past research. It was thought by changing the gradation of this soil one could achieve the desired properties ($\gamma = 100$ pcf, $\phi = 40^\circ$). This turned out to be a very time-consuming task, since there was no rule for fabricating such a soil. For each trial mix, it was necessary to prepare the soil to a unit weight of 100 pcf, and to run a series of triaxial tests to obtain the friction angle. The final conclusion was that one could not achieve the desired properties from the soil available in a reasonable time. Another conclusion drawn from this work was that the relation between grain size distribution and ϕ was extremely sensitive and that changing the gradation slightly would have a drastic effect on the ϕ angle.

The soil finally selected for this test program was a commercially available bagged sand which was obtained from the FHWA Soil Laboratory, McLean, Virginia. This soil had been used in a FHWA model pile testing program. Properties of this soil are summarized in Table 2. Sieve analysis results and the relation between density and friction angle for this soil are presented in Figures 3 and 4.

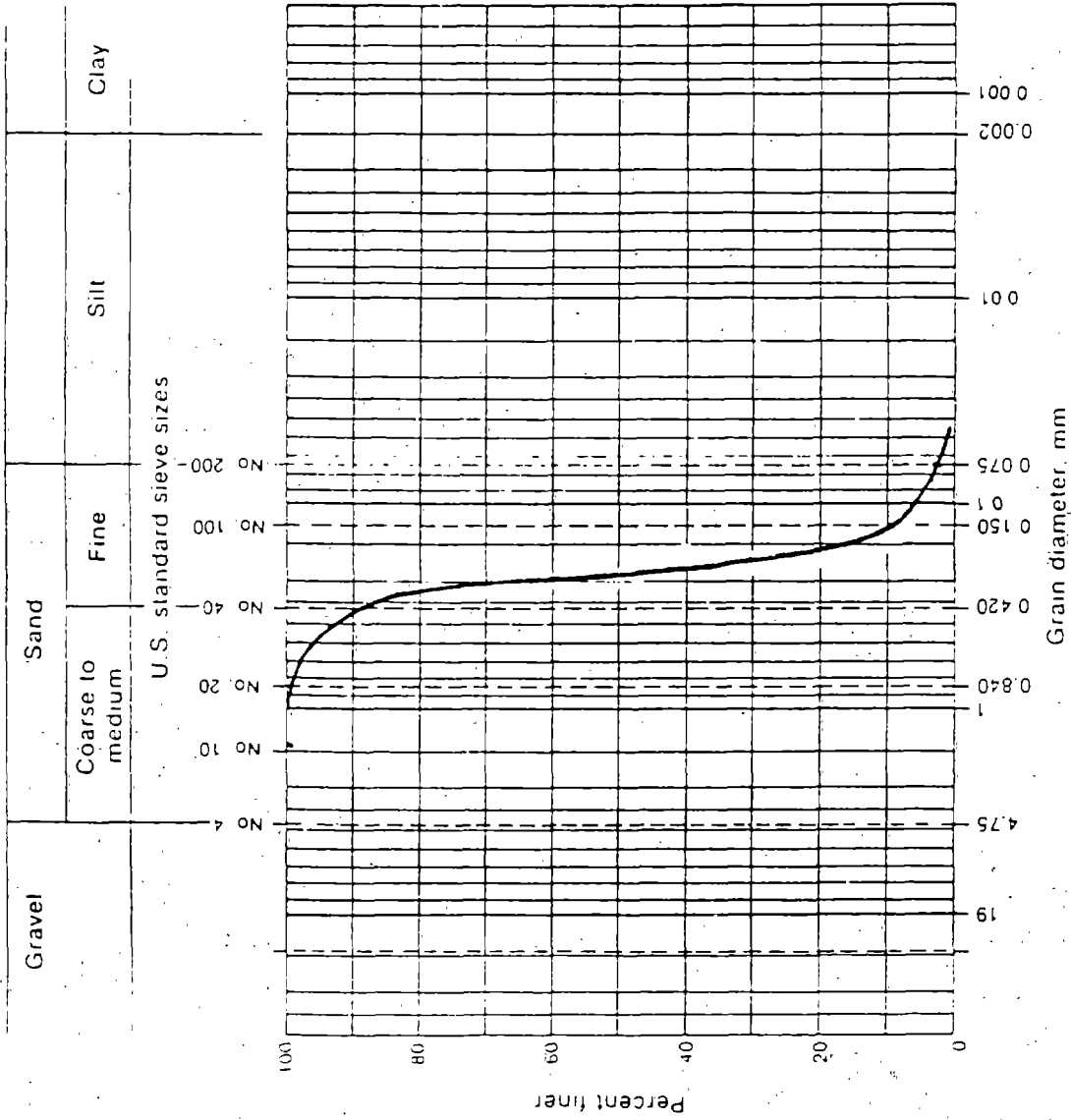


Figure 3. Sieve analysis results.

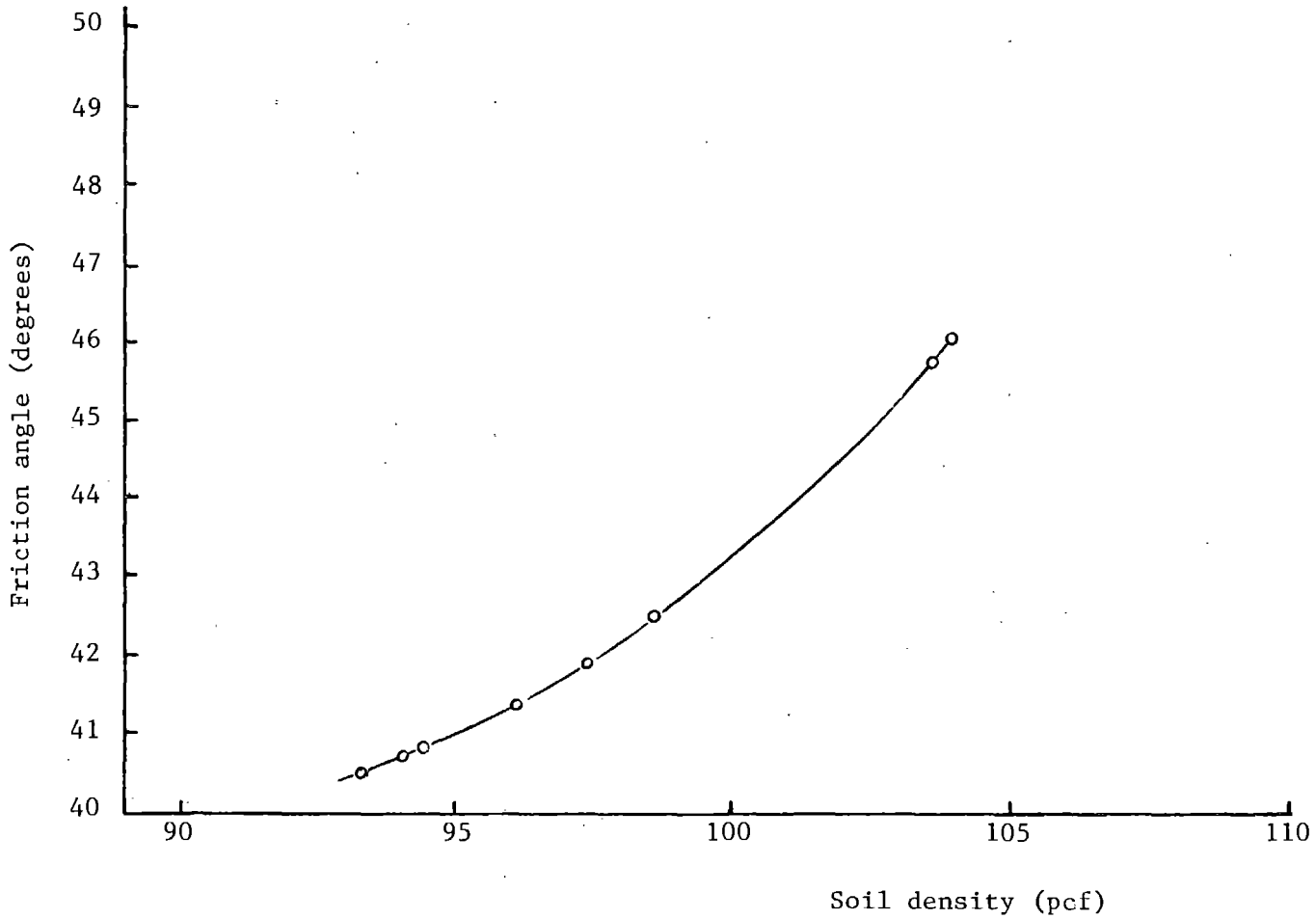


Figure 4. Friction angle versus density
(1 pcf = 0.157 KN/m³)

Table 2. Soil Properties

Dry Density (pcf)	Friction Angle ϕ , deg.	Relative Density %	Soil Modulus (psi)	Saturated Density (pcf)
93.3	40.45	36.0	3200.	-
94.5	-	41.3	-	115.0
96.2	41.4	50.6	3750.	-
97.4	-	56.6	-	116.7
98.6	42.4	62.0	3750.	-
99.3	42.8	65.6	3750.	-

(1 pcf = 0.157 kN/m³; 1 psi = 6.895 kN/m²)

2.2.2 Soil Sample Preparation

The technique used to place the selected soil into the test container is important as slight variations in soil density would produce considerable variations in soil stiffness and strength. The two methods of soil placement evaluated were undercompaction and raining (aerial pluviation).

The method of undercompaction has been proposed by Ladd (1978) for the preparation of reconstituted moist sand specimens for cyclic and static triaxial testing. The technique of undercompaction recognizes that when a typical sand is placed and compacted in layers, the compaction of succeeding layers will cause further densification of layers below. By "undercompacting" the lower layers to a predetermined percentage, the specimen will generally have a uniform density when all layers have been placed and compacted. The advantages of this technique are: (1) segregation of different soil particle sizes is minimized, and (2) samples of uniform density can be obtained.

Although the method seems to be attractive for specimen preparation, there are some difficulties in using the method:

1. The method is cumbersome and time-consuming.
2. It is very hard to compact the granular material by means of static loading to a high density without crushing the soil particles.
3. Within each layer, the rebound is different, making it difficult to include the effect of rebound in the analysis.

4. In cases where the optimum moisture content is too high, the water will squeeze out of the sample during the compaction.

Since the majority of the tests in this program were to be conducted in a dense soil, and both the soil particle crushing and the rebound problems were noticed in preliminary experiments, use of the undercompaction method was abandoned.

In the raining method sand is "rained" into the container from a specified height and through a specified size opening. By changing the height or the size of the opening it is possible to get samples at different densities. Greater drop heights or smaller openings produce higher soil densities. The attractiveness of this method is the ease of use and the absence of layering. Furthermore, for a fixed drop height and opening size the raining method is able to provide reproducible densities from sample to sample.

Some of the disadvantages of this method are:

1. If a well-graded soil is placed by the raining method, segregation of different soil size particles can occur. Since the soil selected for this study was uniform and poorly graded this disadvantage did not apply.
2. The height and size opening for a desired density must be determined by trial and error.
3. To obtain a soil with a very high density, the size of opening will be very small, resulting in a slow rate of soil placement.
4. The method is very operator-dependent. The speed or the path that the operator uses to move the hose around inside the sample container can significantly affect the density of the soil. This makes it important to weigh each completed sample to check its density.

The following procedure was followed in preparing the soil samples by the raining method.

A bucket having a volume of almost twice that of the sample container was filled with the soil and raised to the desired height by a crane. An aluminum pipe with the proper sized opening at one end was attached to this bucket, and the soil was released through the opening. By moving the pipe around in the container with a constant speed and a fixed path, the receiving container was filled. During this process, the supply bucket was raised at the same rate as

soil accumulation in the receiving container in order to maintain a constant height of fall to achieve a uniform density. This process continued until the soil level was approximately .25 in (0.5 cm) above the edge of the container. The excess soil was then trimmed using a straight edge. The next step was to weigh the sample and calculate its density from the known volume and weight. This process is illustrated in Figure 5.

If a saturated specimen was desired, the dry soil was prepared with the above procedure and then water was supplied through the bottom of the container. After the sample was completely saturated it was weighed again and the saturated unit weight was calculated using the measured amount of water used to saturate the soil.

The samples used for the triaxial tests were made with the same method. The same height and opening will give different densities if the receiving containers are of different sizes, for example, 2.0 in (5.08 cm) diameter for the triaxial tests compared to 15-in (38.1 cm) diameter samples for centrifuge tests. A curve of drop height vs. soil density is shown in Figure 6 for soil rained into a 15-in diameter container through a 0.30-in (0.76 cm) diameter size opening.

2.3 Pile Modeling

Two different types of piles were modeled in this study: wooden tapered piles and hollow steel pipes. The first type was used to model the prototype from Lock and Dam No. 26, whereas the second was used to study load transfer in sand.

A model pile can be said to be an accurate model of the prototype if the modulus of elasticity of the model is the same as that of the prototype and if geometric similarity with the prototype is maintained. This means that all physical dimensions of the model are reduced by a factor of λ from those of prototype. However, a model pile may not have all the physical dimensions modeled, and still represent the behavior of the prototype pile correctly. This can occur if one considers what affects the performance of the pile. For example, for laterally loaded piles the bending stiffness is determined by the EI (flexural stiffness of pile) of the pile while for axially loaded piles the axial stiffness is determined by the EA of the pile, where E = modulus of elasticity of the

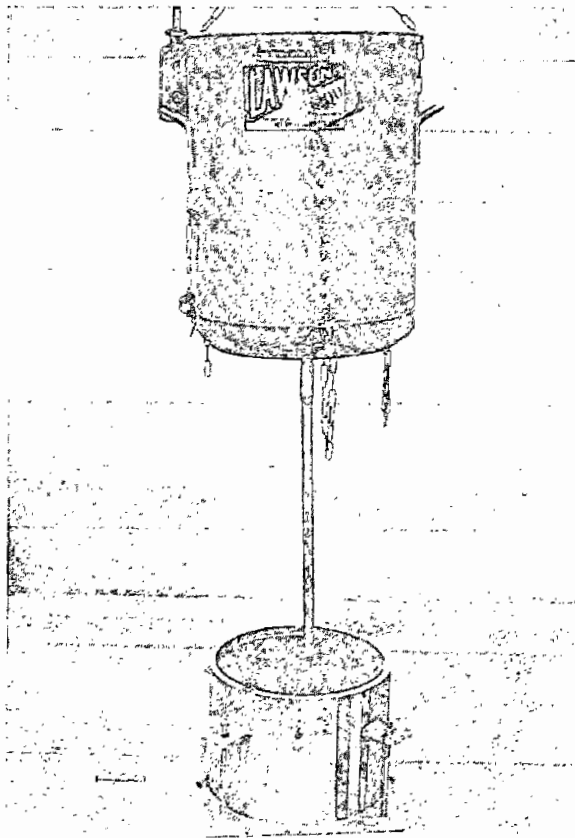


Figure 5. Raining process.

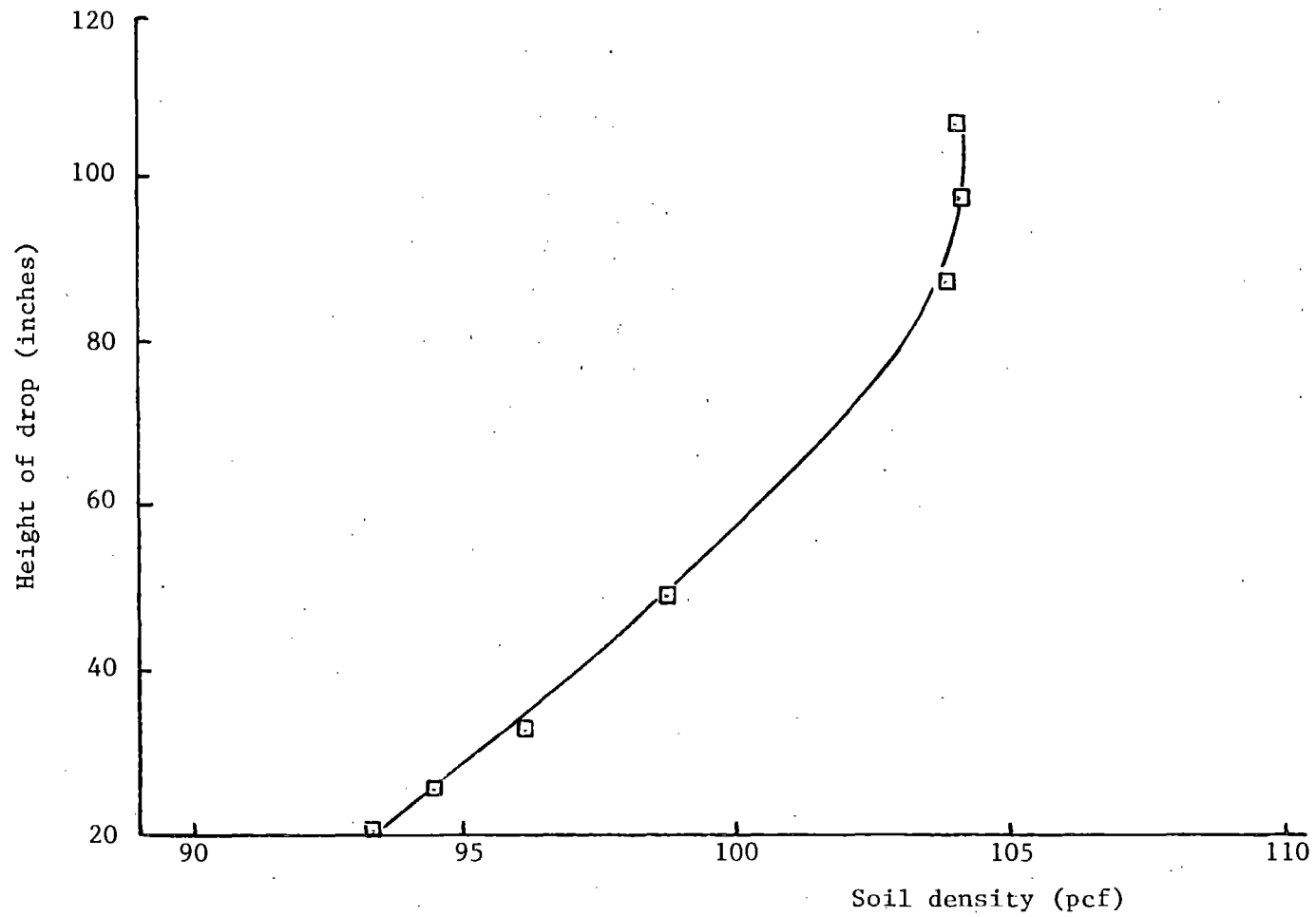


Figure 6. Height versus soil density
(1 pcf = 0.157 KN/m³, 1 in = 2.54 cm)

pile, I = moment of inertia, and A = cross-sectional area.

If the pile to be tested is only loaded axially or laterally, it can be modeled correctly by modeling just EA or EI , respectively, providing the surface area in contact with the soil is correctly modeled since that controls the skin friction on the pile and the lateral resistance of the soil. This is important in the case of steel piles, as a 1/70 scale model of a pile of 0.36 inch (.92 cm) wall thickness would have a wall thickness of 0.005 in (0.0132 cm) which would result in a difficult machining problem. Since the steel pile was primarily used to study lateral loading, fabrication of the model from aluminum with a wall thickness of 0.025 inch (0.0635 cm) will provide the correct bending stiffness and will be much easier to manufacture.

The solid wooden piles were fabricated from wood dowels whose axial modulus was determined to be identical to the listed modulus values for the Douglas fir prototypes. Initially Douglas fir was considered for use in the models, but considerable variations among samples tested were observed. Model piles were turned on a lathe to obtain the correct taper.

Dimensions of the model wooden piles for the 1/50, 1/70, and 1/100 scale sizes tested and of the aluminum pile at the 1/70 scale factor are shown in Table 3.

Table 3. Pile Properties

Pile Type	Property	Scale Factor			
		1	50	70	100
Tapered	Tip Diameter (inch)	11.25	.224	.161	.113
Wooden	Butt Diameter (inch)	14.0	.280	.200	.140
Pile	Length (inch)	480	9.60	6.86	4.80
	Young's Modulus (ksi)	1885	1885	1885	1885
Aluminum	Outer Diameter (inch)	10.80		.154	
Pile	Inner Diameter (inch)	6.58		.094	
	Length (inch)	480		6.86	
	Young's Modulus (psi x10 ⁶)	10.0		10.0	
Straight	Diameter (inch)	12.70		.181	
Wooden	Length (inch)	480		6.86	
Pile	Young's Modulus (ksi)	1885		1885	

(1 in = 2.54 cm; 1 x 10⁶ psi = 0.689 x 10¹⁰ N/m²)

2.4 Modeling of Models

In order to model a problem it is necessary to show that the scaled model results can be projected to prototype behavior regardless of the scale used for modeling. This can be done by a "modeling of models" procedure in which a series of models of different scales all representing the same prototype are tested at different gravity levels appropriate to the model scale and the results are extrapolated to prototype scale for comparison with each other. If all the models produce the same prototype projections, one can say that the scaling relations are valid. Obviously, the series of models to be tested should extend to and include the prototype. However, prototype structures usually involve many uncertainties such as inhomogeneity of presumably homogeneous zones, foundation conditions, and loading conditions. Also, testing the prototype to failure may not be possible for economic or safety reasons. However, the internal consistency of a series of models can still be verified on its own, without involving the actual prototype. The prototype pile in this study was modeled at 1/50, 1/70 and 1/100 scale factors in the centrifuge.

The same soil was used for all the different scales since the ϕ angle and the unit weight of the soil are independent of the scale factor.

The depth of the soil beneath the model piles was varied for the 70- and 100-scale factors to maintain geometric similarity. These depths were 6.00 inches (15.24 cm) and 4.20 inches (10.67 cm) for the 1/70 and 1/100 scale factors, respectively. According to Meyerhof (1959), the lateral zone of influence of piles on soil compaction is between 3 to 4 diameters. Since the soil container used in the centrifuge test program had a diameter of 15 in (38.1 cm), the side wall of the container was at least 25 pile diameters away from the model pile being tested. The influence of the side walls is considered to be negligible.

CHAPTER 3. EQUIPMENT AND PROCEDURE

All testing was conducted in the geotechnical laboratory of the Department of Civil, Environmental, and Architectural Engineering of the University of Colorado at Boulder utilizing its 10 g-ton geotechnical centrifuge. Much of the equipment was specifically constructed for this particular test program. Monitoring and data recording were accomplished by standard manufactured items. This chapter describes each component's function and, for specially constructed items, the details of their construction.

3.1 The Centrifuge

Specifications and principal dimensions for the Genisco Model 1230 centrifuge, shown schematically in Figure 7, are given in Table 4. A principal advantage of this centrifuge is its swinging baskets which were specially designed for geotechnical experiments. This enables samples to be both placed and tested with resultant gravity and acceleration forces always correctly oriented normal to the base of the sample basket.

A vertical shaft on the rotation axis of the centrifuge contains the electrical and hydraulic slip rings. Of the 56 electrical slip rings, two are committed to a video signal and three to power for the camera and lighting. The remainder are available for test control and data. The shaft also contains two hydraulic slip rings suitable for water or light oil to 3000 psi (20.7 MN/m²) pressure.

Testing is monitored by a video camera mounted near the axis of rotation and rotating with the centrifuge. Pictures are displayed on a black and white television monitor, and a video cassette recorder is used to record each test. Normally only a top view of the sample would be available during a test, but a mirror mounted on the sample basket enables one to have a full side view also.

3.2 The Sample Container

The sample container for all of the tests was an aluminum cylinder 15.0 inches (38.1 cm) inside diameter, 16.0 inches (40.64 cm) outside diameter and 12.0 inches (30.48 cm) deep. The container was mounted on a 17.0 x 18.0 x 0.50 inch (43.18 x 45.72 x 1.27 cm) aluminum plate bolted to the floor of the centrifuge basket. The large container diameter eliminated any lateral boundary effects

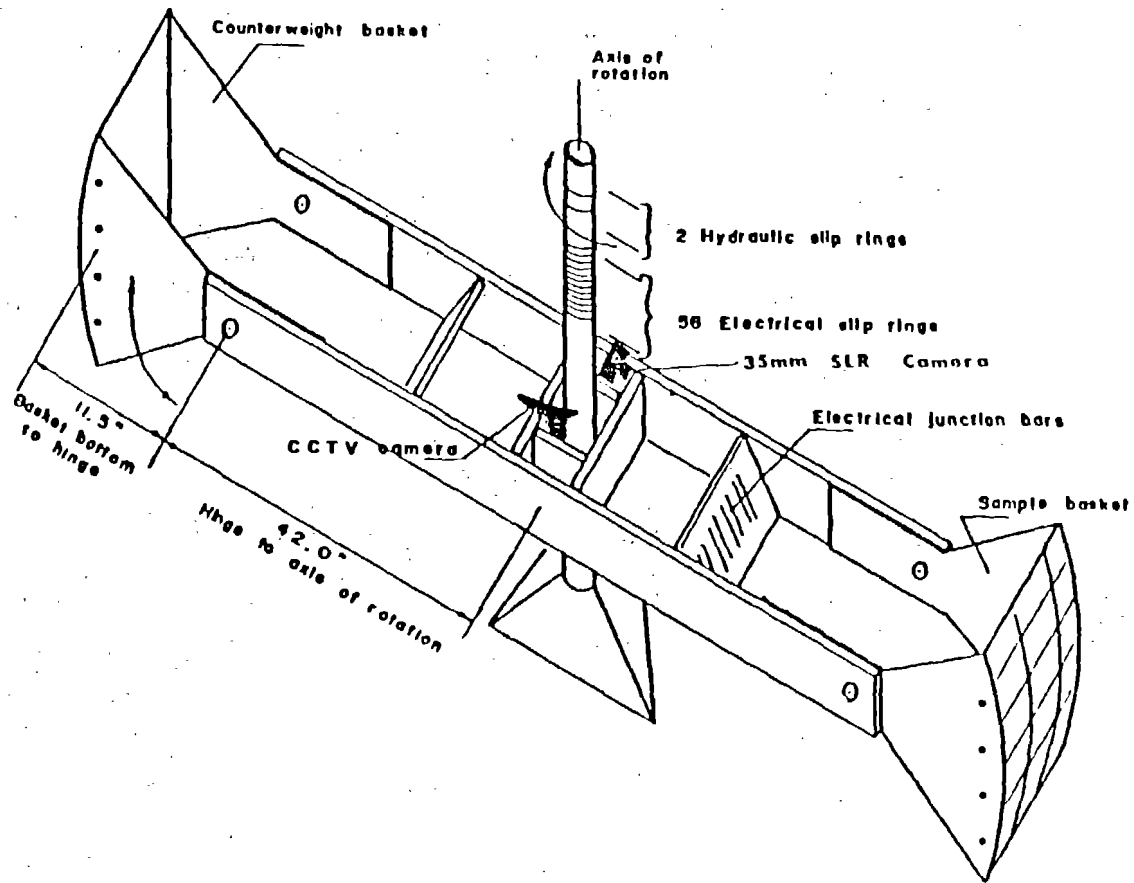


Figure 7. Schematic view of centrifuge

Table 4. Centrifuge Specifications

Manufacturer	GENISCO
Model	1230-5
Driving System	25 H.P. Hydraulic
R.P.M. Range	0-470 R.P.M.
Gravity Range	1-262 g
Payload Capacity	10 g-tons
Radius (Center-Basket Hinge)	41.8 inches (1.06 m)
Radius (Center-Basket Floor)	53.5 inches (1.36 m)
Area (Basket Floor)	18 inch x 18 inch (45.7 cm x 45.7 cm)
Electrical Pick-Ups	56 electrical slip-rings
Fluid Transmission	2 hydraulic slip-rings (rated at 3000 psi, 20.7 MN/m ²)
Test Recording	Closed Circuit TV 35 mm SLR Camera

and permitted more than one test to be conducted in each soil sample.

An O-ring between the container and the bottom plate sealed the container for saturated soil tests. Sample saturation or drainage was accomplished through a series of small (0.005 inch diameter) holes drilled in the base plate. These small holes are intercepted by four horizontal collector grooves that exit on the side of the base plate.

The loading mechanism could be mounted in one of four positions over the soil container, thus permitting four tests to be performed on each prepared soil sample. The separation between two adjacent single pile tests is 3.5 inches (8.89 cm), equal to 17 times the pile diameter at the soil surface in the case of a 70 g test. The four pile test positions in the soil container are located at an equal distance from the container wall. Thus effects of wall disturbance, if any, would be equal for each test position.

3.3 Axial Loading

3.3.1 Hydraulic System

Axial loads were applied to the piles by a Bellofram double acting cylinder manufactured at the University of Colorado. The cylinder, with a maximum load capacity of 1200 lbs (5.34 KN) and a maximum stroke of 7.0 inches (17.78 cm), was employed to drive the model piles in flight under increased gravity conditions to 100 g. The lower part of the cylinder was filled with water and by applying pressure to the upper section, the water would flow out and the loading rod would be pushed out of the cylinder. If necessary a flow valve can be connected to the lower part of the cylinder to control the rate of water flow and therefore the rate of penetration. The hydraulic system is shown in Figure 8.

3.3.2 Load and Displacement Measurements

Measurement of individual pile or group loads required a load cell capable of operating in a 100 g environment. As commercial load cells were unsatisfactory due to their heavy weight (1-2 lbs; 0.45-0.9 kg), it was necessary to design and manufacture a load cell having the required load range and weight. A strain-gauged cylindrical aluminum load cell (Figure 9) was designed to be attached to the ram of the Bellofram cylinder used to apply pile loads. The load cell had a capacity of 1000 lbs (4.449 KN) and a load resolution capacity of 1 lb (4.45 N) force.

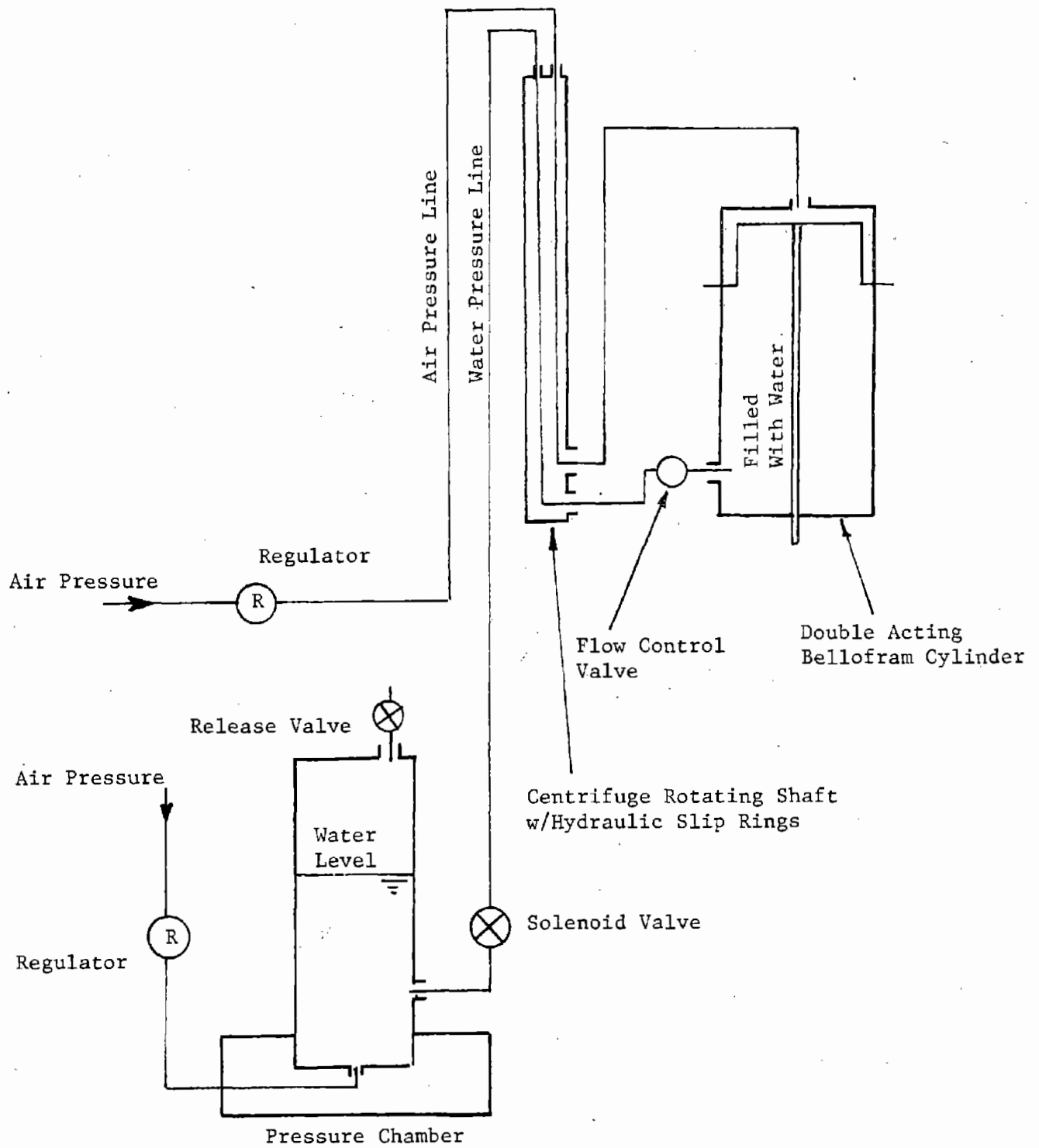


Figure 8. Schematic of hydraulic system.

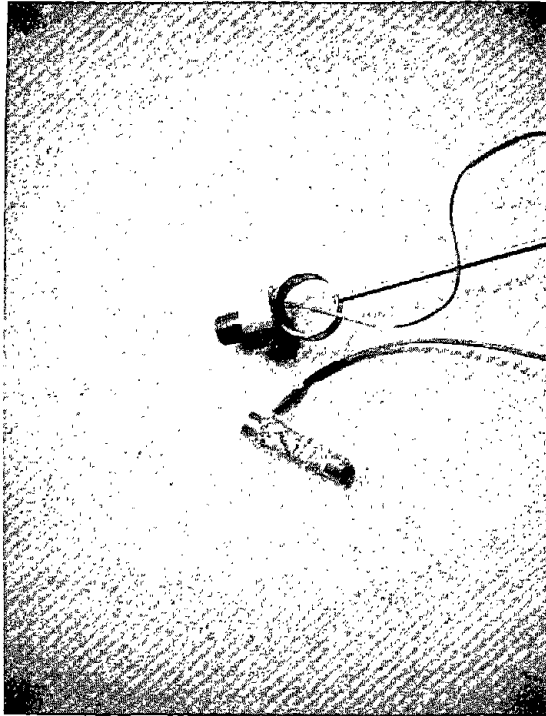


Figure 9. Axial and lateral load cells.

Displacements were measured by Schaevitz linear variable differential transformers (LVDT's). A model 3000HR LVDT with a 6.0-inch (15.24 cm) range was used during the installation of the piles and a model 250HR LVDT with 0.5-inch (1.27 cm) range was used during pile load testing. This smaller LVDT permitted axial deformations to be determined to within 0.005 inch (0.0127 mm). The LVDT's body was fixed to the side of the driving mechanism and the core was attached to the load cell via a lateral extension rod as shown in Figure 10. This arrangement measured displacement of the load cell along with that of the pile. This was necessary because the model piles were too small for an LVDT core to be attached directly to them without introducing significant lateral forces. A correction for the load cell deformation was applied to the settlement of the piles for all the single pile tests. For the group tests the LVDT core was attached directly to the pile group cap.

3.4 Lateral Loading

3.4.1 Hydraulic System

Lateral loads were applied to the pile by a cord which was tied to the top of the pile, and was pulled laterally through a pulley system by means of a small double-acting Bellofram cylinder with a capacity of 400 lbs (1.779 KN). The lower part of the Bellofram cylinder was filled with water to allow control of the rate of loading.

3.4.2 Load and Displacement Measurements

The applied lateral force was measured by a miniature, strain-gauged proving ring (Figure 9) which was attached to the cord.

The lateral deflection was measured by a Schaevitz Model 250 MHR LVDT with 0.50-inch (1.27 cm) maximum range. The LVDT core was slightly spring loaded against the pile top so that it would move with the pile during the lateral loading. The lateral loading system is shown in Figure 10.

3.5 Pile Instrumentation

3.5.1 Aluminum Piles

To obtain load transfer data for piles in sand, hollow, instrumented aluminum piles were used. They were made in two halves which were epoxied together

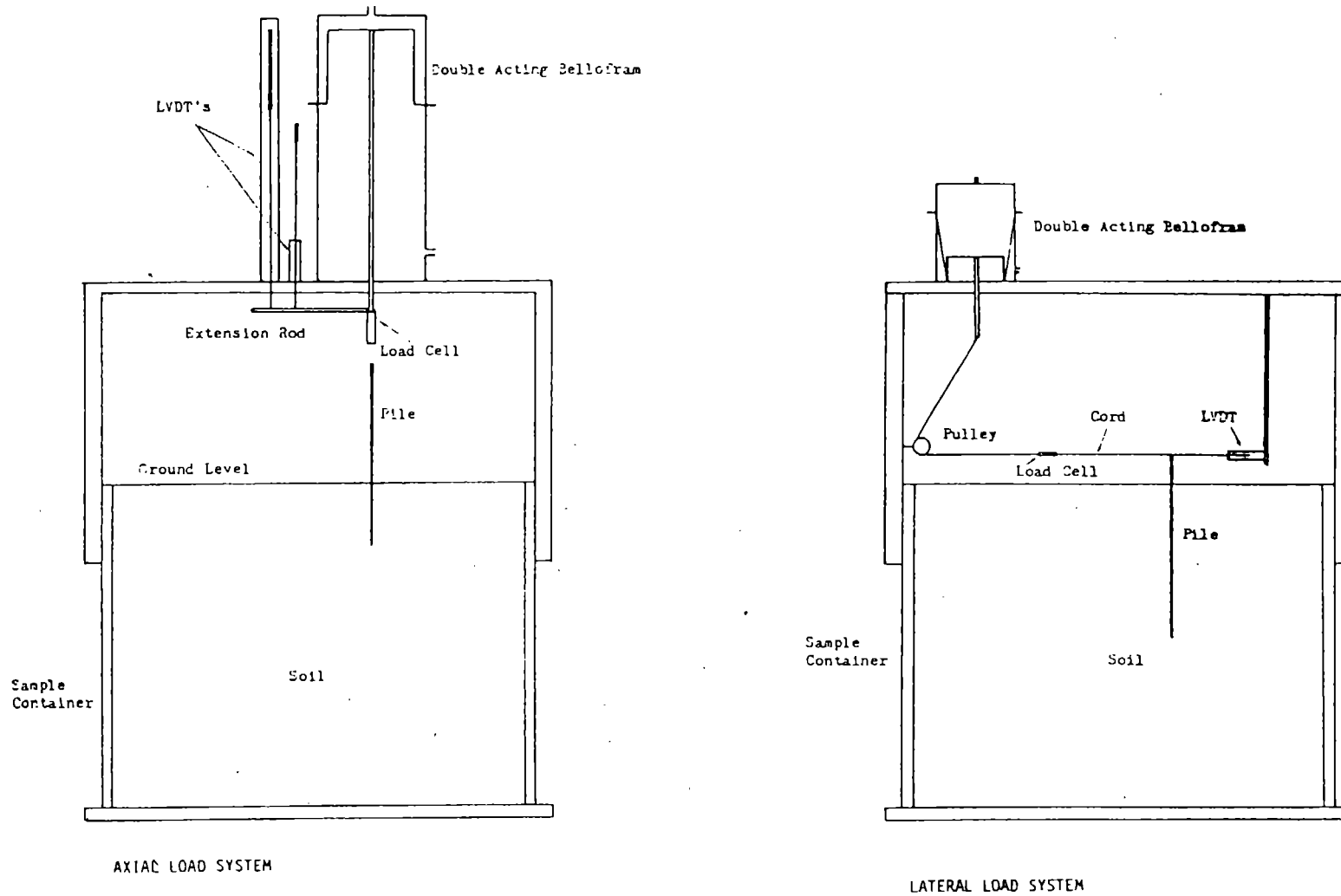


Figure 10. Mechanisms for loading model piles in the centrifuge.

to form the circular cross section. Miniature strain gauges were installed on the inside surface at several locations along the length. At each location, two gauges were applied at opposite ends of the diameter. The positions of the strain gauges installed on the pile are shown in the photograph of one half of the pile in Figure 11.

The strain gauges were 120 ohm Micro Measurement Model EA-06-050AH-120. The two gauges installed at each level along the model pile formed two of the arms of a Wheatstone bridge circuit. The other two arms were supplied by dummy gauges in the balancing and amplifying unit described in Section 3.8.

3.5.2 Wooden Piles

The tapered wooden piles were strain gauged at the top portion above the soil to measure the individual pile loads when a group test was being conducted. An initial problem of heat dissipation with the gauges because of low thermal conductivity of wood was solved by using larger strain gauges. The gauges finally used were Micro-Measurements 120 ohms, Model EA-13-125 BB-120. Of the four arms of a Wheatstone bridge, two were provided by strain gauges on the pile and the other two by dummy gauges on the signal conditioning cards.

3.6 Calibration Procedures

The load cells manufactured for the axial and lateral load measurements were calibrated using laboratory proving rings of known calibration. The LVDT's used for the pile driving and for the model pile testing were calibrated using a mechanical type micrometer or dial gage. These calibrations were conducted at normal gravity levels.

The two strain-gauged piles used in this test program were calibrated at one g by applying a force to the top of the pile using the Bellofram cylinder. The previously calibrated axial load cell was used to determine the applied load. This procedure was used to calibrate the two strain gauges at the top of the wooden piles and the several gage levels on the instrumented aluminum pile.

To avoid a buckling failure of the model pile, the pile was inserted into a small diameter hole (approximately one inch in diameter) for its full length to provide lateral stability under the calibration loading.

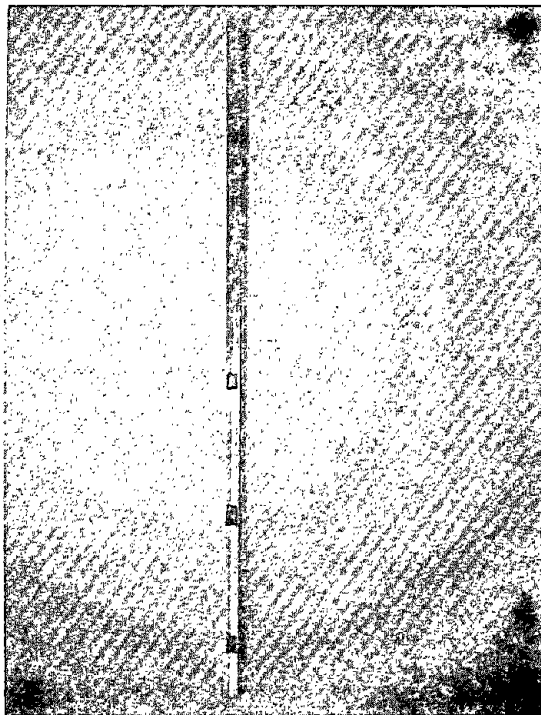


Figure 11. Strain gage positions on one-half of the aluminum pile.

3.7 Test Procedure

3.7.1 Axial Loading

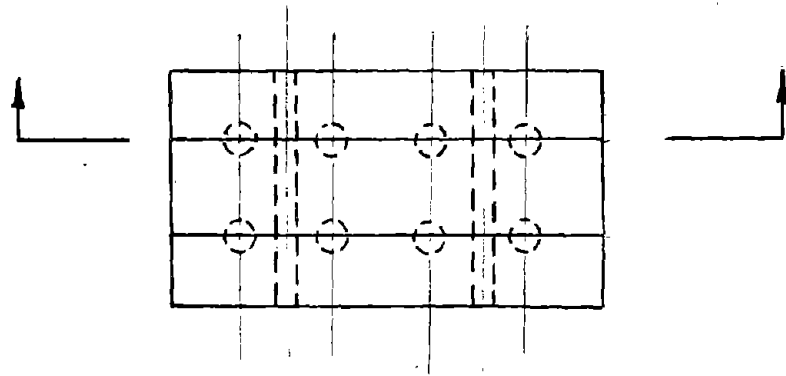
3.7.1.1 Single Pile

The following procedure was followed in installing and load testing the single model pile. The pile is pushed into the soil by hand for a distance of 2.0 inches (5.00 cm) (in case of 70 g test) using a template block for initial alignment purposes. The centrifuge is then brought to the speed required to produce the acceleration needed at the mid-height of the embedded pile, and the installation of the pile is continued under the increased gravity by activating the hydraulic controls on the loading mechanism. Pile penetration is monitored by the 6.0-inch (15.24 cm) range LVDT, whose output is read by a digital voltmeter and also plotted against the load cell signal on a x-y plotter. Towards the end of the pile penetration during the installation, the more sensitive 0.5-inch LVDT (1.27 cm) comes into range and is used to monitor penetration. When the desired driving penetration is reached the load is taken off the pile. A pile loading test is carried out after installation without stopping the centrifuge by bringing the loading ram down again. After an axial loading test has been completed the centrifuge is stopped and the loading mechanism is shifted to the next test location.

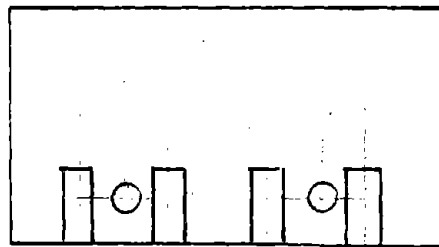
3.7.1.2 Pile Groups

Installation of the pile group is achieved by using a cardboard template with holes punched at locations corresponding to the piles in the 2 by 4 group of the prototype. The pile loading device is positioned sequentially over each of the piles to push it into the soil under the desired gravity, with the centrifuge being stopped between each single pile installation for repositioning of the driving device. Since the template is thin and flexible, the friction between it and the piles can be neglected. The template is left in place during the group testing.

After all piles in the group have been driven the pile cap is installed. The pile cap is fabricated from three pieces of aluminum as shown schematically in Figure 12. The rigid fixed nature of the pile cap means that any horizontal or vertical misalignment of the top of piles from the prescribed group pattern



Top view



Section

Figure 12. Model Pile Cap

can result in some differential lateral or vertical pile displacement as the cap is installed and is initially loaded.

This was observed in the initial pile group test when it was found that the initial group loading after installation of the pile cap required 0.10 to 0.15 inch (.3-.4 cm) vertical settlement to reach ultimate load whereas subsequent tests on the same pile group reached ultimate load in 0.015 to 0.02 inch (0.04-0.05 cm) settlement. The difference was attributed to the effect of individual pile disturbance on the initial loading after pile cap installation.

To provide a uniform state from which to measure response, all pile groups were pushed as a group an additional 0.2 inch (.5 cm) after pile cap installation while the centrifuge was producing the required gravity level. Load-settlement curves were then obtained from this point.

3.7.2 Lateral Loading

After the pile was installed under test gravity conditions the centrifuge was stopped and the lateral loading mechanism installed. The loading cord with the load cell attached was connected to the pile top and the lateral LVDT positioned. The lateral load test was then conducted after the centrifuge had been brought back to the desired speed.

3.8 Data Acquisition System

Strain-gauge signals from the load cells and from the instrumented wood or aluminum piles were amplified by signal conditioning units in which the Wheatstone bridge circuit was completed. The units also provided balancing and zeroing functions. The units were mounted on the arm of the centrifuge as it was necessary to amplify the low output strain-gauge signals to levels greater than the noise levels from the electrical slip rings.

The signal conditioning unit permitted the dummy gauges of the Wheatstone bridge to be in opposite or adjacent positions in the bridge to provide, respectively, an average signal from the two active gauges for axial loading or a differential signal for bending produced by lateral loading.

The applied force vs. pile movement data were recorded on x-y plotters. The individual loads taken by each of the piles in the group test and the load taken

by each of the five sets of strain gauges on the aluminum pile used for load transfer testing were recorded on strip chart recorders.

CHAPTER 4. PRESENTATION OF TEST DATA

4.1 Introduction

In this chapter the test program is summarized in tabular form and the results of individual tests are presented. Results in the form of load-settlement curves have generally been converted to prototype scale to facilitate comparison of pile responses.

4.2 Test Plan

The pile tests conducted in sand are summarized in Table 5. The ultimate loads reported in Table 5 have been converted to prototype scale for all tests to permit convenient comparison of results. The ultimate loads reported produced 2.0 inches (5.1 cm) settlement at prototype scale. This corresponds to 0.040 inch (0.10 cm), 0.029 inch (0.073 cm) and 0.020 inch (0.051 cm) at 1/50, 1/70, and 1/100 scale, respectively.

The test program in sand was conducted in three phases. The first phase, represented by Test Series No. 1 and 2, was required to develop and verify details of model pile installation in the centrifuge. The second phase, which constituted the main portion of the research project, investigated the ability and feasibility of conducting tests on model piles and pile groups in sand in the centrifuge. Test Series No. 3, 4, and 5 provided information on the internal consistency of the data, investigated the sensitivity of test results to friction angle and provided model test data which could be extrapolated to prototype scale for comparison to field test data. The third phase provided information on several topics of interest in pile foundation design and provided load-transfer data necessary for input to a computer program to compute pile and pile group response.

4.3 Presentation of Test Results

Test Series 1: Effect of In-flight Installation vs. 1 g Installation

The effect of in-flight vs. 1 g installation on single pile load test results was investigated with both 50 and 70th scale model piles. One pile was installed at normal gravity and then load tested at increased gravity. A second pile was both installed and tested at the increased gravity level. This test series was conducted to verify the need for in-flight pile installation. Results are presented in Figures 13 and 14.

Table 5. Summary of Testing Programs in Sand

Test Series	Test Group No.	Purpose	Gravity Level g s	Test Condition Unit Weight pcf	φ deg.	Ultimate Load Kips	Special Point of Interest	Comments
1	1	Effect of in flight installation vs. lg installation	70	98.23	42.5	520		
	2		50	103.61	46	1060		
2	1	Effect of interruption between installation and load test	70	98.23	42.5	520		
3	1	Modeling	50	98.23	42.5	470-560		
	2	of	70	98.23	42.5	520		
	3	Models	100	98.23	42.5	540		
4	1	Parametric study	70	92.78	40.45	190		In 4.8 test group, at 13 inch left for installation to be completed, two of the piles broke at approximately 1.2 inch below the soil level.
	2		70	93.54	40.7	250		
	3		70	93.99	40.8	260		
	4		70	95.70	41.35	340		
	5		70	96.96	41.85	470		
	6		70	98.23	42.5	520		
	7		70	103.16	45.7	890		
	8		50	103.61	46.0	1060		
5	1	Group	70	93.99	40.8	2800	Efficiency 1.32	The weight of the cap (103.8 Kip) is not included in the load-settlement curves but it is included in the calculation of efficiency factors.
	2	Tests	70	95.70	41.35	3100	1.15	
	3		70	96.96	41.85	4360	1.16	
	4		70	98.29	42.5	4790	1.15	
6	1	Tapered	70	95.32	41.25	270	Tap. Str. Ratio: Tap/St. -	The straight pile had the same diameter as the mid-height diameter of the tapered pile.
	2	vs.	70	95.70	41.35	340 290	1.15	
	3	Straight piles	70	98.23	42.5	520 415	1.24	
7	1	Saturated	70	93.99	40.8	2800 2350	Dry Sat. Ratio: Dry/Sat. 1.19	Test 7.1 is a group test, and at the end of the test water level was 5.2 ft below soil level. Test 7.2 was a single pile test, and at the end of the test water level was 7.0 inch above soil level (prototype).
	2	Tests	70	96.96	41.85	470 290	1.61	
8	1	Lateral Load Tests	70	92.78	40.45	16.8		The lateral deflections were measured at 5 ft above the soil level. The ultimate loads at 5.5 inch of deflection (prototype).
	2		70	93.54	40.7	19.5		
	3		70	98.23	42.5	24.0		
	4		70	103.61	45.7	27.0		
9	1	Instrumented Aluminum pile Test	70	95.32	41.25	170		

1 Kip = 4.45 KN, 1 pcf = .158 KN/m³

All quantities expressed in prototype scale

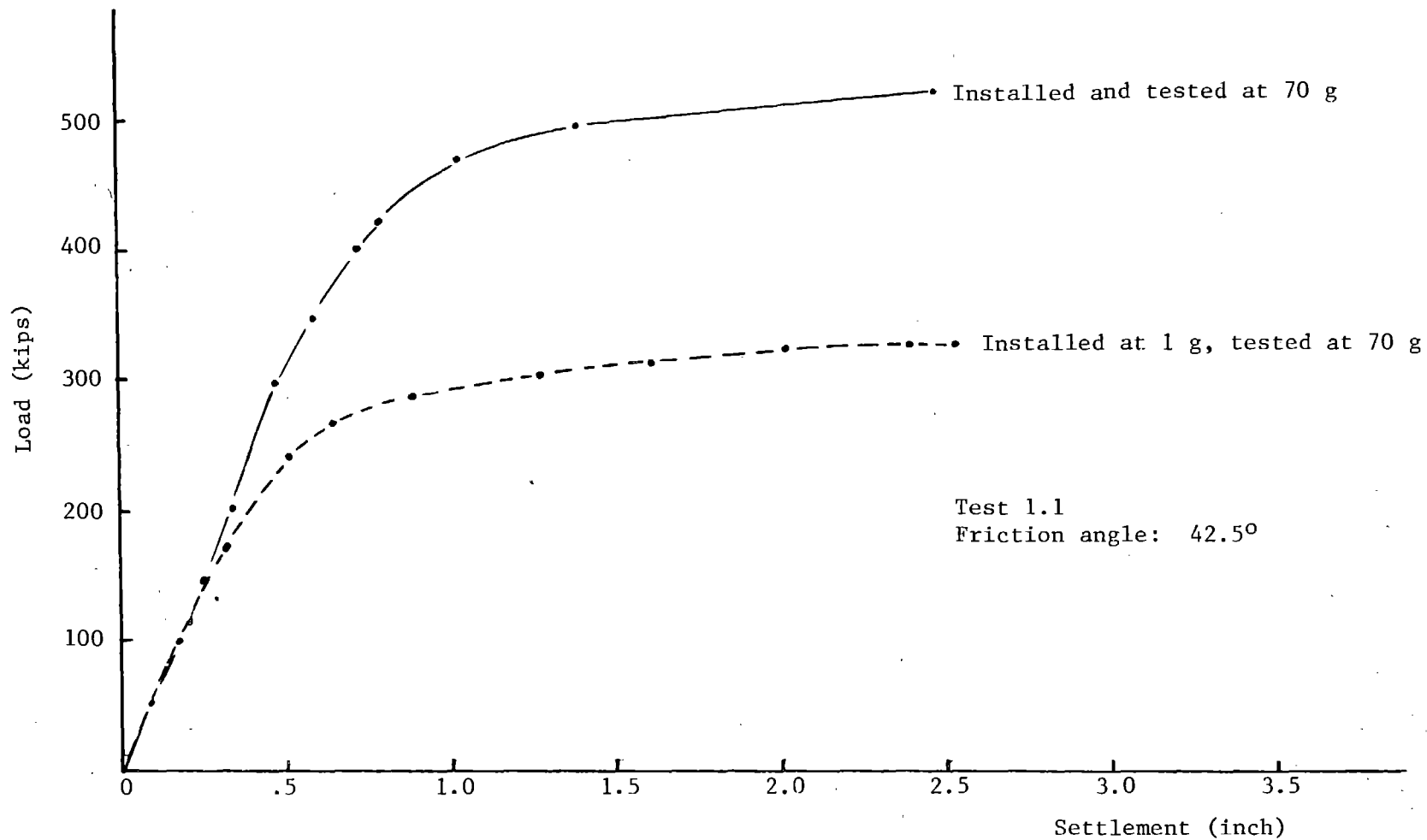


Figure 13. Effect of in-flight vs 1 g Installation (prototype scale), 1/70 scale.
(1 in = 2.54 cm, 1 kip = 4.45 kN)

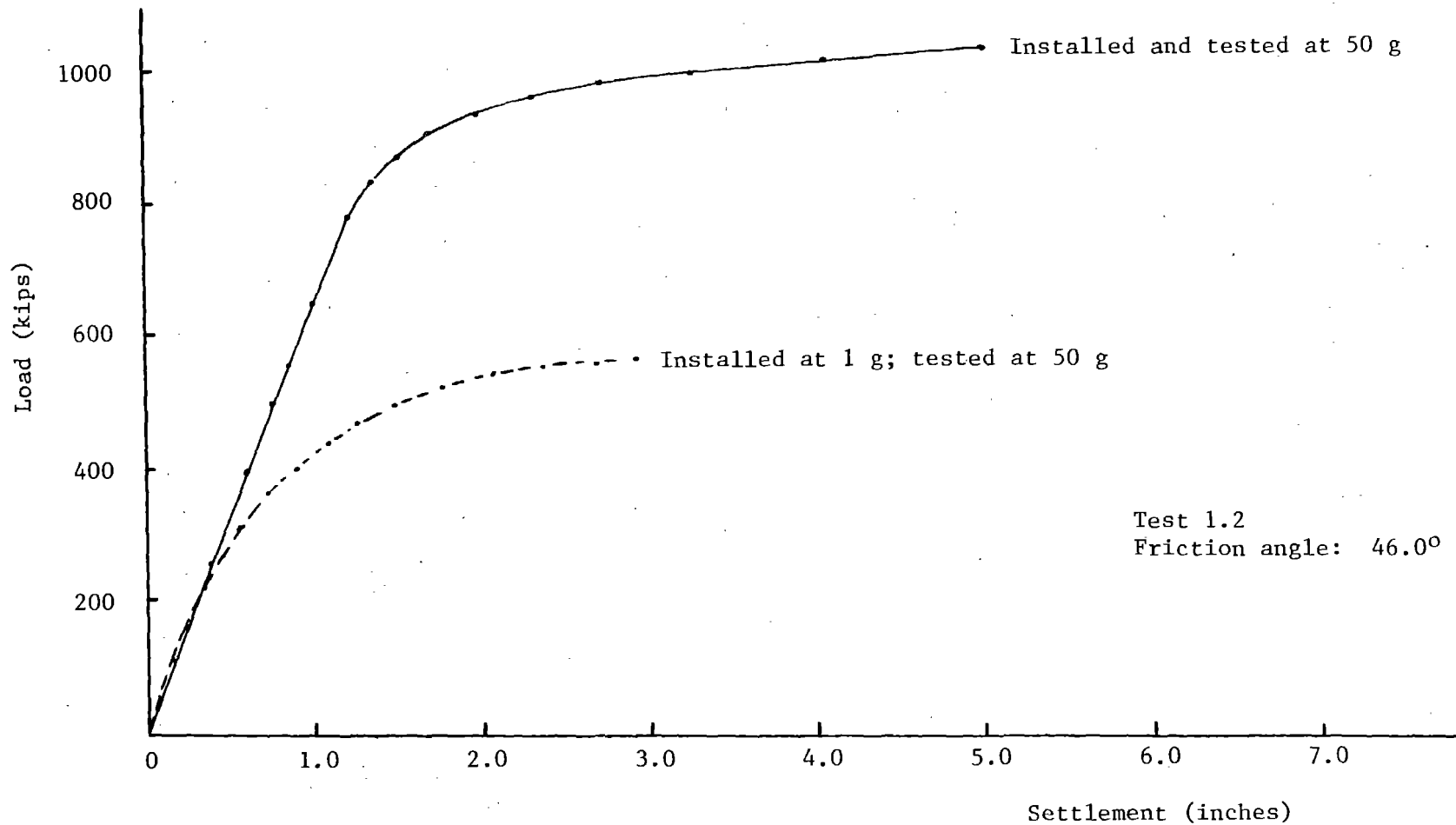


Figure 14. Effect of in-flight vs 1 g installation (prototype scale), 1/50 scale.
(1 in = 2.54 cm, 1 kip = 4.45 kN)

Test Series 2: Effect of Interruption Between Installation and Load Testing

For the group tests the centrifuge had to be stopped after installation of each pile so that the loading mechanism could be repositioned over the next pile. This raised the question of whether or not stopping the centrifuge after installation would have any effect on pile behavior. This was investigated by installing a pile and load testing it without interruption. The same pile was then tested after the centrifuge had been stopped and brought up to speed again. Results are shown in Figure 15.

Test Series 3: Modeling of Models

To verify the similitude relationships and the internal consistency of the centrifuge results, a modeling of models study was performed. The tests were conducted at 50, 70, and 100 g levels. Two tests were conducted at each model scale (g level) for a total of six tests. All tests were conducted in sand having a friction angle of 42.5 degrees. The load-settlement curves of the tests at their respective g levels are shown in model scale in Figure 16.

Test Series 4: Parametric Study

The effect of soil density on the load-settlement behavior of model piles was investigated using 1/70 scale model piles. Results from one 1/50 scale test were also included in this test series. Results are shown converted to prototype scale in Figures 17 to 19. A minimum of two and up to four tests were conducted on each prepared soil sample. Where a single curve is shown for a given friction angle it is representative of test results which had identical measured responses. Some tests show two or more curves as a result of the different responses obtained from the same soil sample.

Test Series 5: Group Tests

Four successful group tests were performed. Because of some differences in the test procedure, they will be divided into two groups for discussion.

Tests 5.2 and 5.4

For these two pile group tests the LVDT used to measure group settlement was attached to the top of the load cell as previously described in the discussion of the single pile loading equipment. Thus it was necessary to correct the measured settlement value for the elastic deformation of the load cell. The magnitude of

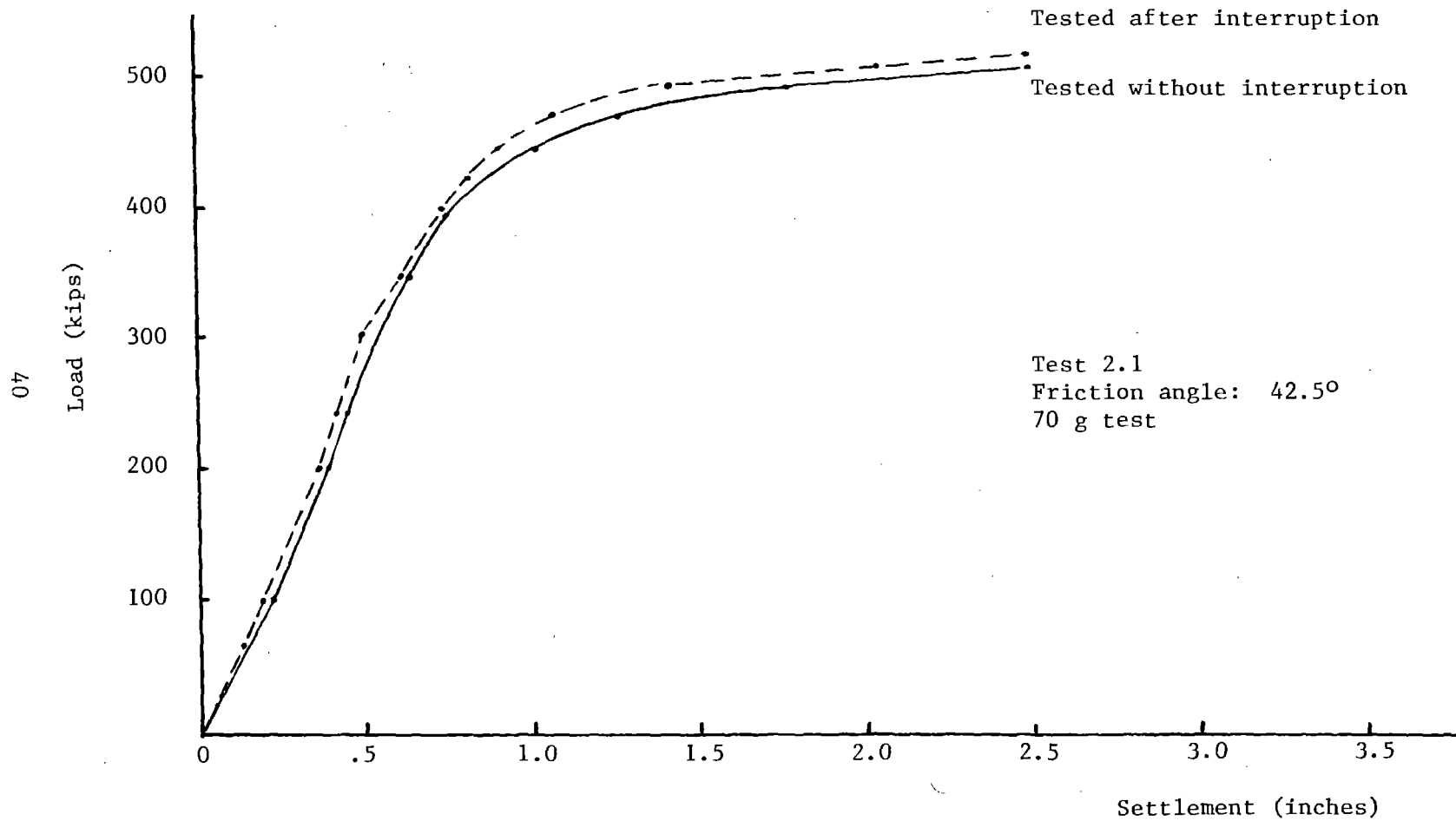


Figure 15. Effect of centrifuge stoppage between pile installation and testing (prototype scale).
(1 in = 2.54 cm, 1 kip = 4.45 kN)

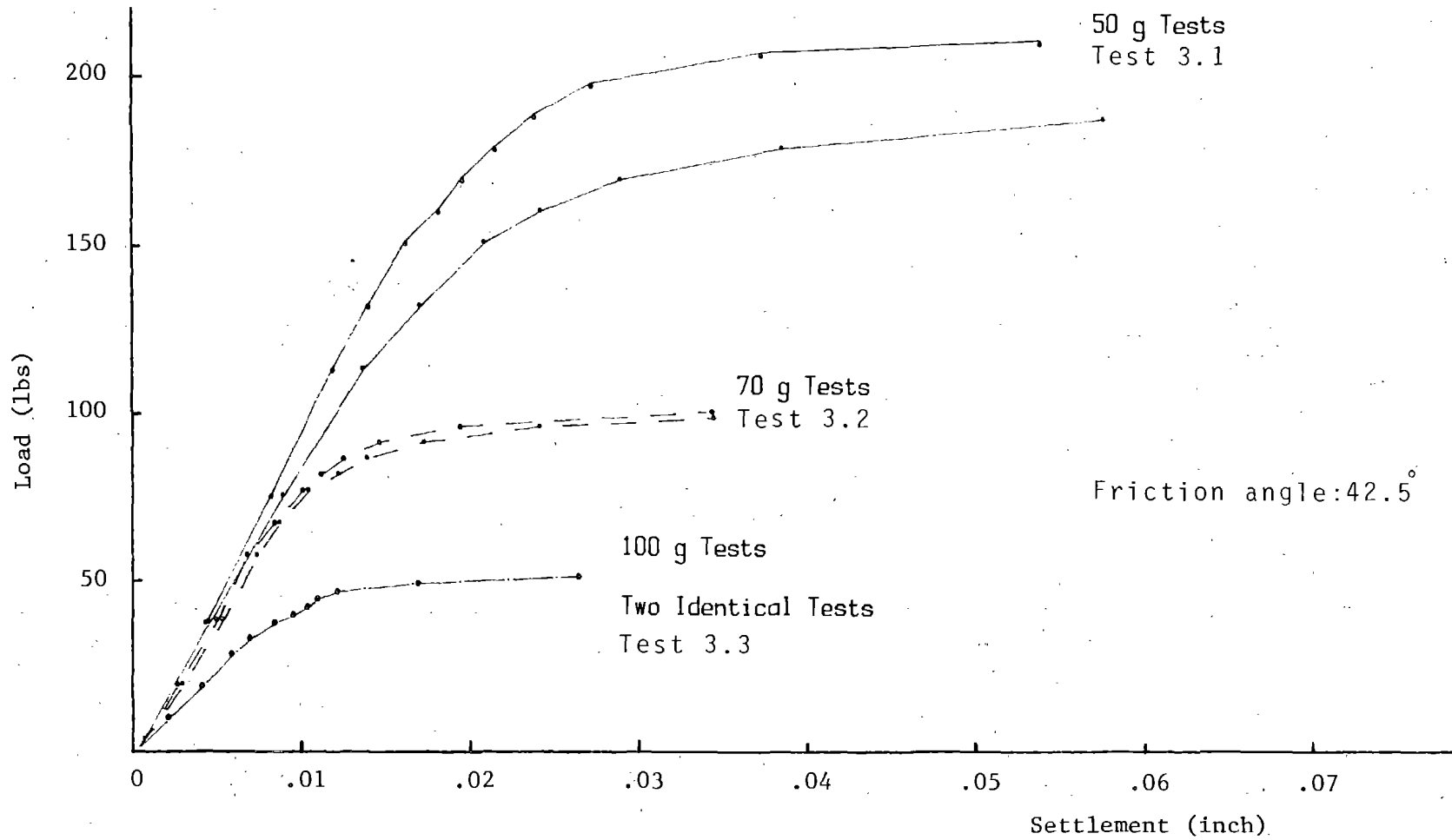


Figure 16. Load-settlement curves from modeling of models test series.
(model scale) (1 in = 2.54 cm, 1 lb = 0.224 N)

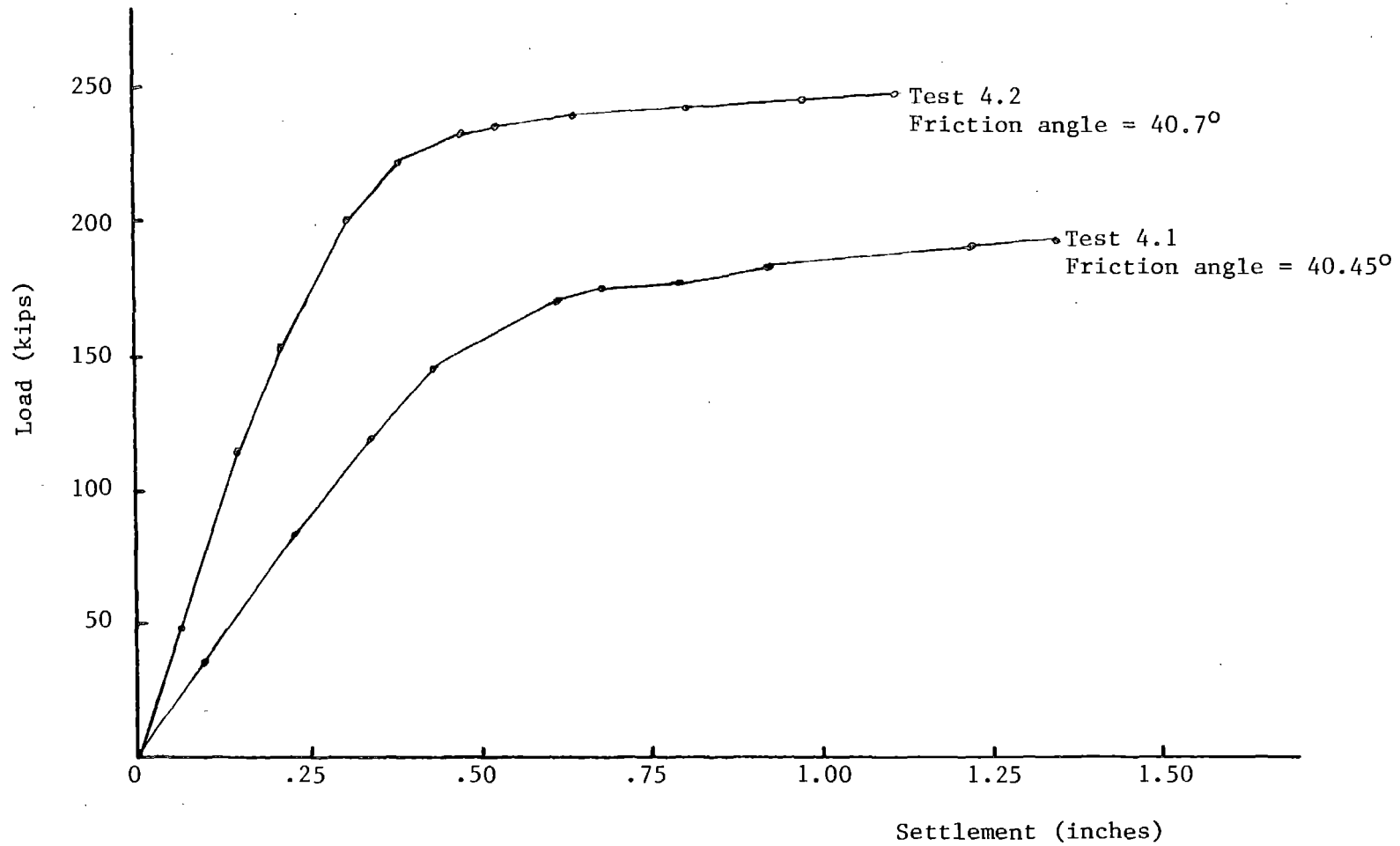


Figure 17. Parametric study load-settlement curves, Tests 4.1 and 4.2 (prototype scale). (1 in. = 2.54 cm, 1 kip = 4.45 kN)

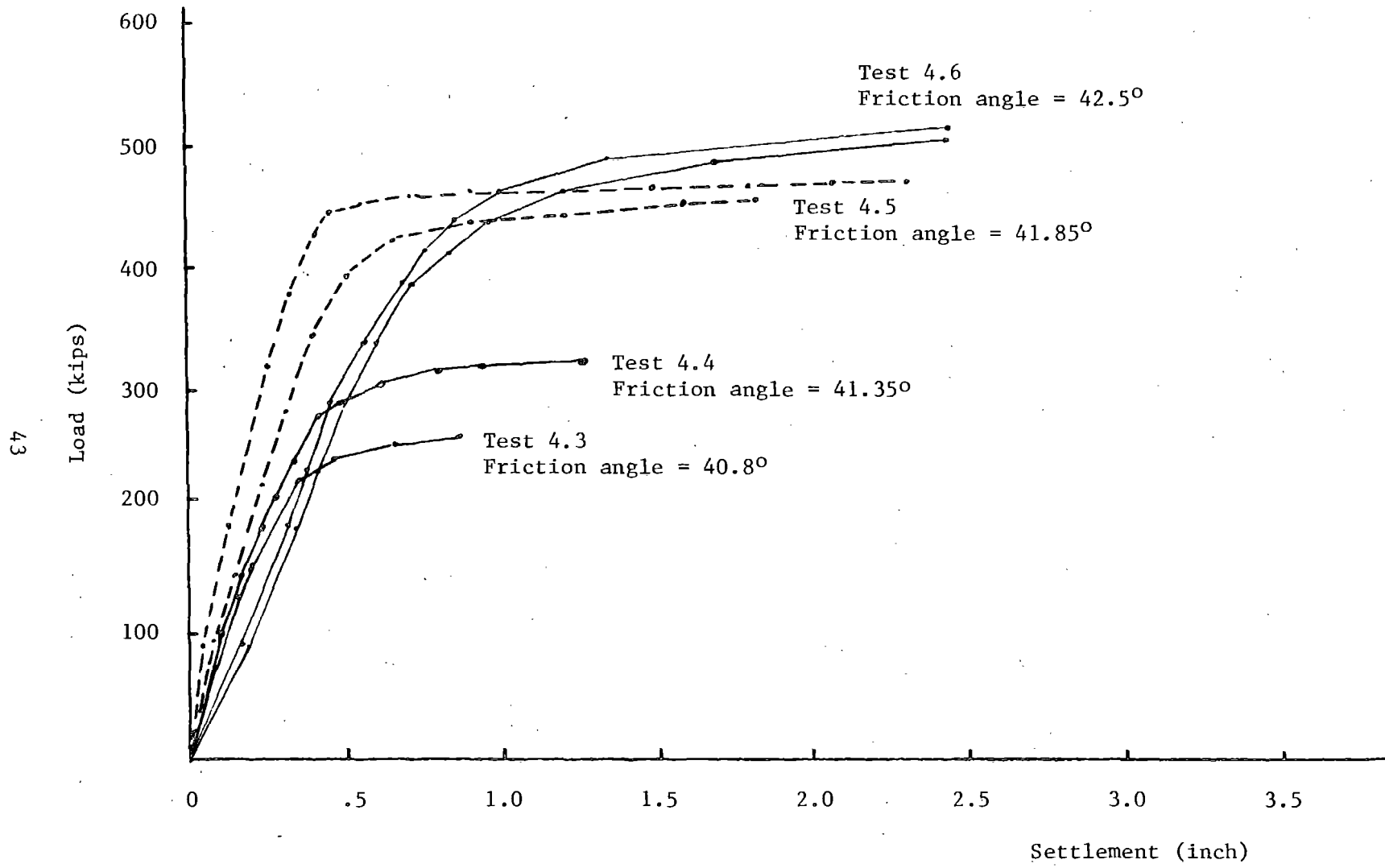


Figure 18. Parametric study load-settlement curves, Tests 4.3, 4.4, 4.5, and 4.6 (prototype scale). (1 in = 2.54 cm, 1 kip = 4.45 kN)

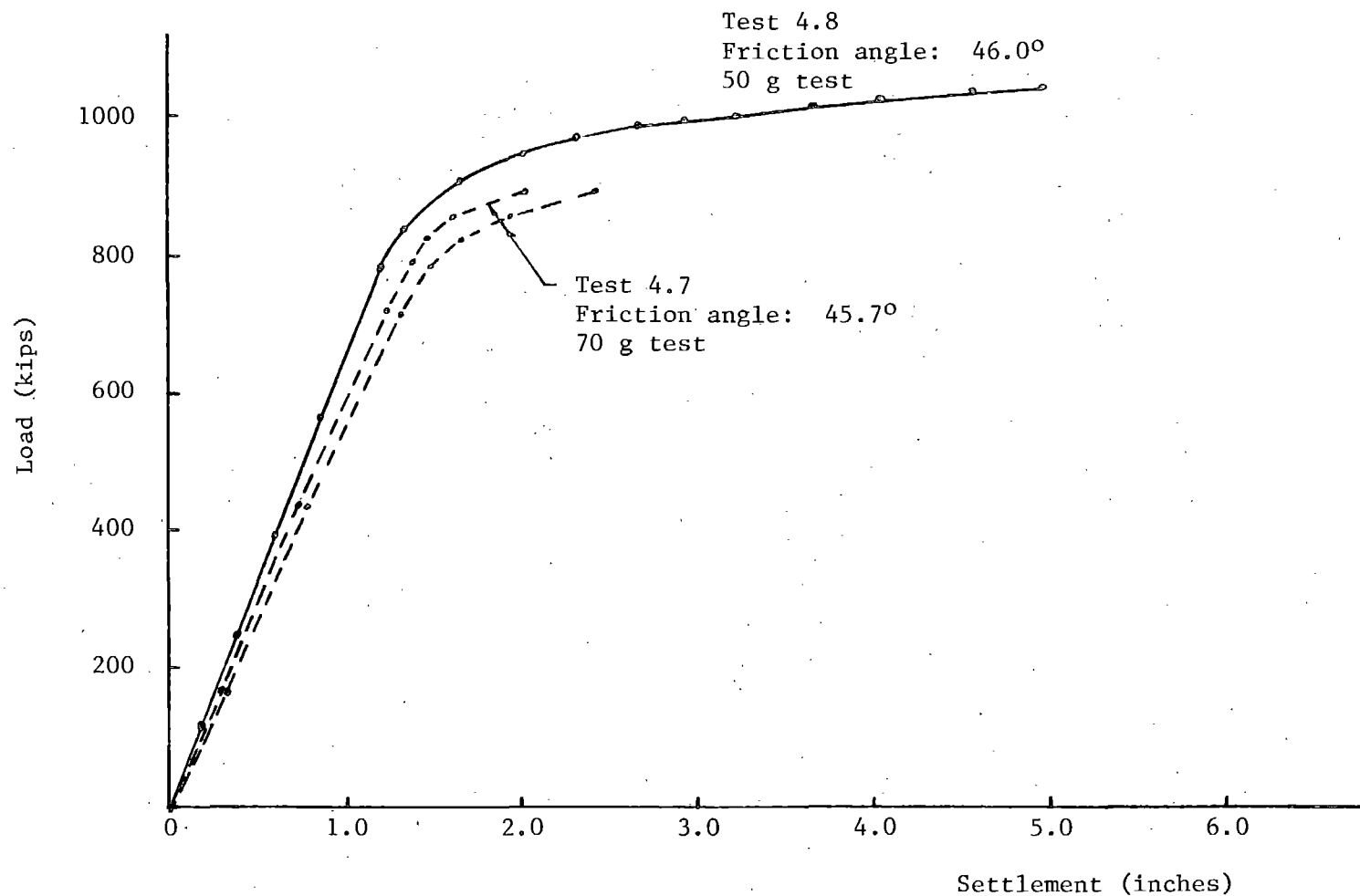


Figure 19. Parametric study load-settlement curves, Tests 4.7 and 4.8 (prototype scale). (1 in = 2.54 cm, 1 kip = 4.45 kN)

this correction was sufficiently large that a different arrangement was adopted for Tests 5.1 and 5.3.

All model piles in these two tests were installed to a depth of 5.2 inches (13.3 cm). The three-piece pile cap (Figure 12) was then clamped to the top of the driven piles. The diameter of the individual pile sockets in this cap was such that after the pile cap was clamped in place the pile tops were considered to be fixed against rotation and displacement relative to the pile cap. Because it was not possible to install the piles so that their tops exactly aligned with the pile sockets in the aluminum pile cap, clamping the pile cap in place resulted in lateral displacement of the pile top and some degree of disturbance from the as-installed state. As described in Chapter 3, the group was pushed into the soil an additional 0.20 inch (0.5 cm) before the load-settlement test was conducted.

The strain gauges installed on the top of the individual wooden piles permitted the driving record of each pile to be recorded as shown in Figures 20 and 21 for Tests 5.2 and 5.4, respectively. Individual pile loads, as well as the total group load as measured by the load cell, were measured during the load-settlement test.

The group load-settlement curves for Tests 5.2 and 5.3 are presented at prototype scale in Figures 22 and 23, respectively. Individual pile loads and the measured group load at ultimate load are presented in Table 6.

Tests 5.1 and 5.3

Two modifications to the equipment were made prior to group tests 5.1 and 5.3. First, the core of the two LVDT's used to measure axial deformation were connected directly to the pile cap to avoid having to subtract the correction for load-cell deformation from the measured settlement data. Secondly, the sockets in the aluminum pile cap were enlarged. This reduced the lateral pile disturbance introduced when assembling the pile cap. This also allowed the top ends of the model piles to rotate during load testing.

Individual piles in these tests were driven to a model depth of 5.95 inches (15.1 cm), the pile cap assembled, and the piles and pile cap were then driven as a group an additional 0.05 inch (0.13 cm) prior to conducting the group load test. This additional driving would correspond to 3.5 inches at prototype scale for the

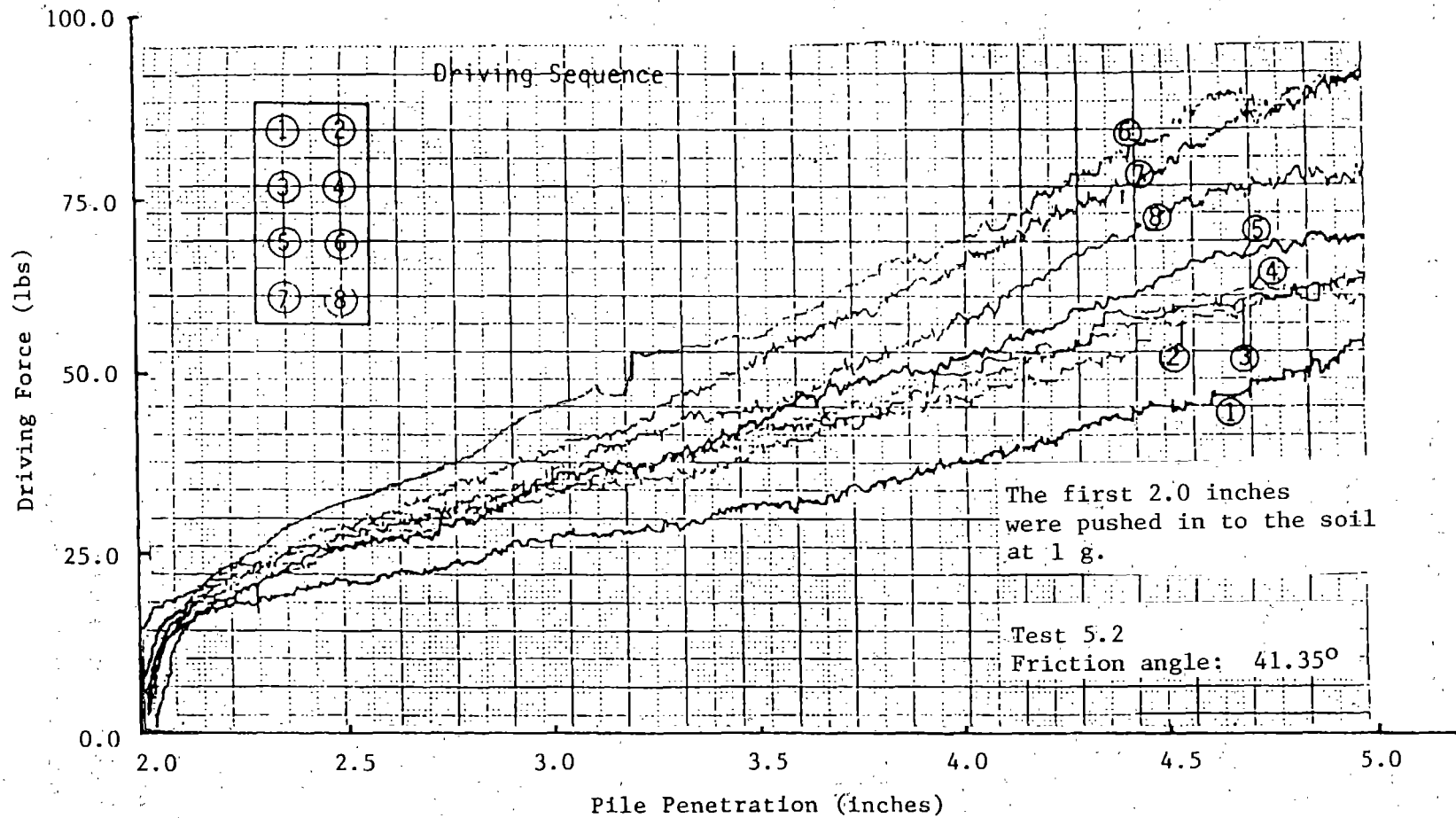


Figure 20. Influence of driving order, Test 5.2 (model scale).
(1 in = 2.54 cm, 1 lb = 4.45 N)

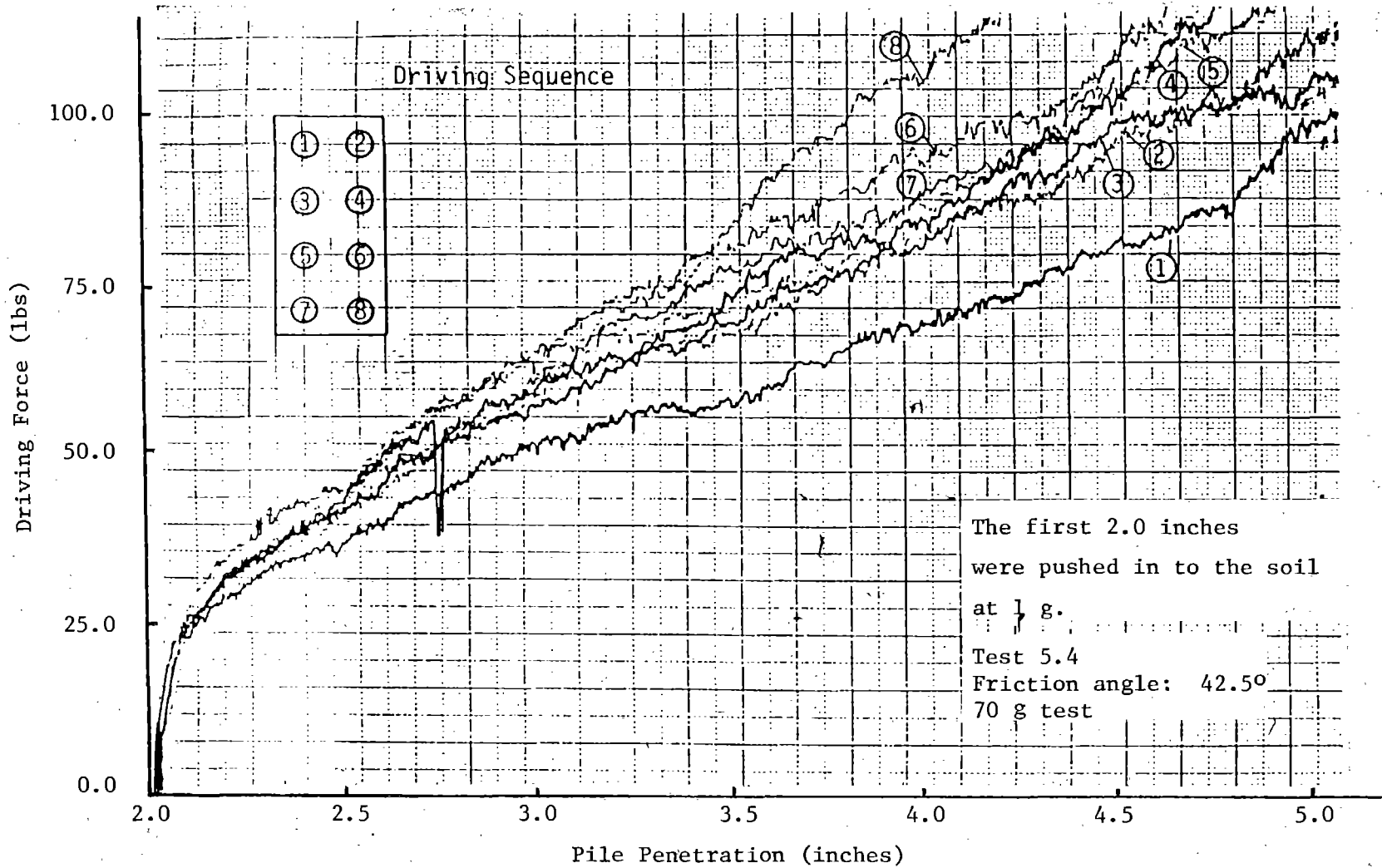


Figure 21. Influence of driving order, Test 5.4 (model scale).
 (1 in = 2.54 cm, 1 lb = 4.45 N)

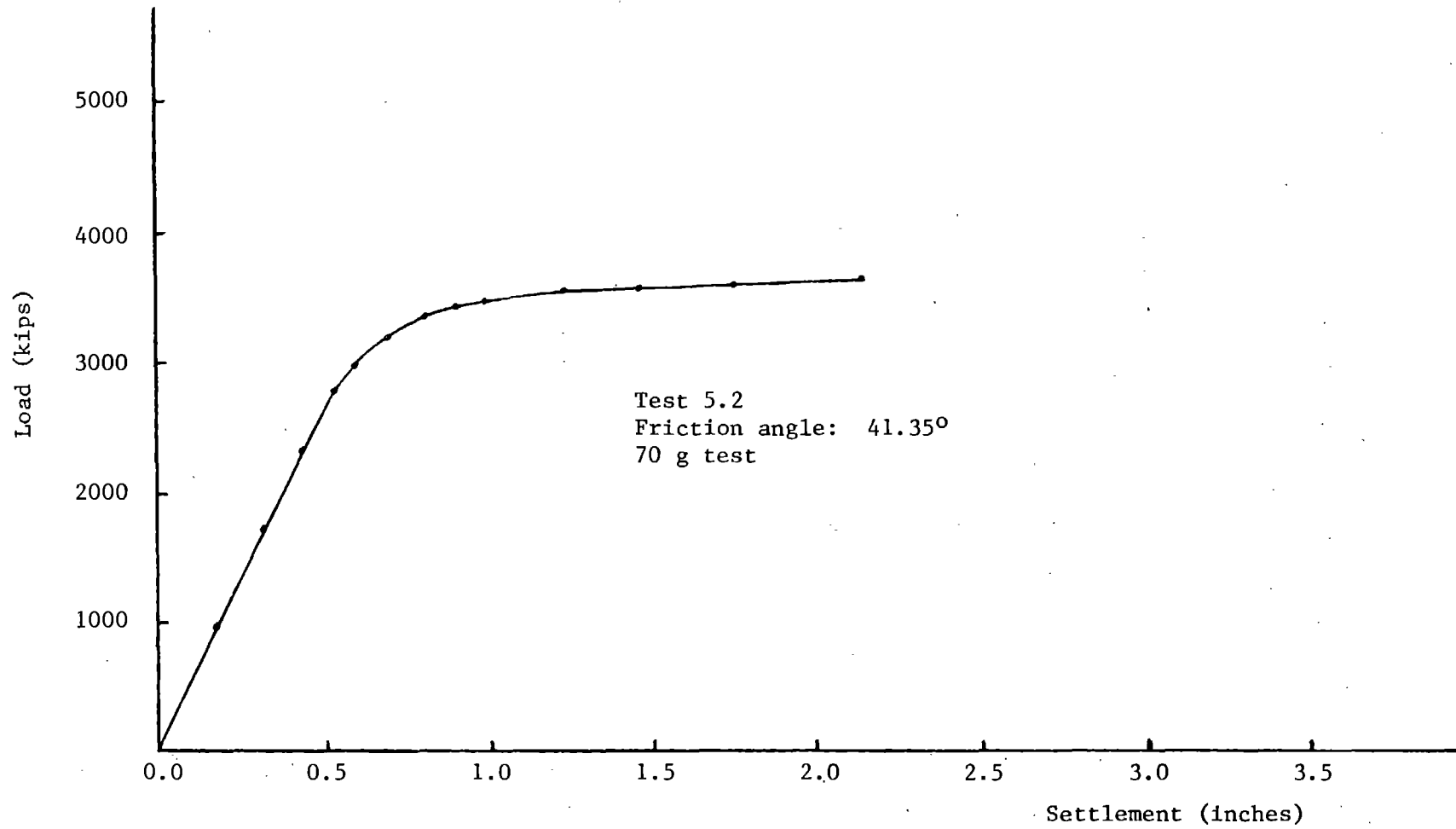


Figure 22. Load-settlement curve, group Test 5.2 (prototype scale).
(1 in = 2.54 cm, 1 kip = 4.45 kN)

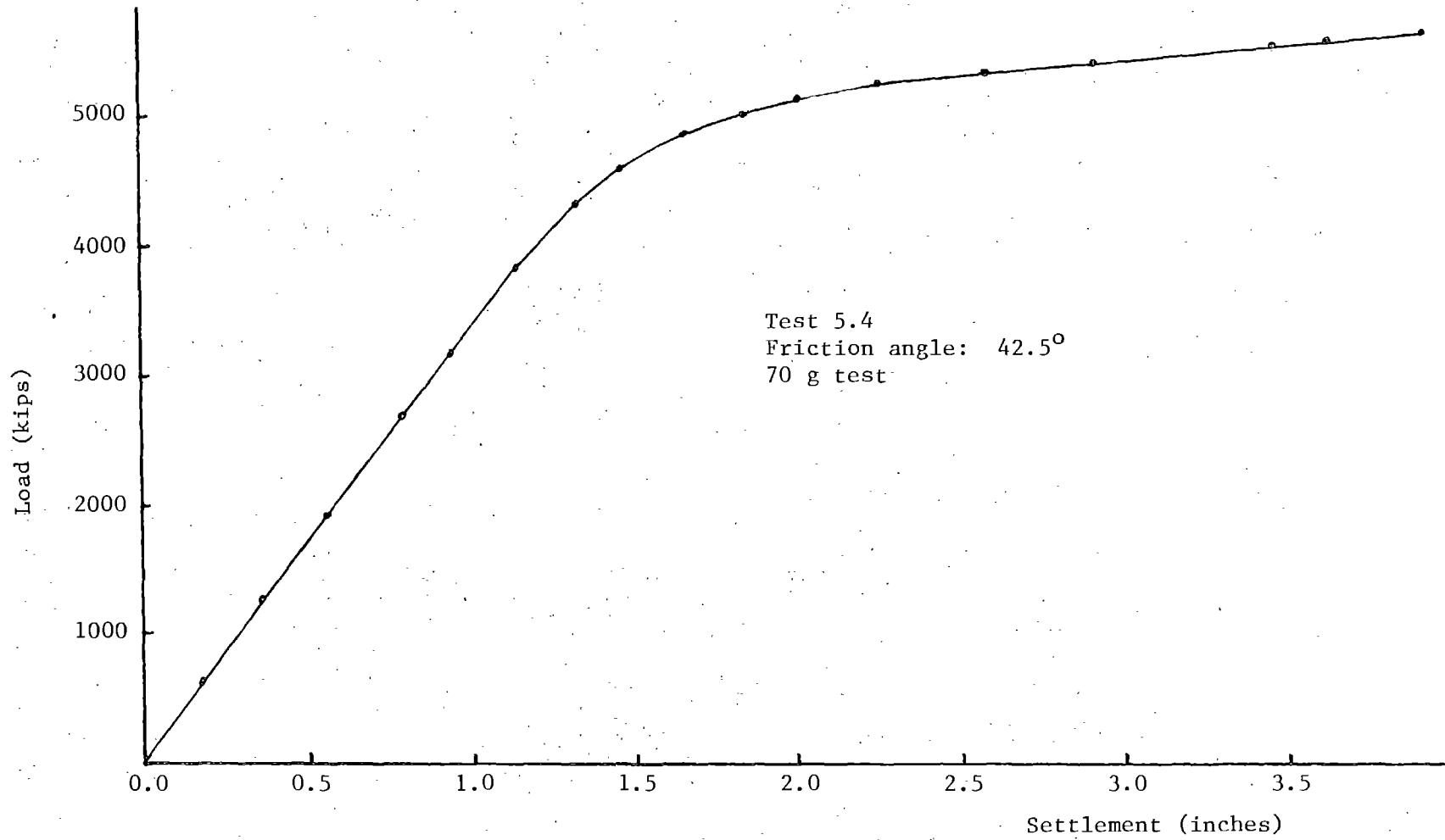


Figure 23. Load-settlement curve, group Test 5.4 (prototype scale).
(1 in = 2.54 cm, 1 kip = 4.45 kN)

Table 6. Group Test Data, Sand

Individual Pile Capacities (lbs)				
Pile No.	Test 5.1	Test 7.1	Test 5.2	Test 5.4
1	54.7	57.6	57.1	102.4
2	67.1	59.1	72.8	103.0
3	69.2	60.2	74.4	114.9
4	70.8	*	73.6	114.9
5	*	58.4	75.6	144.4
6	76.6	63.5	82.4	114.2
7	70.8	58.6	72.8	142.6
8	77.0	64.0	80.8	113.5
Total load from individual piles	-	-	589	952
Total load from load cell	550	482	600	1016

* Gages did not work

Note: Weight of the cap not included

Scale: 1/70

All pile capacities reported at model scale
1 lb = 4.45 N

1/70 scale used for these models.

Load-settlement curves from Tests 5.1 and 5.3 are shown in Figures 24 and 25, respectively, and ultimate load data is presented in Table 6.

Test Series 6: Tapered vs Straight Pile

Three tests were performed on straight wooden piles. The piles had the same diameter as the mid-height diameter of the 1/70 scale tapered piles. Results are shown in Figure 26. For tests 6.2 and 6.3 companion tests on tapered wooden piles tested at the same time in the same soil sample are also shown.

Test Series 7: Saturated Tests

Two tests were conducted under saturated conditions to investigate the effect that soil saturation would have on pile behavior. Test 7.1 was conducted on the pile group of Test 5.1 after the initial group test (5.1) in the dry sand. The soil was saturated as described in Chapter 2 and another test conducted at 70 g acceleration on the pile group in the saturated soil. The load-settlement curve is presented in Figure 27, and individual pile and pile group results at ultimate load are presented in Table 6. After Test No. 7.1 was completed the water level in the test container was observed to be 0.89 inch (2.26 cm) below the soil surface. This water was believed lost during centrifuge spin-up when gravity was not exactly perpendicular to the soil surface.

Test No. 7.2 was conducted on a 1/70 scale single pile. A single pile was first driven and load-tested under dry conditions. The test container was then saturated and another single pile was driven and tested under saturated conditions. The water level prior to the start of the saturated test was 1.1 inch (2.87 cm) above the soil surface. After the test the water level was 0.1 inch (.25 cm) above the soil surface. The load-settlement curves from these tests are shown in Figure 28.

Test Series 8: Lateral Load Tests

Four lateral load tests were conducted on 1/70 scale piles following test procedures described in Chapter 3. Load-deflection curves from these tests are presented in Figures 29 to 32.

Test Series 9: Aluminum Pile Test

To obtain load transfer data for use in the computer analysis, a test on a strain-gaged straight aluminum pile was performed. The position of the strain

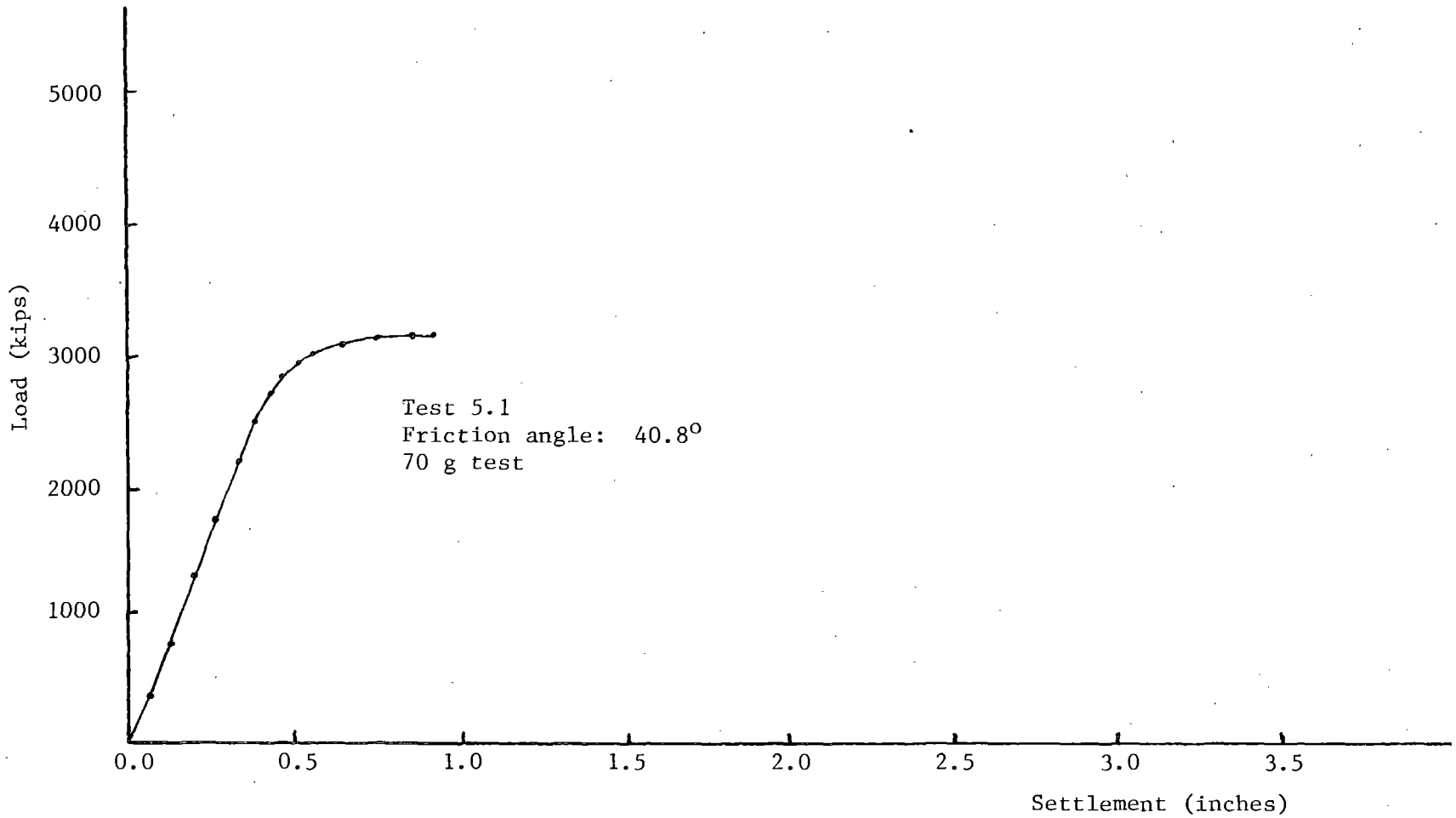


Figure 24. Load-settlement curve, group Test 5.1 (prototype scale).
(1 in = 2.54 cm, 1 kip = 4.45 kN)

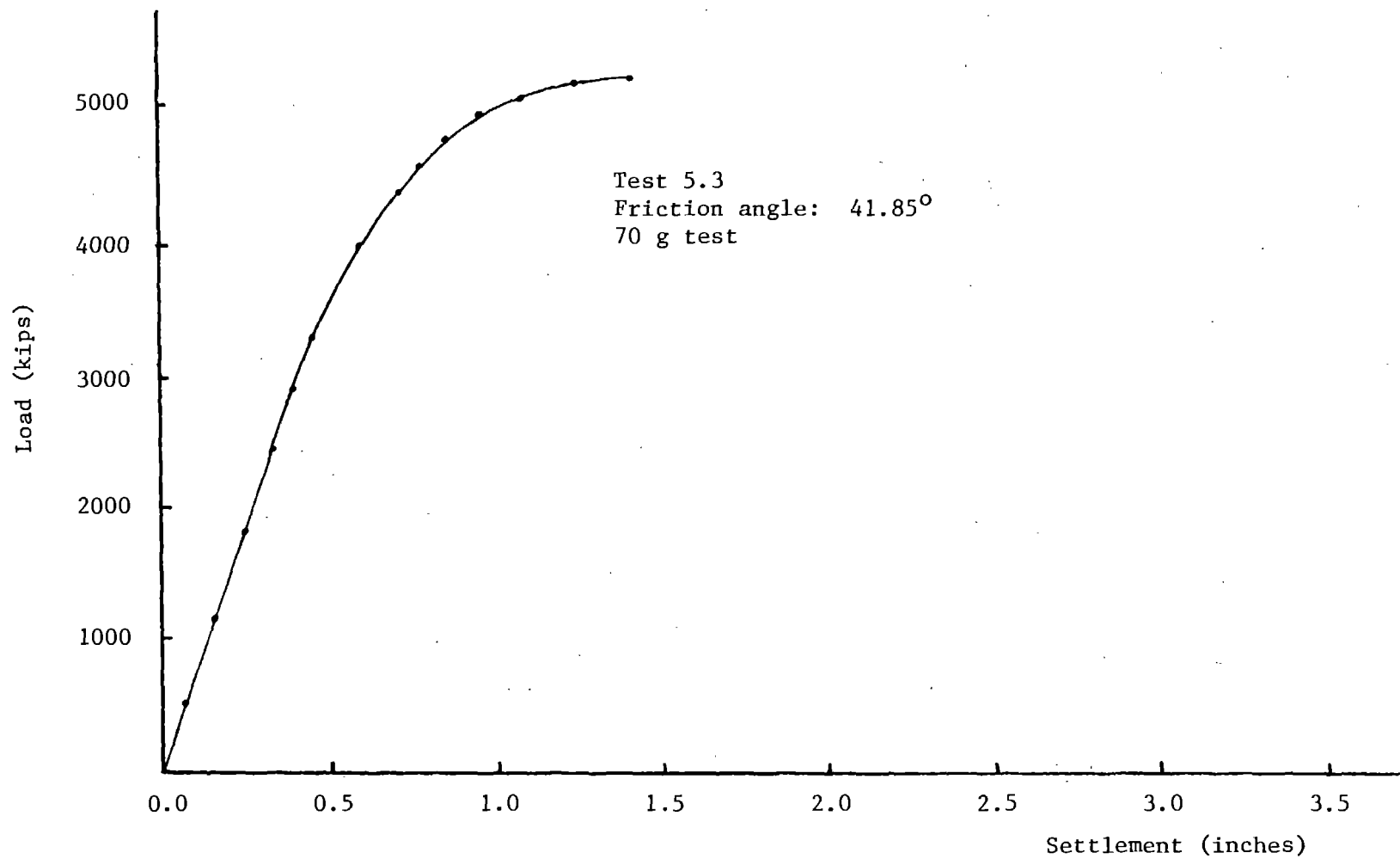


Figure 25. Load-settlement curve, group Test 5.3 (prototype scale).
(1 in = 2.54 cm, 1 kip = 4.45 kN)

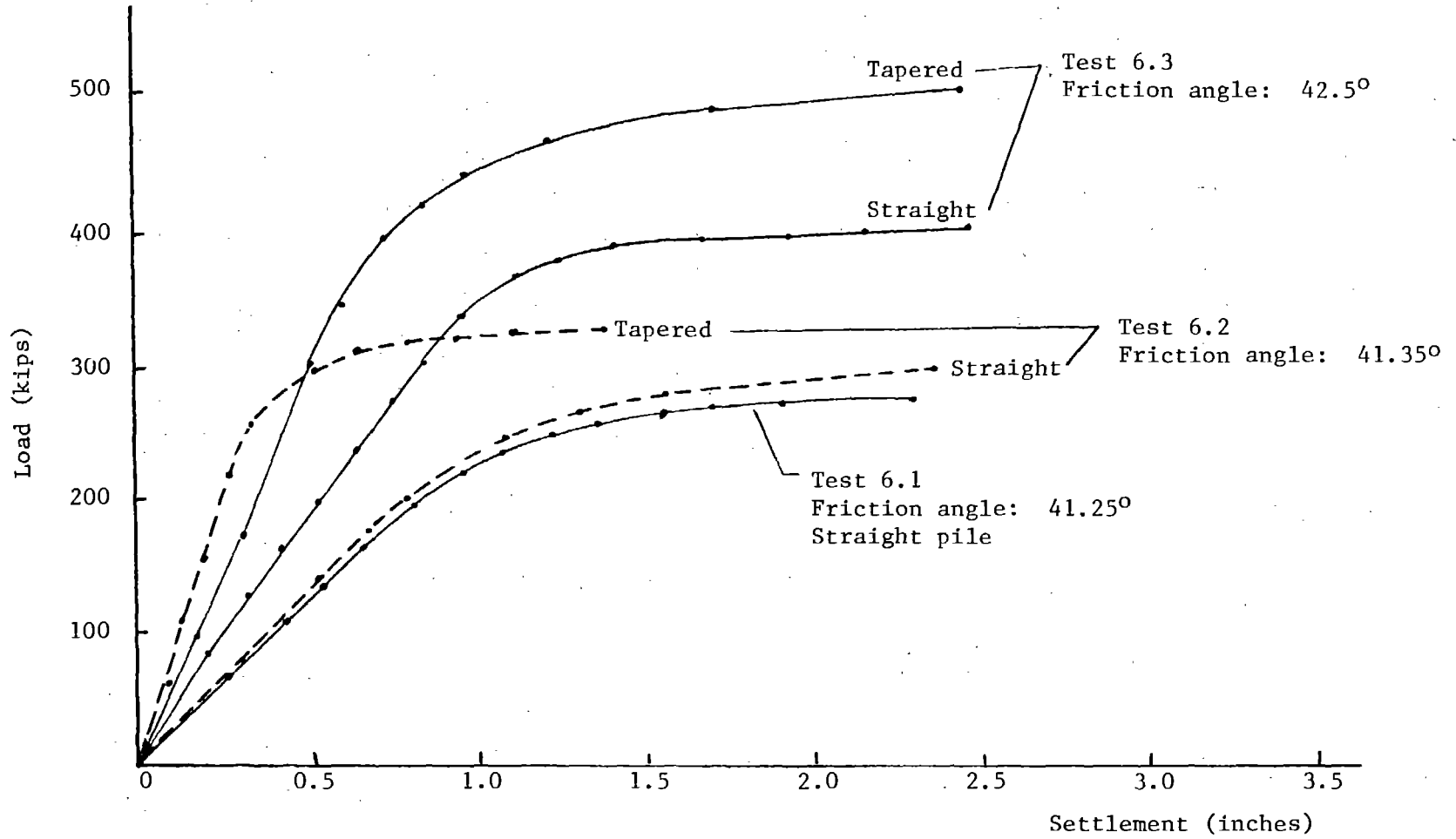


Figure 26. Tapered versus straight pile response (prototype scale).
(1 in = 2.54 cm, 1 kip = 4.45 kN)

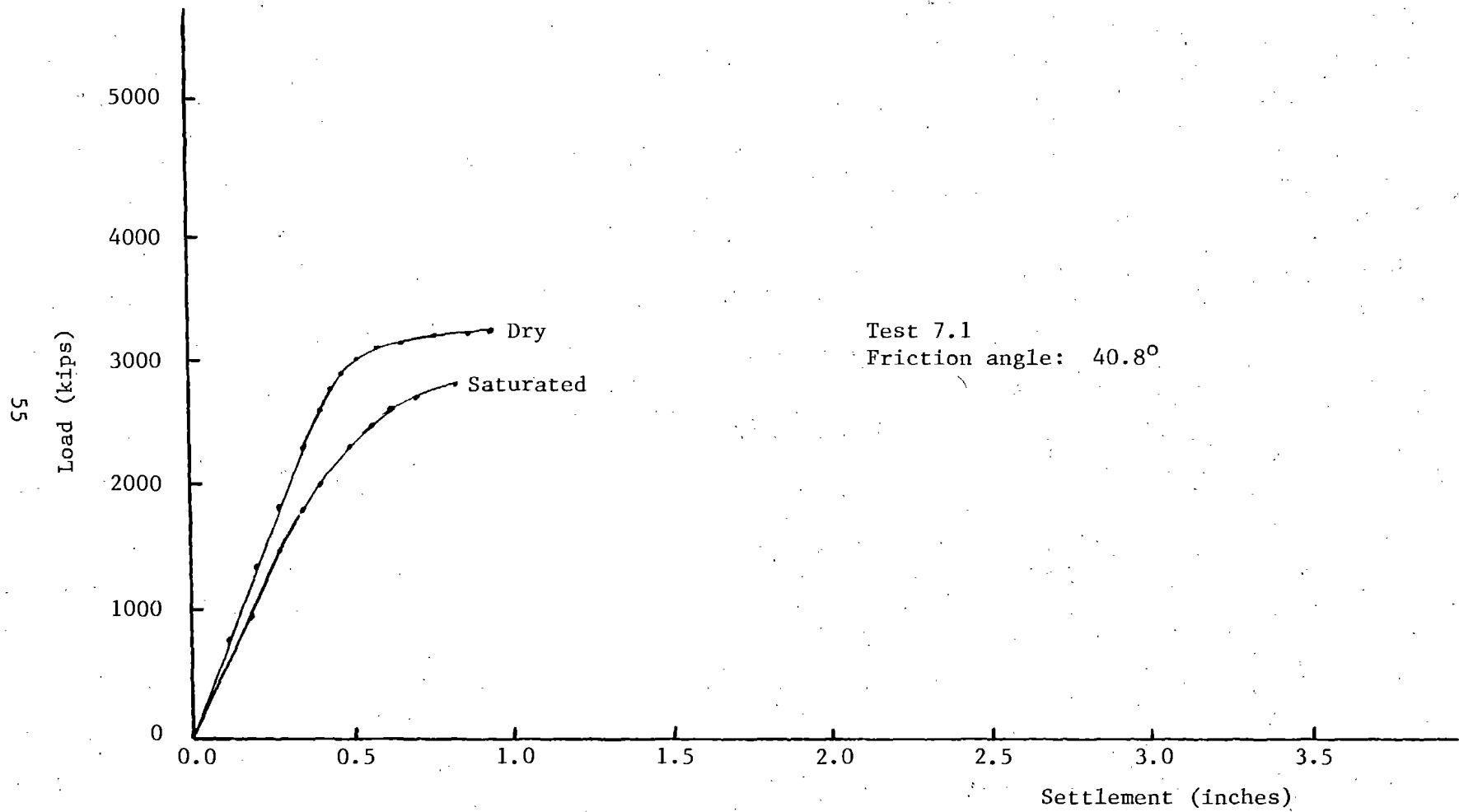


Figure 27. Saturated versus dry pile group test (prototype scale).
 (1 in = 2.54 cm, 1 kip = 4.45 kN)

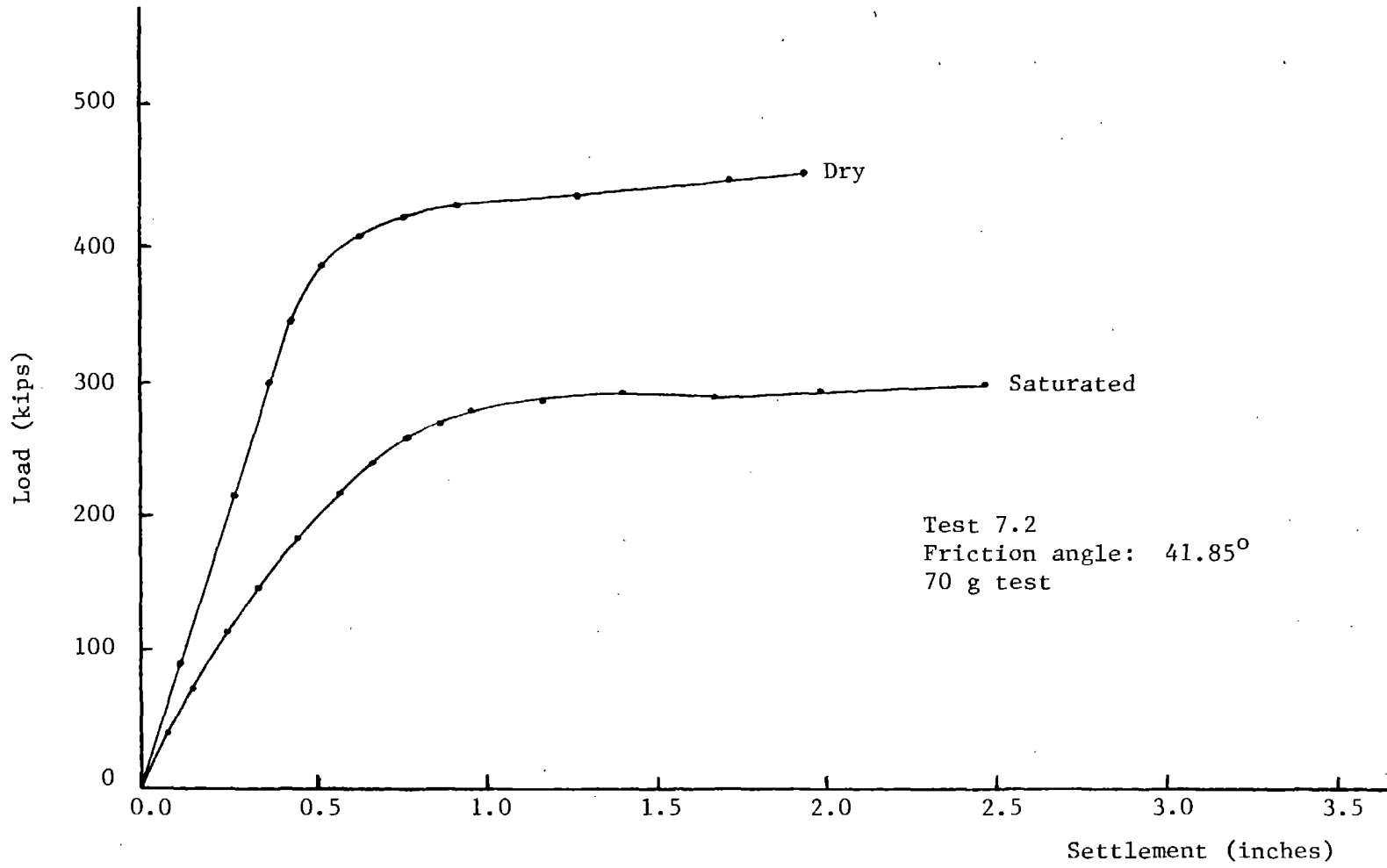


Figure 28. Saturated versus dry single pile test (prototype scale).
(1 in = 2.54 cm, 1 kip = 4.45 kN)

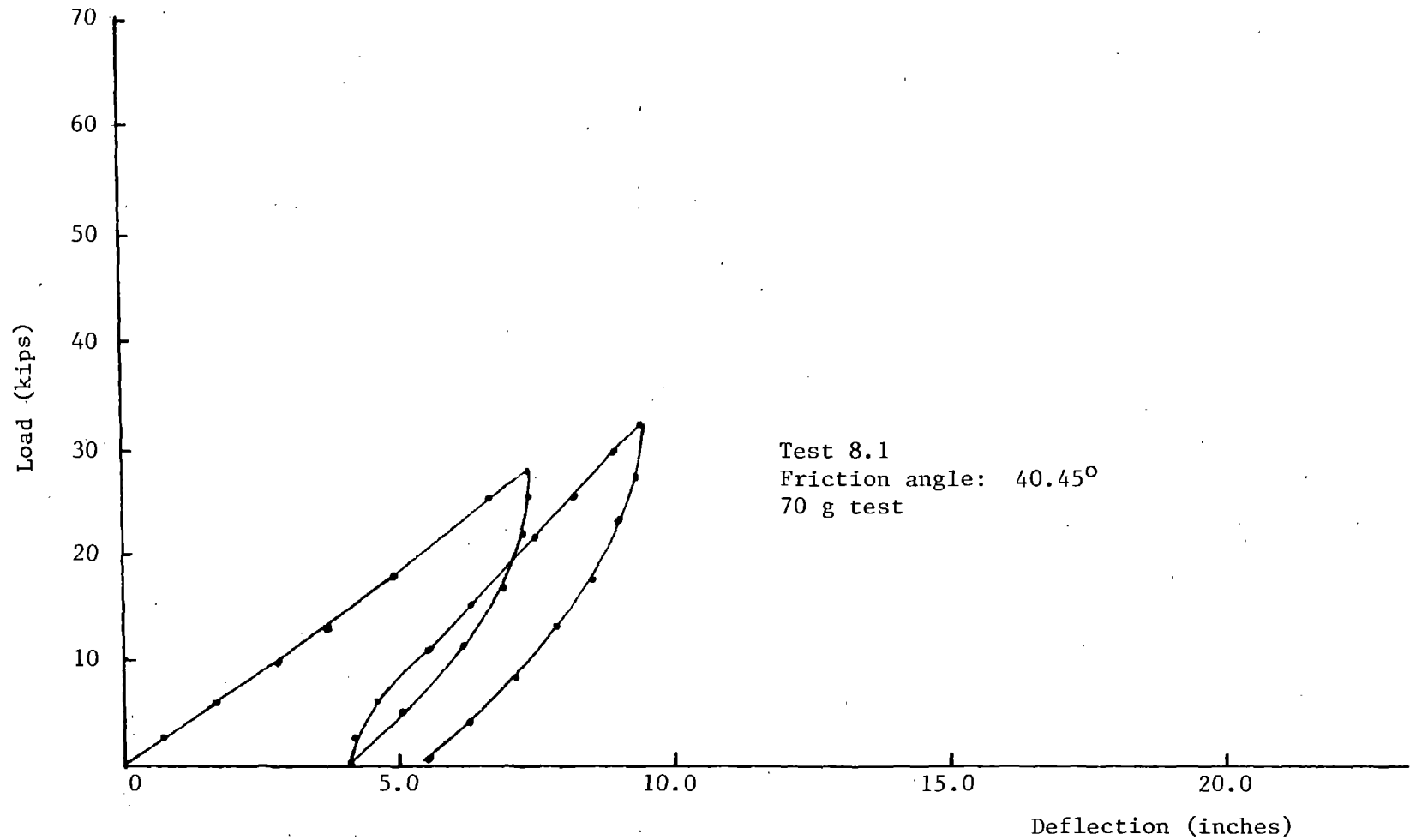


Figure 29. Lateral load Test 8.1 (prototype scale).
(1 in = 2.54 cm, 1 kip = 4.45 kN)

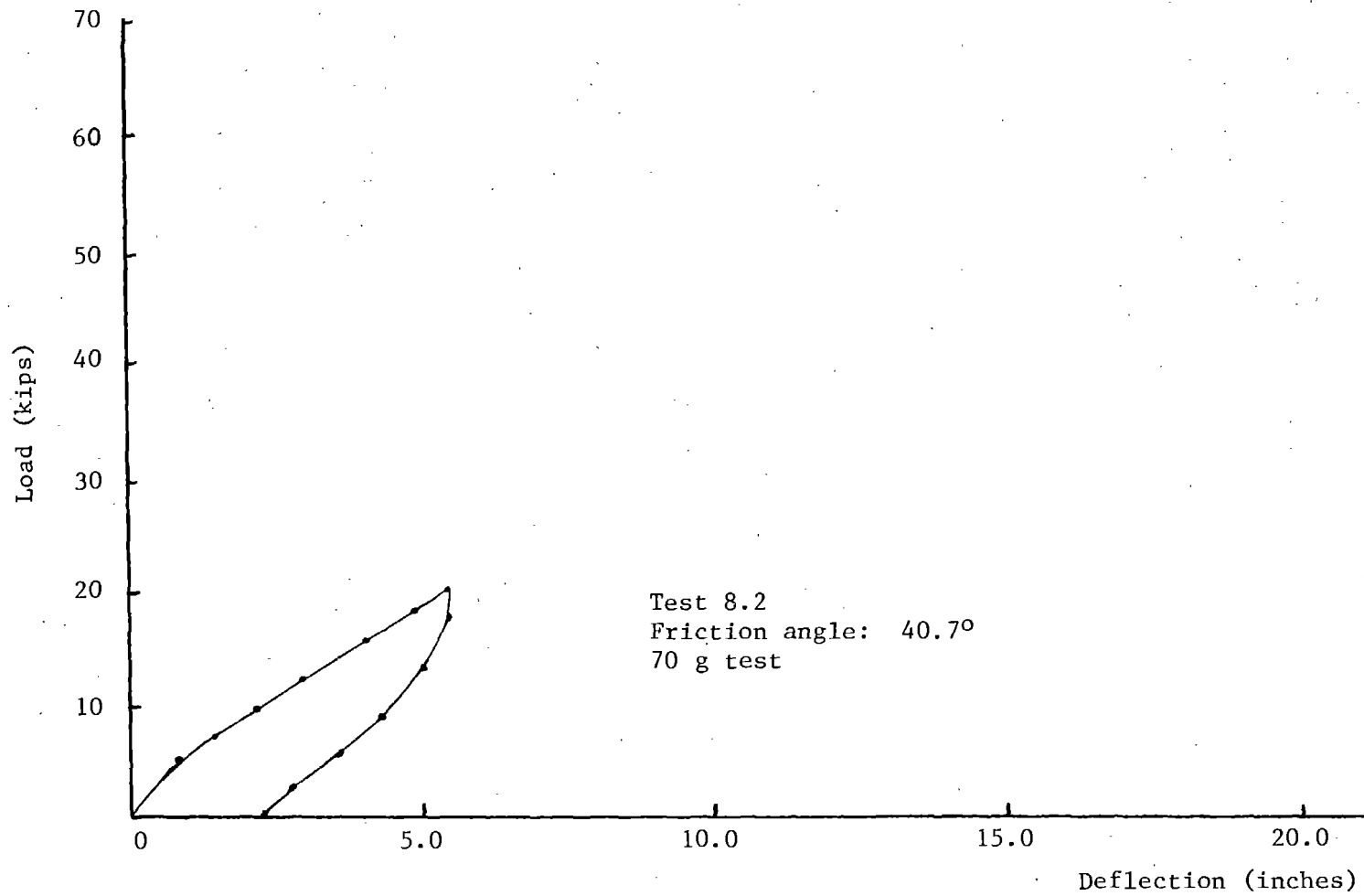


Figure 30. Lateral load Test 8.2 (prototype scale).
(1 in = 2.54 cm, 1 kip = 4.45 kN)

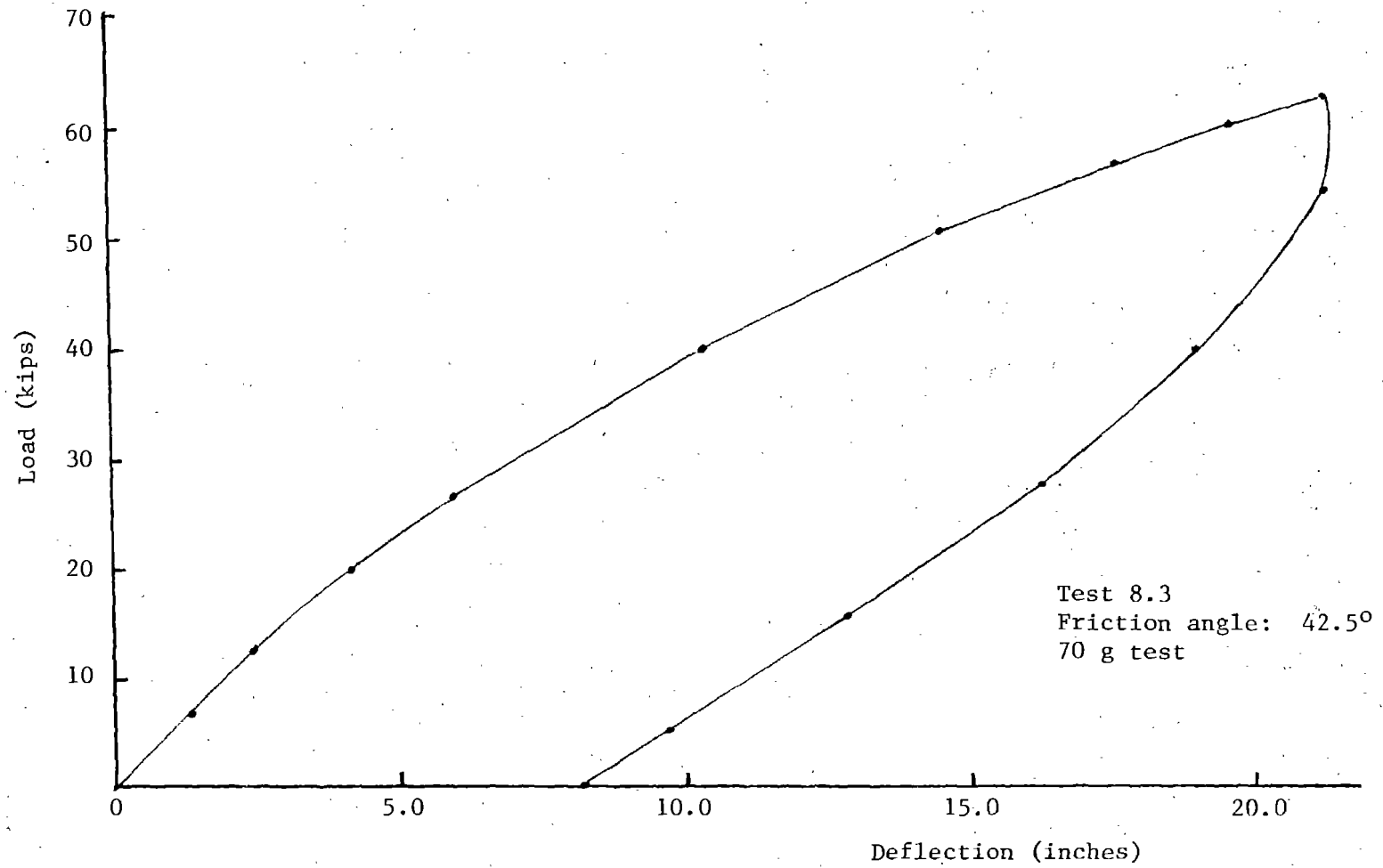


Figure 31. Lateral load Test 8.3 (prototype scale).
(1 in = 2.54 cm, 1 kip = 4.45 kN)

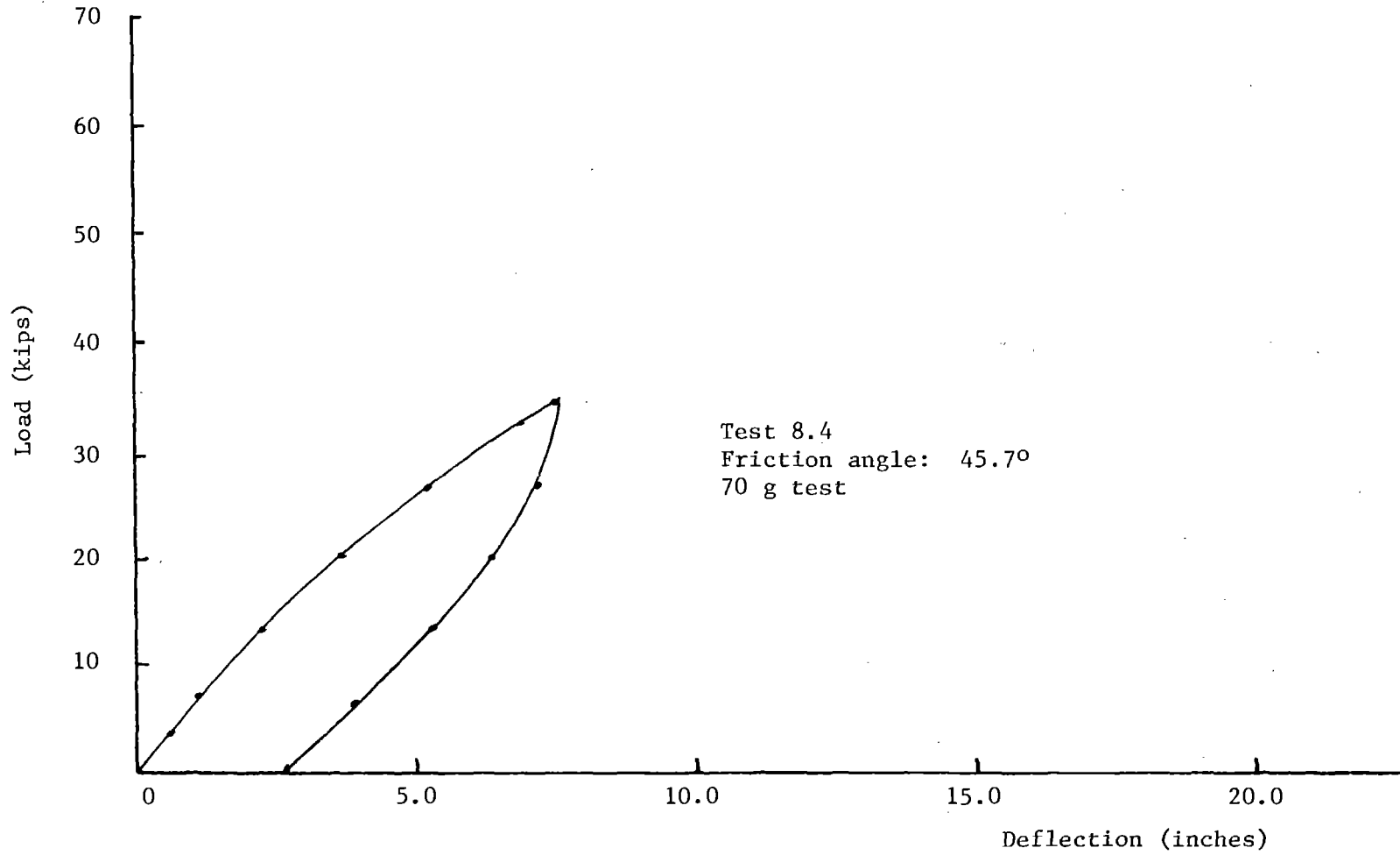
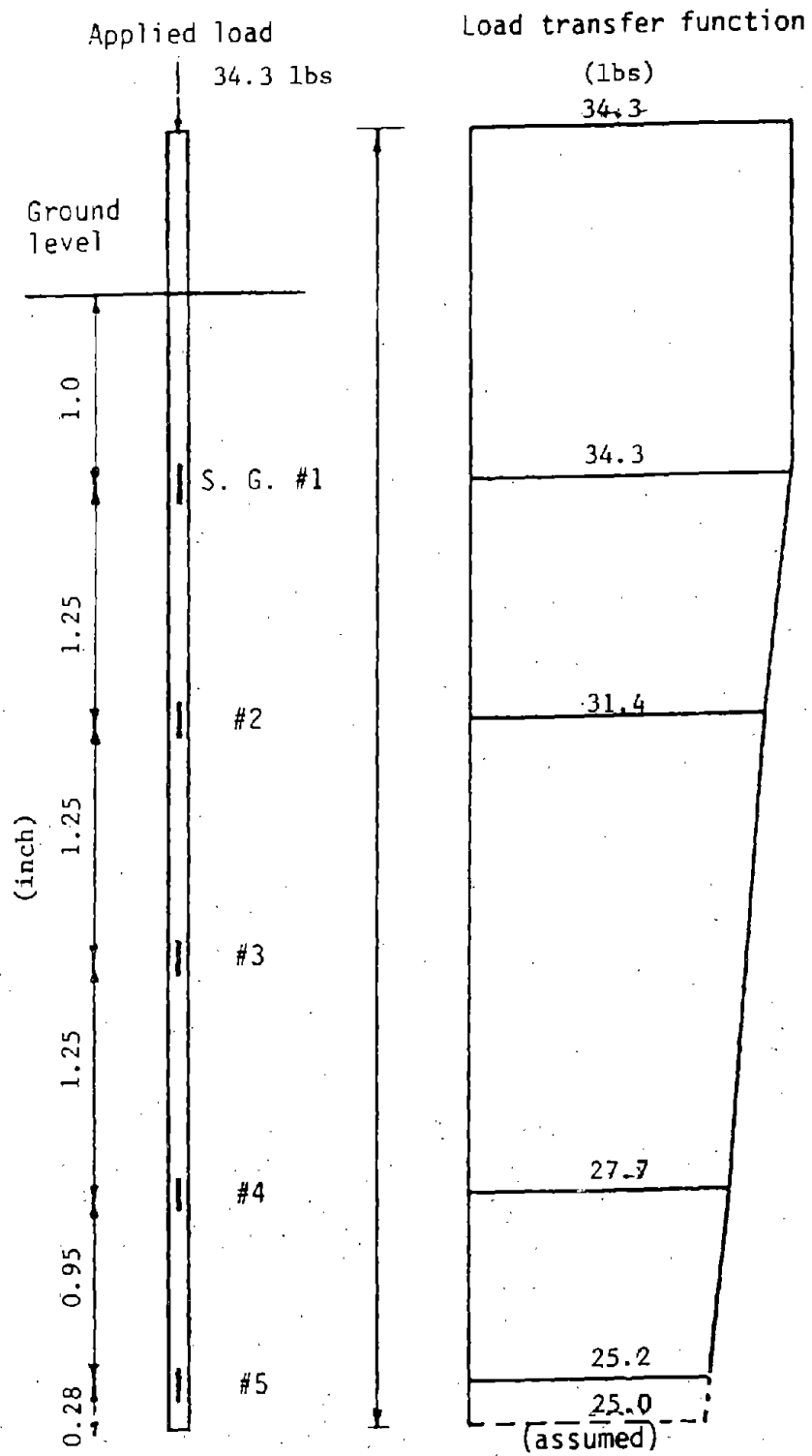


Figure 32. Lateral load Test 8.4 (prototype scale).
(1 in = 2.54 cm, 1 kip = 4.45 kN)

gages and the load transfer curve are shown in Figure 33. The load-settlement curve is shown in Figure 34.



Note: 1" = 2.54 cm
 1 lb = 4.45 N

Tip resistance: 73%
 Skin friction: 27%

Figure 33. Load-transfer curve, aluminum pile in sand.

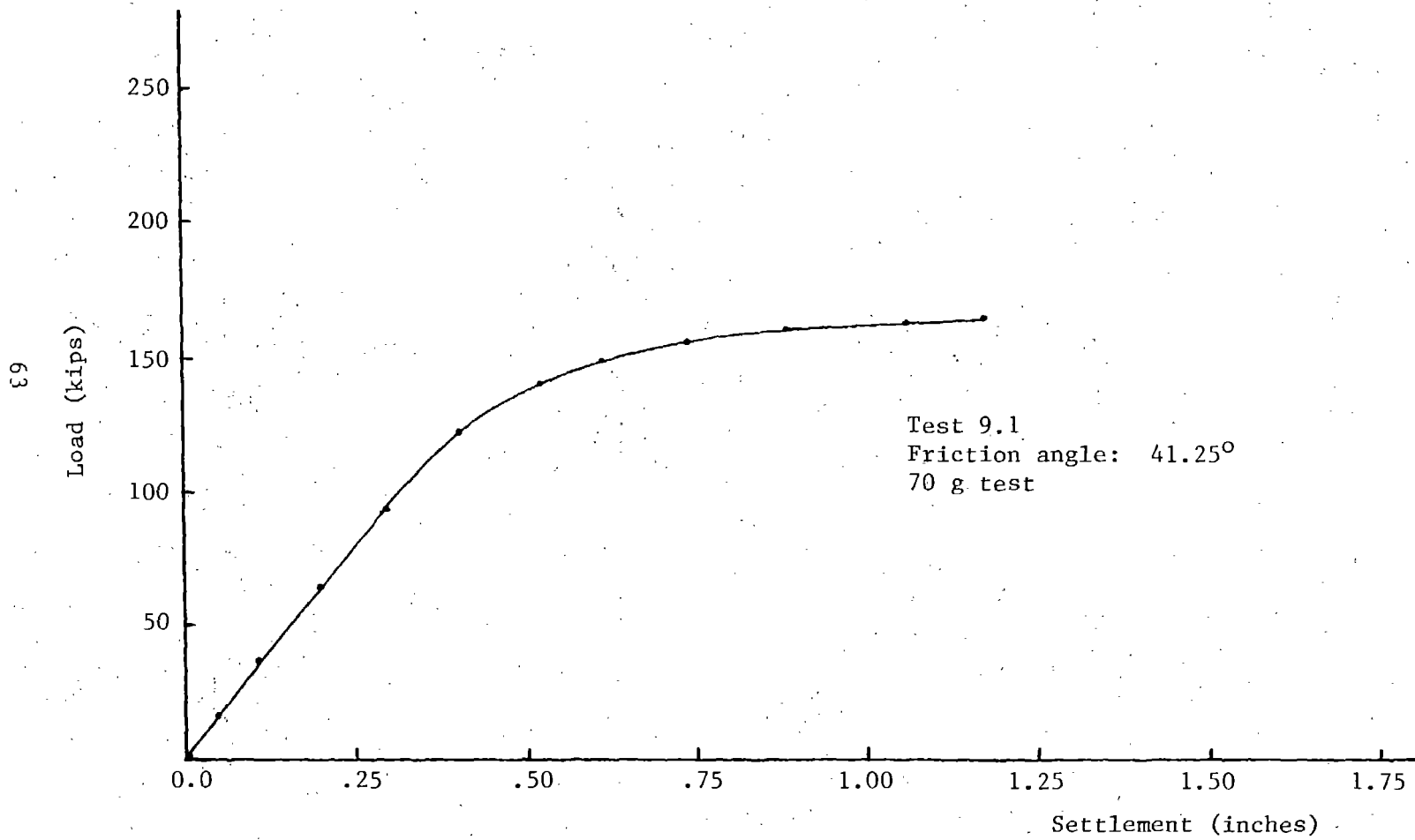


Figure 34. Load-settlement curve, aluminum pile (prototype scale).
(1 in = 2.54 cm, 1 kip = 4.45 kN)

CHAPTER 5. ANALYSIS OF DATA

5.1 Introduction

In this chapter the data presented in Chapter 4 is analyzed and discussed. Where possible, conclusions are drawn from the data. In other cases the need for additional research and testing is pointed out.

5.2 Test Series 1: Effect of In-flight Installation vs. 1 g Installation

From the results shown in Figures 13 and 14, it is seen that a substantial difference in pile capacity exists between the two methods of installation. In both figures, the pile that was installed and tested at high g showed a much higher capacity than the one installed at 1 g and then tested at high 8. These results show that it is important to have proper simulation of the stress field not only during loading but also during installation. As a result of this conclusion, all piles installed in the remainder of this study were driven under the gravity condition appropriate to the model scale.

It is speculated that the observed difference in capacity reflects the extent of soil disturbance produced by pile installation.

Comparison of the results of the 50 g (Figure 13) and 70 g test (Figure 14) suggests that the degree of disturbance in sand may be scale related with less disturbance occurring as the size ratio of prototype to model decreases. Additional tests over a broad scale range would be required to verify this suggestion. These tests would have significance for model pile tests in sand conducted at 1 g.

5.3 Test Series 2: Effect of Interruption Between Installation and Load Testing

From the results shown in Figure 15 it is seen that there is essentially no difference in the load-settlement curves between the two tests. It is concluded that stopping the centrifuge will have no effect on the subsequent performance of the pile embedded in sand.

5.4 Test Series 3: Modeling of Models

The load-settlement curves of the six tests conducted at 50-g, 70-g and 100-g gravity level in the same soil ($\phi = 42.5^\circ$) were replotted at prototype scale in Figure 35. All curves, except for one 50 g curve which is slightly off, plot in a

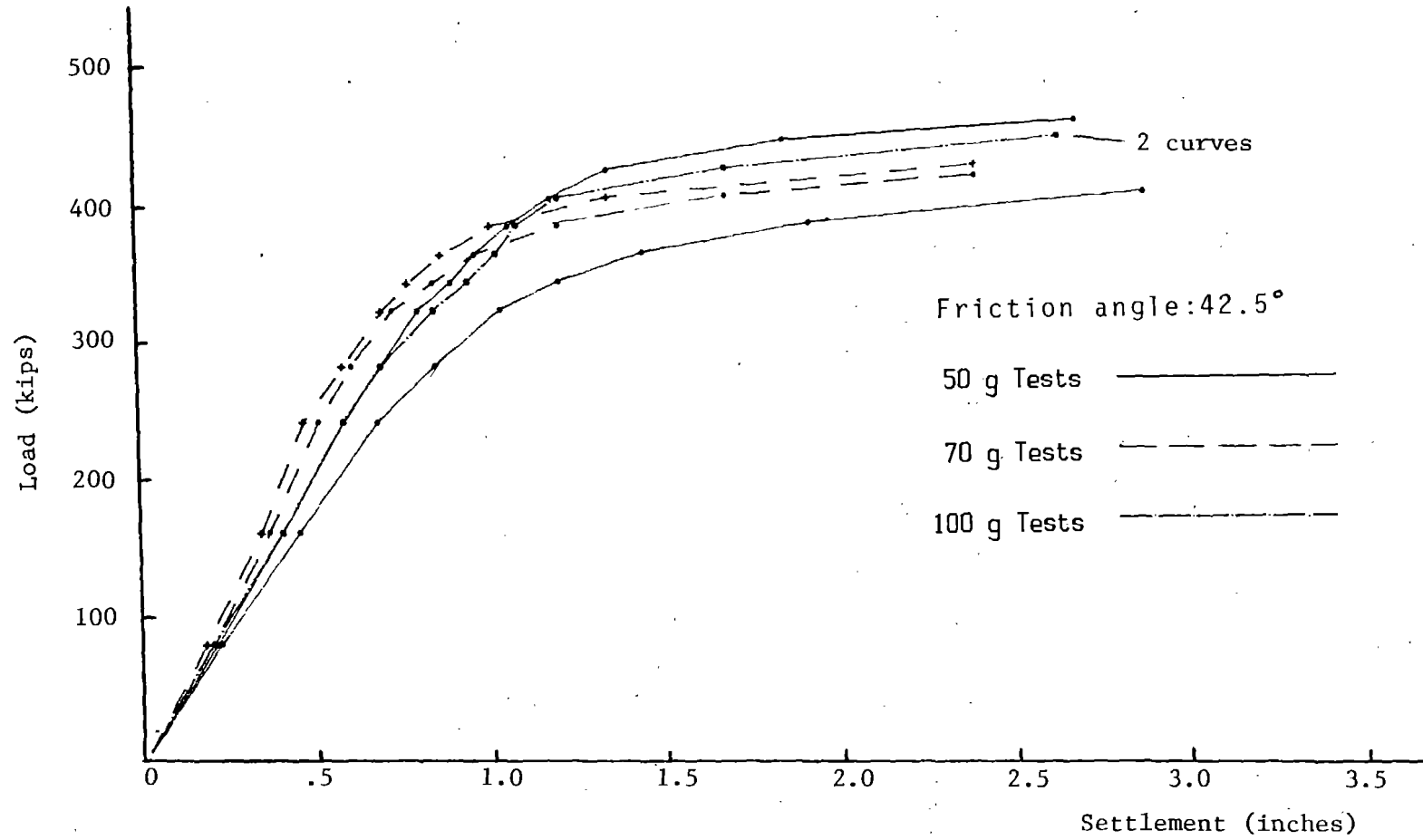


Figure 35. Load-settlement curves from 'modeling of models' test series (prototype scale). (1 in = 2.54 cm, 1 kip = 4.45 kN)

tight band. This result proves the internal consistency of the model pile test results and verifies the similitude theory and testing procedures employed in this study at least over a scale range from 50 to 100.

The results of this modeling of models experiment provides the basis for plotting and comparing at the prototype scale the results of model tests in the centrifuge. The results also permit one to extend the model range to prototype and to extrapolate model test data to prototype scale and to compare this with the field test results as discussed in Chapter 6.

5.5 Test Series 4: Parametric Study

From the results shown in Figures 17 through 19, it is seen that the ultimate load capacity increases as the soil gets denser. These ultimate load capacities are plotted versus the soil's friction angle in Figure 36 where a linear least-squares curve was fitted to these data. Most of the points fall close to this line suggesting that the ultimate load increased linearly with the increase of the soil's friction angle for the range of 40 to 46 degrees.

Except for test 4.1, which was carried out on the loosest uniform soil achievable, all the tests have almost identical initial slopes for their load-settlement curves. Thus the results of this Test Series 4 indicate a strong dependence of pile ultimate load with sand density but little or no dependence of the initial slope of the load-settlement curve on density.

Two causes for the insensitivity of the slope of the initial load-settlement curve can be advanced. First, the modulus of the sand used in these tests increased by only 15 percent as the relative density increased from 36.0 percent for a ϕ of 40.45° to 65.6 percent for a ϕ of 42.8°. Secondly, the installation of the pile by the steady jacking force likely created a zone of disturbed soil adjacent to the pile. The disturbance produced by the pile installation probably affected the structure of the sand for a distance of approximately one diameter around the pile circumference as shown by Vesic (1977) for dense sand. The method of pile installation, i.e., a steady jacking force vs. dynamic repeated blows, could affect the nature and extent of soil disturbance. This, however, needs to be investigated by a specific study of pile installation procedures.

5.6 Test Series 5: Group Tests

The group tests will be analyzed for four different behavior characteristics. These are detailed in the following sections.

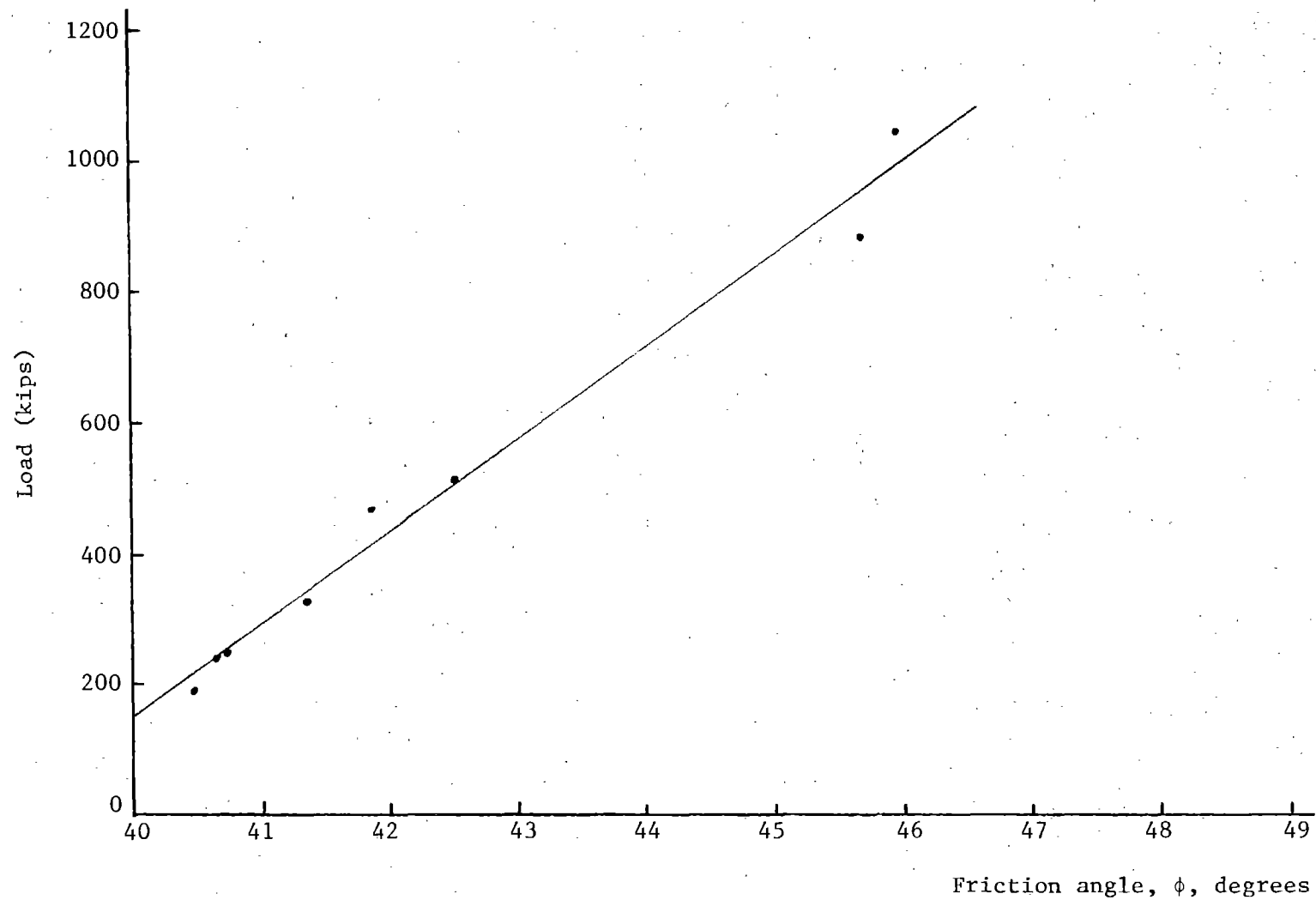


Figure 36. Ultimate load versus friction angle (prototype scale),
(1 kip = 4.45 kN)

5.6.1 Driving Records

The driving records are available only for tests 5.2 and 5.4 which are shown in Figures 20 and 21, respectively. In both tests the effect of driving order is clearly seen. In test 5.2, pile No. 2 required 20% more installation force than pile No. 1 while this difference was 16% for test 5.4. The denser soil in test 5.4 may have resulted in less densification due to installation of pile No. 1.

The increase in driving force continued up to the 7th pile, which required less installation force than pile No. 6. Pile No. 8 in test 5.2 required less installation force than pile No. 7, but in test 5.4 pile No. 8 required more installation force than any other pile. This may be the result of a change in the driving rate which is suspected because of the sudden jump in the driving force at 3.5 inches (8.9 cm) of installation.

5.6.2 Individual Pile Loads in the Group at Failure

This information is available from tests 5.1, 5.2, and 5.4 as shown in Table 6. Although in all three tests pile No. 1 had less load at failure than the other piles, the influence of driving order is not obvious. Good correlation is observed between the total load measured from the load cell and the sum of the loads measured by the strain gages installed on the individual piles, thus verifying the accuracy of the load measurement instrumentation.

5.6.3 Ultimate Load and Efficiency

The ultimate loads for these tests are shown in Table 5. It is seen that as the soil gets denser the ultimate load increases as should be expected.

The group efficiency was calculated as the ratio of the group load at failure divided the number of piles in the group to the load at failure of a single isolated pile test. The single pile test results are reported in Series 4, Parametric Study, and are from single pile tests conducted on the same soil as the corresponding group test. The efficiency for the loosest soil, test 5.1, was 1.3 while the measured efficiency for the other three tests was 1.1.

5.6.4 Slope of the Load-Settlement Curves

Load-settlement curves from the four tests are shown in Figures 22, 23, 24, and 25. In order to compare these results to the single pile test results, the

load-settlement curves from tests 5.1 and 5.3 were redrawn with the loads divided by the number of piles in the group. They are shown in Figures 37 and 38, respectively. In both cases the slope of the initial portion of the load-settlement curve for the group tests is slightly less than the single pile tests. This may be a result of the stress field produced by adjacent piles causing additional settlement (group effect).

5.7 Test Series 6: Tapered vs. Straight Piles

The results of these tests are shown in Figure 26. The ultimate load was 24 percent larger for the tapered pile than for the straight pile for test No. 6.3 which had the greater soil strength ($\phi = 42.5^\circ$). The increase for test No. 6.2 which had a soil ϕ angle of 41.35° was approximately 17 percent. This suggests that as the soil gets denser the effect of taper becomes more pronounced.

Also from these results, it can be seen that the slope of load-settlement curves for tapered piles was substantially higher than for the straight piles (up to three times for test No. 6.2). The higher load capacity and the stiffer slope of load-settlement curve can probably be attributed to the greater normal stresses developed between the tapered pile and the soil.

The prototype wood piles being modeled in this study had a diameter change from 14.0 in (35.5 cm) to 11.25 in (28.6 cm) from the butt end to the tip end over a length of 40 ft (12.2m). This relatively small taper of 0.069 in (0.17 cm) per 12-in length (30.5 cm), however, produced significant increases in pile capacity and slope of the load-settlement curve. The geotechnical centrifuge would seem to be an ideal tool to investigate in a systematic manner the effects of pile shape and soil density on pile performance. Among the variables that could be investigated are pile type (step-taper, straight, taper, drilled piers with belled ends, etc.), degree of taper, soil density, among others.

5.8 Test Series 7: Saturated Tests

Results of the saturated tests are shown in Figures 27 and 28. In test 7.1, which was the group test, it does not appear that the measured load for the saturated soil was reduced by the ratio of $\gamma_{\text{buoyant}}/\gamma_{\text{dry}}$. Several factors are believed to contribute to this discrepancy. First, because of the loss of water (see discussion, Section 4.3) the pore pressures at the tip of the pile, where most of the load resistance was generated, were reduced. Also, since the soil was wet

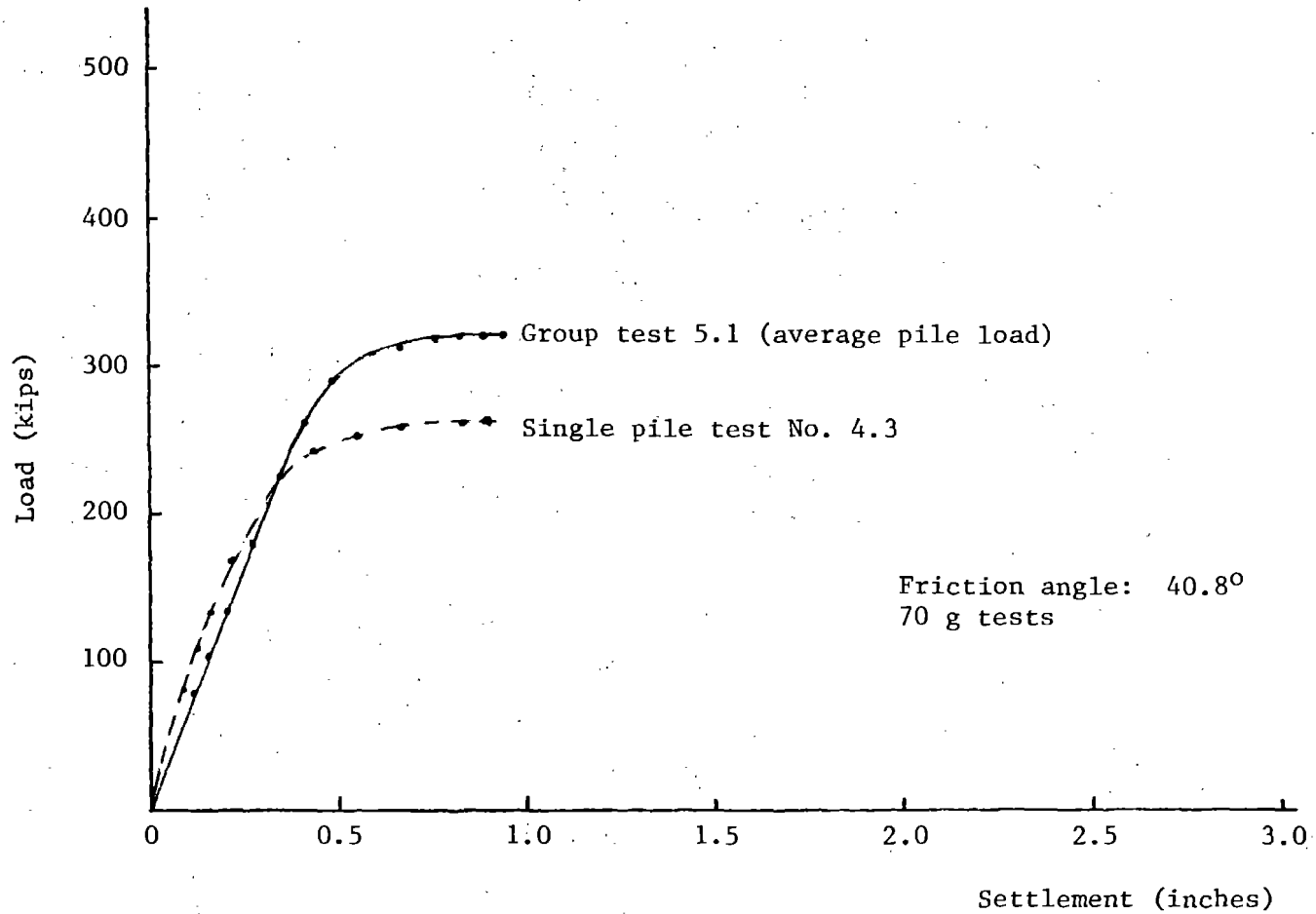


Figure 37. Comparison between single pile and pile group tests, Tests 4.3 and 5.1, (prototype scale).
(1 in = 2.54 cm, 1 kip = 4.45 kN)

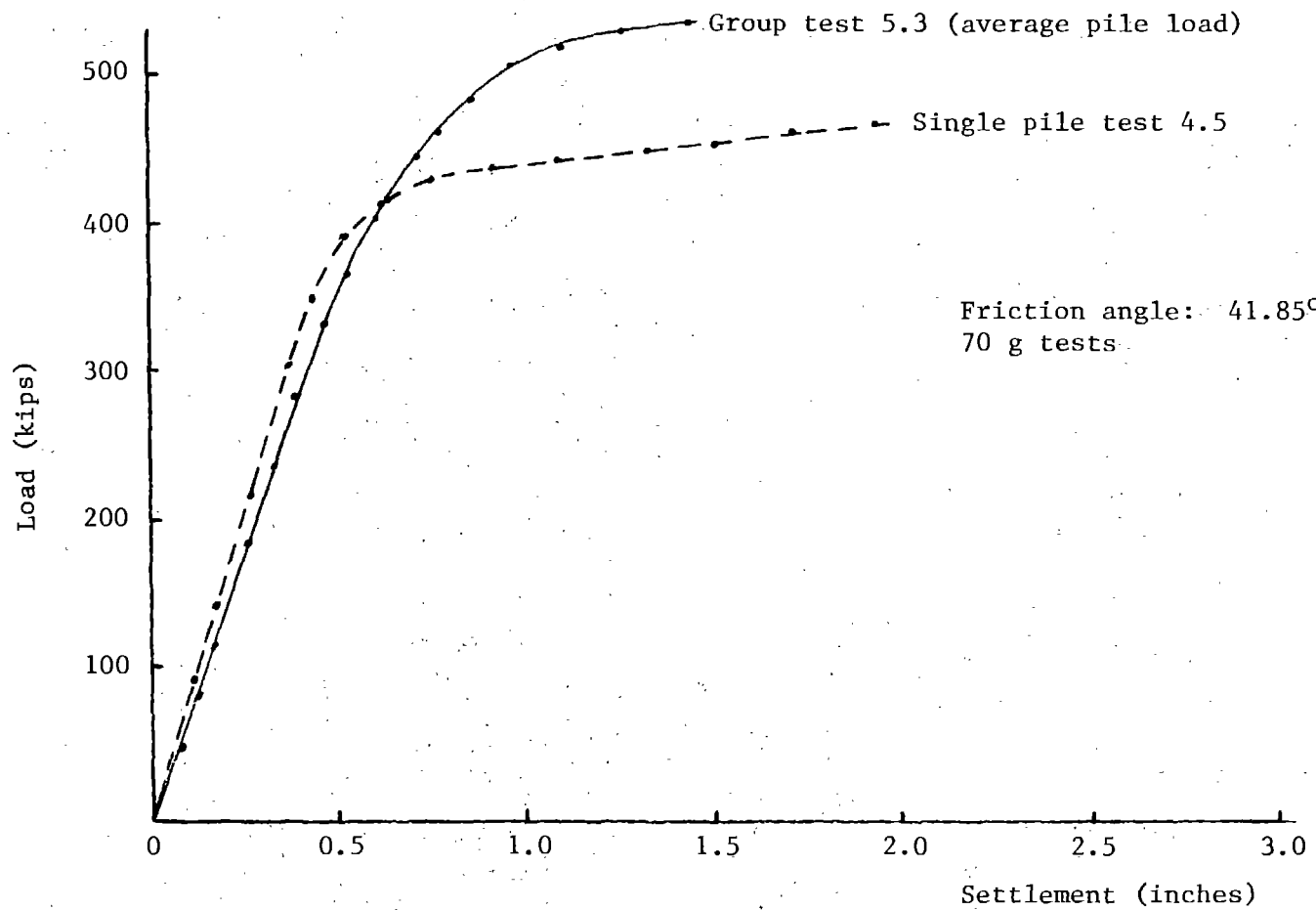


Figure 38. Comparison between single pile and pile group tests, Tests 4.5 and 5.3; (prototype scale).
(1 in. = 2.54 cm, 1 kip = 4.45 kN)

from the surface to the depth of 0.89 inch (2.26 cm), some apparent cohesion may have been developed. Second, by the time the load testing of the dry group test was completed, the group had been pushed into the soil 0.19 inch (0.5 cm). Thus the load test conducted after saturation started at a depth of 0.19 inch (0.5 cm) greater than the dry test, and the load resistance would be increased due to greater pile embedment. Third, after the saturated test was completed, it was noticed that the wooden piles were swollen due to exposure to water. The pile diameters were measured and on the average they had increased by almost 5.0 percent. The swelling may have increased the lateral stresses on the pile and hence increased the frictional resistance developed during load testing.

For test 7.2, which was a single pile test, the above discrepancies were removed. The load-settlement curve is shown in Figure 28. The ratio of $\gamma_{\text{buoyant}} / \gamma_{\text{dry}}$ is 0.56 while the measured load for the test in the saturated soil was reduced by a factor of 0.67 which can be considered as satisfactory. Also from Figure 28, it is seen that the slope of the saturated test was approximately 50 percent of that in the dry test.

5.9 Test Series 8: Lateral Load Tests

Results of these tests are shown in Figures 29 through 32. For test 8.1, two cycles of loading were performed on the pile; and, as expected, the load-deflection curve for the second cycle was stiffer than the first cycle. Also, comparing the slope of the load-deflection curves of tests 8.1 to 8.4 shows that as the soil gets denser the lateral resistance of the soil increases, which was also expected.

All the piles were pushed into the soil for 2.0 inches (5.1 cm) at 1 g before completing the remainder of the installation under increased gravity.

Thus the upper region of the pile that provides the greatest resistance to lateral loading may be significantly influenced by the method of pile installation. This should be considered in evaluating the deflections observed in these tests.

5.10 Test Series 9: Aluminum Pile Test

From the load transfer curve shown in Figure 34 it is seen that approximately 73% of the ultimate load came from tip resistance. There was no load transfer measured at the first strain gage level located 1.0 inch (2.5 cm) below the soil surface. This may reflect the disturbance produced by installing the initial 2.0 inches (5.1 cm) of the pile at 1 g.

The load transfer curve is almost a straight line meaning that the skin friction was uniform over the entire length of the pile. This is in contrast with the theoretical assumption that the shaft resistance increases linearly with the depth, but it is in good agreement with results of field tests obtained by Vesic (1967) who showed that the shaft resistance became constant after depth of 11.6 feet (3.53 m) for piles driven in dense sand.

The ultimate load at prototype scale for this test was 168 kips (750 KN). To compare this value to the results from the straight wooden pile test it is necessary to account for the different pile diameters and different l/d ratios. Using Figures 3.13 and 3.14 from Poulos and Davis (1980) the ultimate shaft and base load were increased by 1.6 and 1.87 times respectively. A value of 249 kips (1,111 KN) was obtained for the transformed ultimate load capacity which is in good agreement with the 269 kips (1200 KN) measured from the straight wooden pile test (test 6.1, Figure 26).

CHAPTER 6. COMPARISON OF MODEL TEST RESULTS TO
FIELD DATA AND ANALYTICAL PREDICTIONS

6.1 Introduction

In this chapter the results from model tests in the centrifuge are compared to predicted responses obtained using currently available computer analysis methods. The centrifuge results are also compared to field test results from the Lock and Dam 26 site.

6.2 Ultimate Bearing Capacity of Piles

The ultimate bearing capacity of piles can be estimated using limiting equilibrium, pile driving, or wave equation formulas. Values of bearing capacities estimated using these approaches can be in considerable error when compared to actual field test results. Moreover, these methods provide only estimates of capacity and do not provide information on the slope of the load-settlement curve.

The load carried by a pile is transferred to the soil by either end-bearing, skin friction, or a combination of the two. In computing the ultimate load, Q_T , each of the two components is calculated separately, and the two are then added:

$$Q_T = Q_b + Q_f \quad (6.1)$$

where

Q_b = ultimate tip resistance, and

Q_f = ultimate shaft resistance.

The ultimate shaft and base resistance are given by Equation 6.2 which is the general expression for the ultimate load capacity of a single pile in sand (Poulos and Davis, 1980).

$$Q_T = \int_0^L F_\omega C(\sigma'_v K_s \tan \phi_a) dz + A_b \sigma'_{vb} N_q \quad (6.2)$$

where

L = pile embedment length

F_ω = correction factor for tapered pile (= 1 for uniform diameter pile)

C = pile circumference

σ'_v = effective vertical stress along shaft which is the effective overburden stress for depths up to the limiting depth below which σ'_v is assumed constant

K_s = coefficient of lateral pressure

ϕ_a = angle of friction between pile and soil

Z = vertical distance

A_b = area of pile tip

σ'_{vb} = effective vertical stress in soil at the level of the pile tip which must not exceed the limiting stress

N_q = bearing capacity factor based on the soil friction angle

6.3 Settlement of Pile Foundations

The three solution methods available to calculate the settlement of pile foundations may be categorized as:

1. Step integration methods, which use measured relationships between pile movement relative to the soil and the resulting resistance at various locations along the pile length.
2. Methods using the theory of elasticity, which employ equations of Mindlin for subsurface loading within a semi-infinite mass.
3. Numerical methods and, in particular, the finite element method.

Two computer programs using the first and the second methods were used to analyze the data. These two methods will be briefly described.

6.3.1 Step Integration Method

This method was first described by Seed and Reese (1957) and then developed by Coyle and Reese (1966) and Coyle and Sulaiman (1967). The method employs a finite difference approach for modeling the axially loaded pile and requires the satisfaction of compatibility between loads and deformations. This method uses measured pile load-transfer data and hence requires no assumptions regarding linearity of soil behavior. However, it inherently assumes that the shear stress developed at a given point along the pile is dependent only on the movement of the pile relative to the soil at that point and is not affected by soil stresses elsewhere along the pile. Since this disregards the continuity of the soil, the method by itself cannot be used for analyzing pile groups.

In a recent research study (Ha and O'Neill, 1981), this method was combined with the elasticity solution to analyze pile groups. This solution will be used to analyze some of the data presented in Chapter 4.

The usual approach in developing load transfer curves experimentally from load tests is to assume that, prior to loading, the residual side shear stresses (and tip load) are zero and that the pile itself is free of axial stresses. This leads to the initial distribution of load along the unloaded pile indicated by curve 1 in Figure 39. When the pile is loaded with an axial compressive load F_u ,

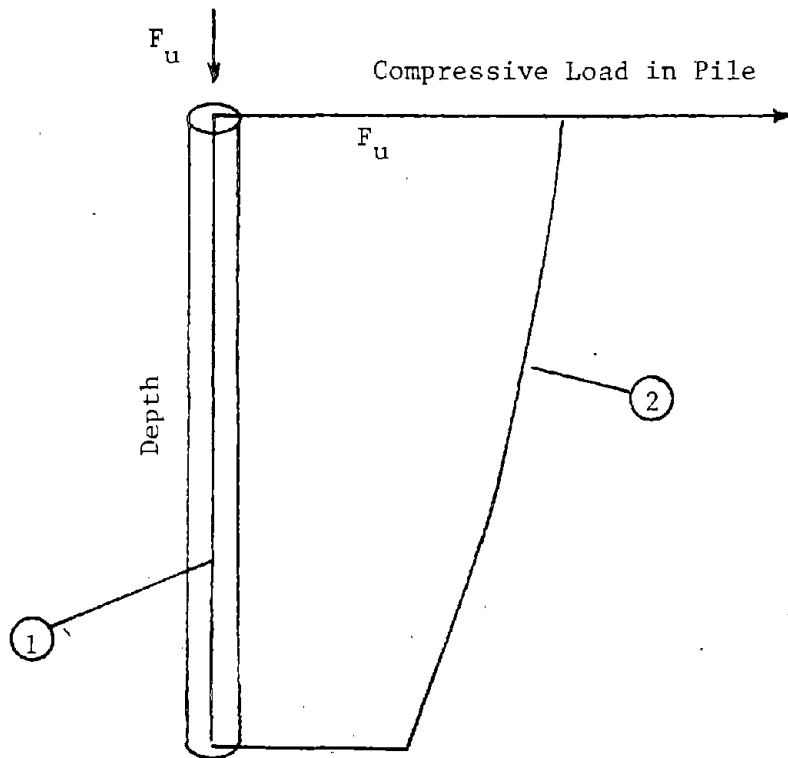


Figure 39. Axial load transfer curve

changes in the indicated load occur along the pile length. These changes may be sensed by strain gages in a physical test. When the changes in load are added to the initial load, in this case curve 1, curve 2 ensues. Curve 2 is the apparent load distribution in the pile under applied load F_u . The unit side shear resistance, f , at any level is the derivative of load in the pile with respect to depth divided by the pile circumference, $\pi D(dF/dz)$.

The corresponding value of relative displacement between pile and soil is the settlement of the head of the pile less the area between curves 1 and 2 from the head to the depth at which the curve is derived, divided by the elastic stiffness (AE) of the pile. By varying F_u experimentally and the depth of calculation, a family of apparent load transfer curves can be generated. The load transfer curve for the tip can be developed in a similar manner, except that in this case, the tip load is plotted directly against downward movement at the level of the pile tip. Analysis of numerous load tests on instrumented piles indicate that apparent load transfer curves have certain characteristic properties at various depths in various types of soil.

6.3.2 Methods Based on the Theory of Elasticity

These methods have been described by several investigators, including Poulos and Davis, (1968) and Salas and Belzunce (1965). All assume the soil to be a linear elastic material. In this method a set of equations expressing displacement compatibility between elements of the pile and the adjacent soil are solved for the pile-soil stresses and the element displacements. These equations are valid as long as the pile soil stress at that element remains elastic. If the computed stress reaches or exceeds the limiting value at any element the displacement compatibility equation for that element is replaced by the condition that the pile-soil stress equals the limiting value. The effect of an adjacent pile is allowed for by evaluating the additional soil displacements due to the adjacent pile, as described by Poulos (1968).

6.4 Computer Solutions

6.4.1 Step Integration Method

The load transfer and the load settlement curves from test 9.1 are shown in Figures 33 and 34, respectively. From the load transfer curve it is seen that no load was transferred to the soil for the first 1 in (2.5 cm) of depth corresponding to a depth of 5.8 ft (1.8 m) at prototype scale. Below this level the slope of the curve is almost constant meaning the shear stress between the pile and soil was constant for the remaining length of the pile. All computer runs were conducted at prototype scale to avoid problems encountered using model scale dimensions in the program. Problems were encountered with format on input and

output and with certain fixed parameters internally located in the program.

The pile prediction program PILGP1 developed by Ha and O'Neill (1981) for the FHWA was used to analyze the aluminum pile test since it was the only test for which load transfer data was available.

Since only the maximum skin friction (f_{\max}) and the maximum tip resistance (Q_{\max}) were available, it was not possible to get the f - z (shear stress-relative displacement) and Q - z (tip load-relative displacement) curves directly from the data available. This problem could have easily been solved if the strain gage signals from each location and the total load from the load cell were obtained versus time or versus each other. Unfortunately this was not accomplished.

For the first computer run the shape of the f - z and Q - z curves used were obtained by using equations suggested by the PILGP1 user's manual. The value of z_c (deflection needed to mobilize maximum resistance) in the input Q - z curve was taken to be 8% of the pile tip diameter, and the value of z_c in the input f - z curve was taken to be 0.0108 inch (.027 cm) at model scale. These selections were based on the recommendations by Reese and Awoshika (1980), on the basis of the relative density of the soil and triaxial test results under a confining pressure equal to the overburden pressure at the pile tip. The same f - z curve was used for the entire length of the pile except for the first 1 inch (2.54 cm) for which a zero value was assigned to f_{\max} . The computed pile response is compared in Figure 40 with the results from test No. 9.1, the centrifuge test on the straight aluminum pile at 1/70 scale factor.

While the ultimate load predicted by the computer program is quite close to the model test results, the predicted slope of the initial load-settlement curve and the pile settlement at working loads are not close. A lower value of z_c used for the Q - z curve would have improved the predicted behavior.

In order to show the f - z and Q - z curves in the same graph, the values of f were multiplied by the acting circumferential area of the pile to obtain the total side shear force on the pile versus settlement curve, f - z , as shown in Figure 40.

To obtain the best match of the computer solution to the test data, a series of computer runs using different values for z_c and different slopes for the f - z and Q - z curves were made. In all runs the values of Q_{\max} and f_{\max} were kept equal to the values obtained from test 9.1 in the centrifuge. Figures 41 and 42 show the best possible matches obtained. In both cases, a value of 0.35 in (0.9 cm) prototype scale was used for the z_c of the f - z curves compared to 0.2-0.5 in (0.5 to 1.3 cm) suggested in the user's manual. The value of z_c for the Q - z curve

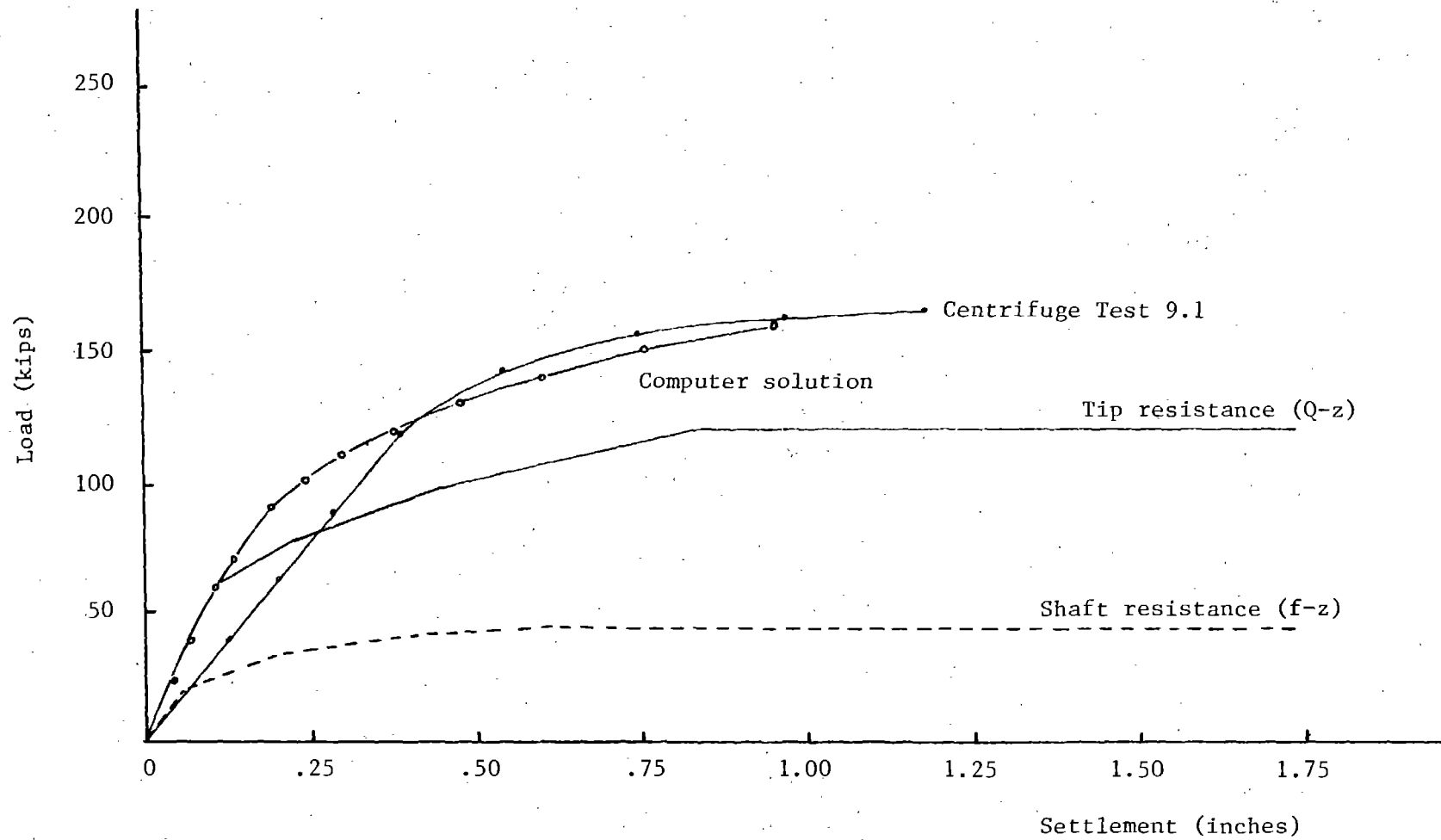


Figure 40. PILGPI predictions vs centrifuge results, recommended load transfer curves (prototype scale). (1 in = 2.54 cm, 1 kip = 4.45 kN)

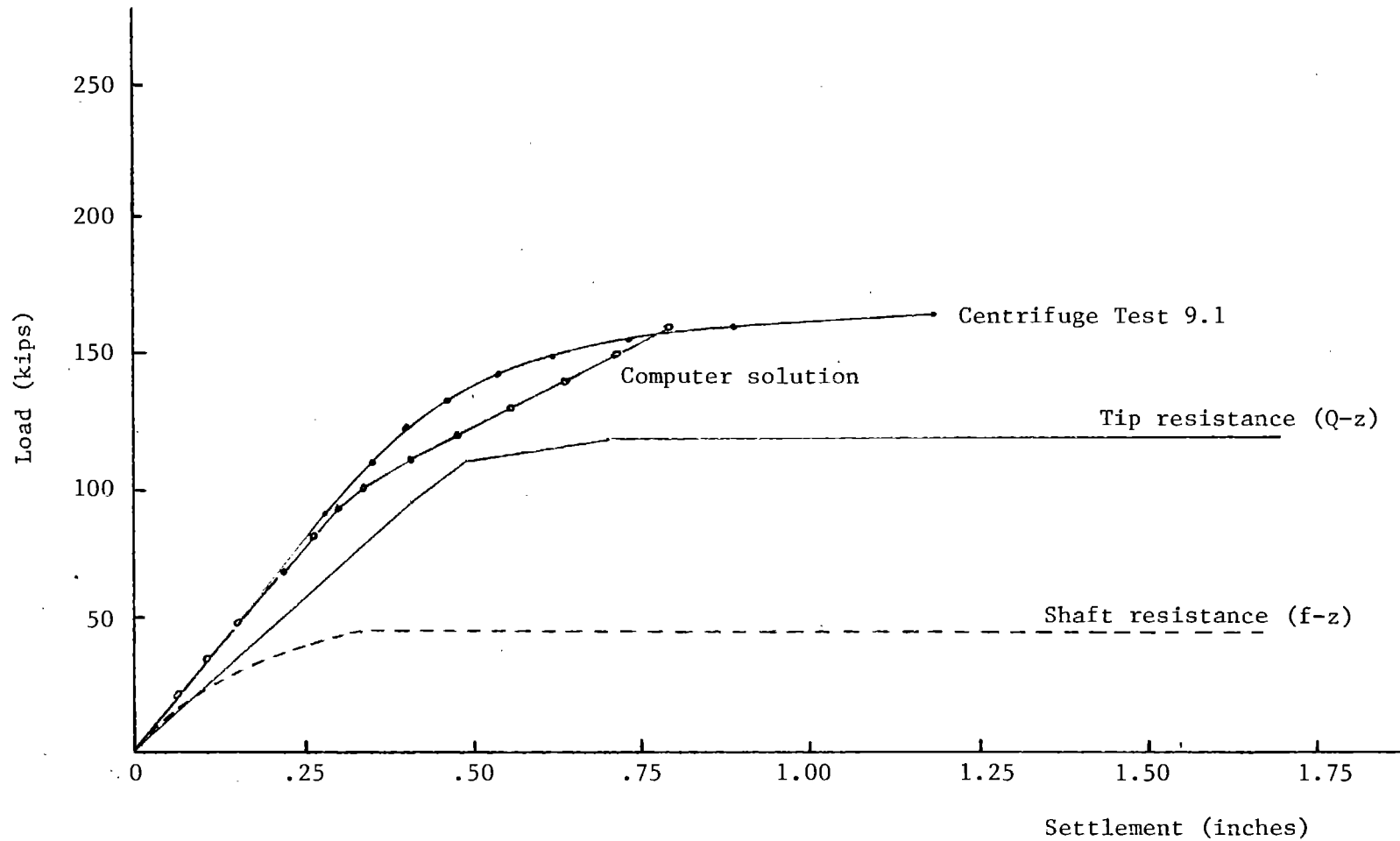


Figure 41. PILGP1 predictions vs centrifuge results, adjusted load transfer curves, (prototype scale). (1 in = 2.54 cm, 1 kip = 4.45 kN)

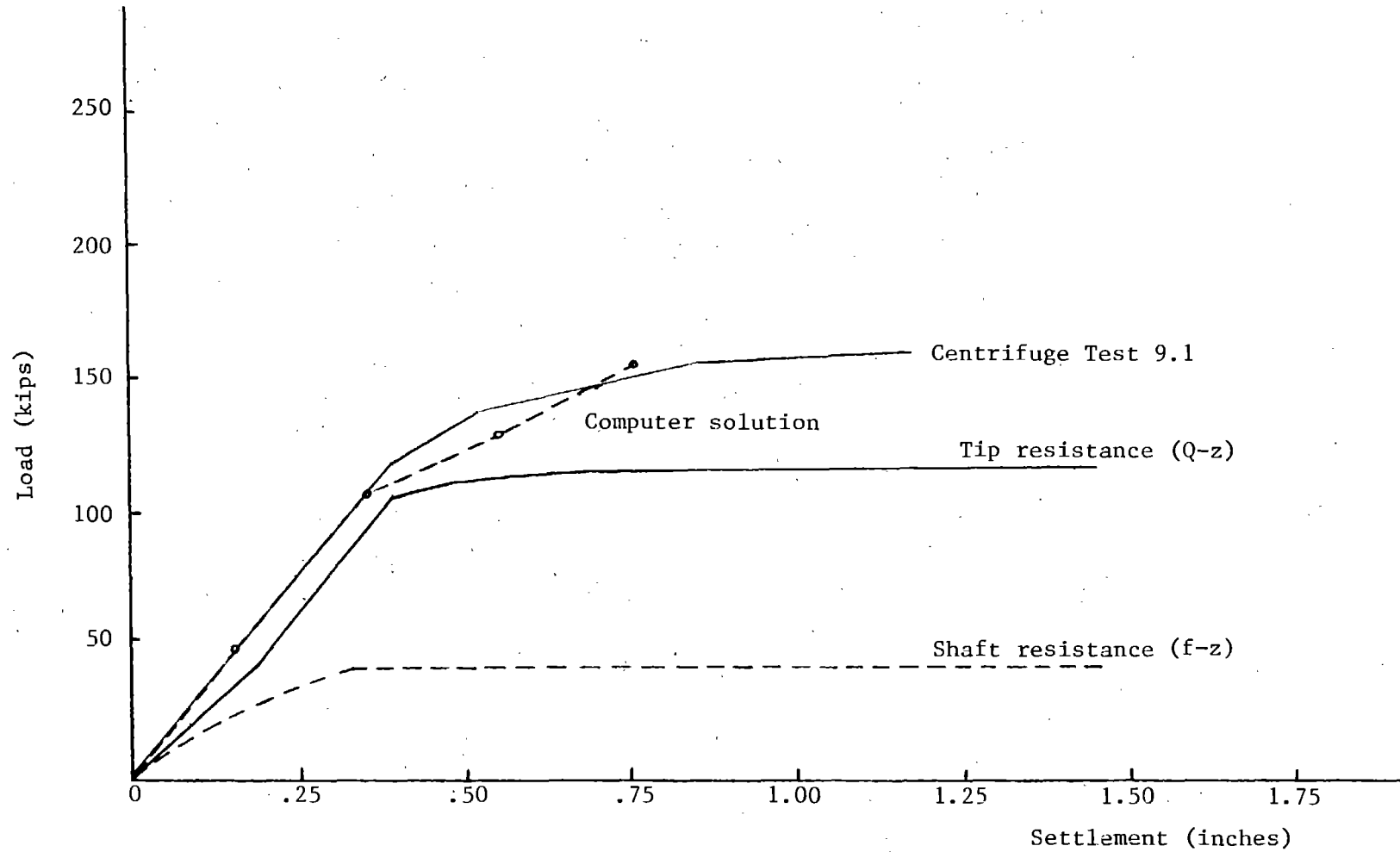


Figure 42. PILGP1 predictions vs centrifuge results, adjusted load transfer curves, (prototype scale). (1 in = 2.54 cm, 1 kip = 4.45 kN).

was 6% of the pile tip diameter, 0.64 in (1.64 cm), at prototype scale compared to 5% suggested by the manual. The shape of the f-z curves used is identical in Figures 41 and 42 but the Q-z curves have slightly different shapes up to z_c .

From Figure 41 it is seen that the computer solution is identical with the centrifuge data up to the z_c point of the f-z curve. Beyond this point the slope of the predicted load-settlement curve changes since the value of skin friction has reached a constant value while the tip resistance continues to increase. This occurs before the centrifuge curve has started to yield, and regardless of the f-z and Q-z curves input, this problem could not be overcome if maximum skin friction is to be mobilized before maximum tip resistance. Although, the same phenomenon (change of slope) was noticed for computer solutions obtained for clay (see Vol. III), the fact that approximately 70% of the ultimate load in clay is taken by skin friction causes the change in slope of the predicted curve to occur about where the slope change occurs in the experimentally measured curve in the centrifuge.

This can be illustrated schematically in Figure 43 where the same ultimate load is divided into 75% tip resistance, 25% skin friction for sand and 25% tip resistance, 75% skin friction for clay. In both cases, the skin friction is mobilized first, and the values for the z_c 's are the same. The f-z and Q-z curves are then added to give the resultant dashed line. As it is seen the resultant curve for the clay looks more like the field test data available in the literature.

Since the f-z and Q-z curves were not obtained from the test data directly (except for Q_{max} and f_{max}), it is not possible to make specific comments on the accuracy of the computer solution. However, the z_c 's used for the f-z and Q-z curves to make the computer solution match the centrifuge data are the ones suggested by the computer manual, and only the shape of these curves is slightly different from the manual's suggestion. The general conclusion reached from the above predictions and discussions is that, for the model tests in the centrifuge, the program PILGP1 provided good predictions of pile response up to only approximately 60% of ultimate load. The load-settlement predictions in this range, which would include most working loads is, however, excellent.

6.4.2 Elasticity Method

The computer program AXPIL5 written by Poulos (1978) was also used to predict

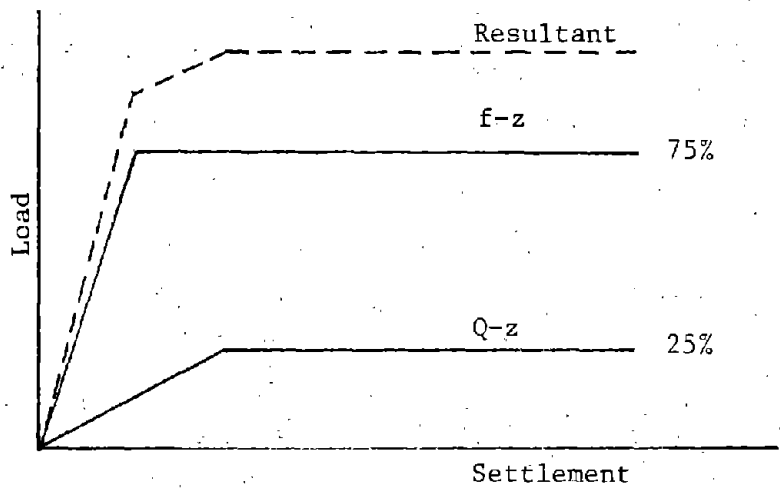
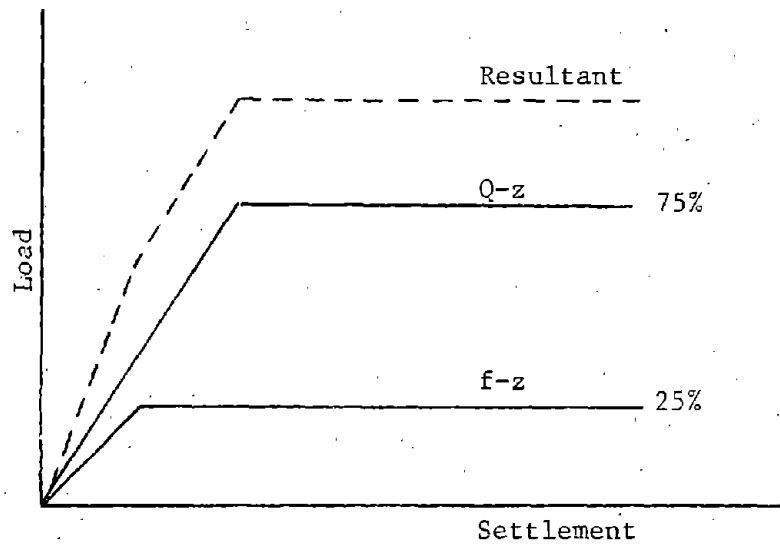


Figure 43. Schematic illustrating differences between predicted sand and clay pile response.

centrifuge test results. The program computes the load-settlement curve and stresses in the pile based on elastic theory. Provisions are made to permit soil-pile slip and tip failure thus allowing the load-settlement curve for the pile up to failure to be calculated.

The program is limited to considering only straight, uniform diameter piles and thus was used to analyze the straight wooden pile of test 6.1. The ultimate load of this pile was divided into 73% tip and 27% shaft resistance. The shaft resistance was uniformly distributed over the embedded circumferential area of the pile.

For the first series of computer runs the pile was considered to be floating. In an attempt to match the centrifuge test data, various values of modulus of elasticity were given to the soil. The measured limiting soil-pile shear stress, f_{\max} , determined from test 9.1 was also used as an input quantity. Computed results are compared with those from test 6.1 in Figure 44. As it is seen, the same problem (change of slope) noticed with the PILLGP1 program is also present in the elasticity solution, but the problem is more pronounced.

For the second series of runs the pile was considered to be end bearing. Results are shown in Figure 45. It again was not possible to match the model test data (test 6.1) regardless of the input soil modulus.

It is concluded that using the load-transfer data obtained from the model tests in this elasticity approach does not provide acceptable predictions of model pile behavior.

6.5 Comparison of Model Tests to Field Tests Results

6.5.1 Description of Field Tests

The field test program conducted at Locks and Dam No. 26 is described in great detail in the reports by Woodward-Clyde (1979) to the Corps of Engineers. A total of seven single pile or pile group test structures were constructed and tested at this site. Only the results from Monolith M-5, a 2 x 4 group test, and Monolith M-6, a single pile test, will be used for comparison in this report.

The timber piles used in Monoliths M-5 and M-6 were jettted with some driving to a depth of 30 feet (9.1 m) below grade. The timber piles were then driven an additional 5 feet (1.5 m) to a 35-foot (10.6 m) embedment depth using a Vulcan 1 single-acting air/steam hammer of 15,000 ft·lb (20.3 m-kN) rated energy.

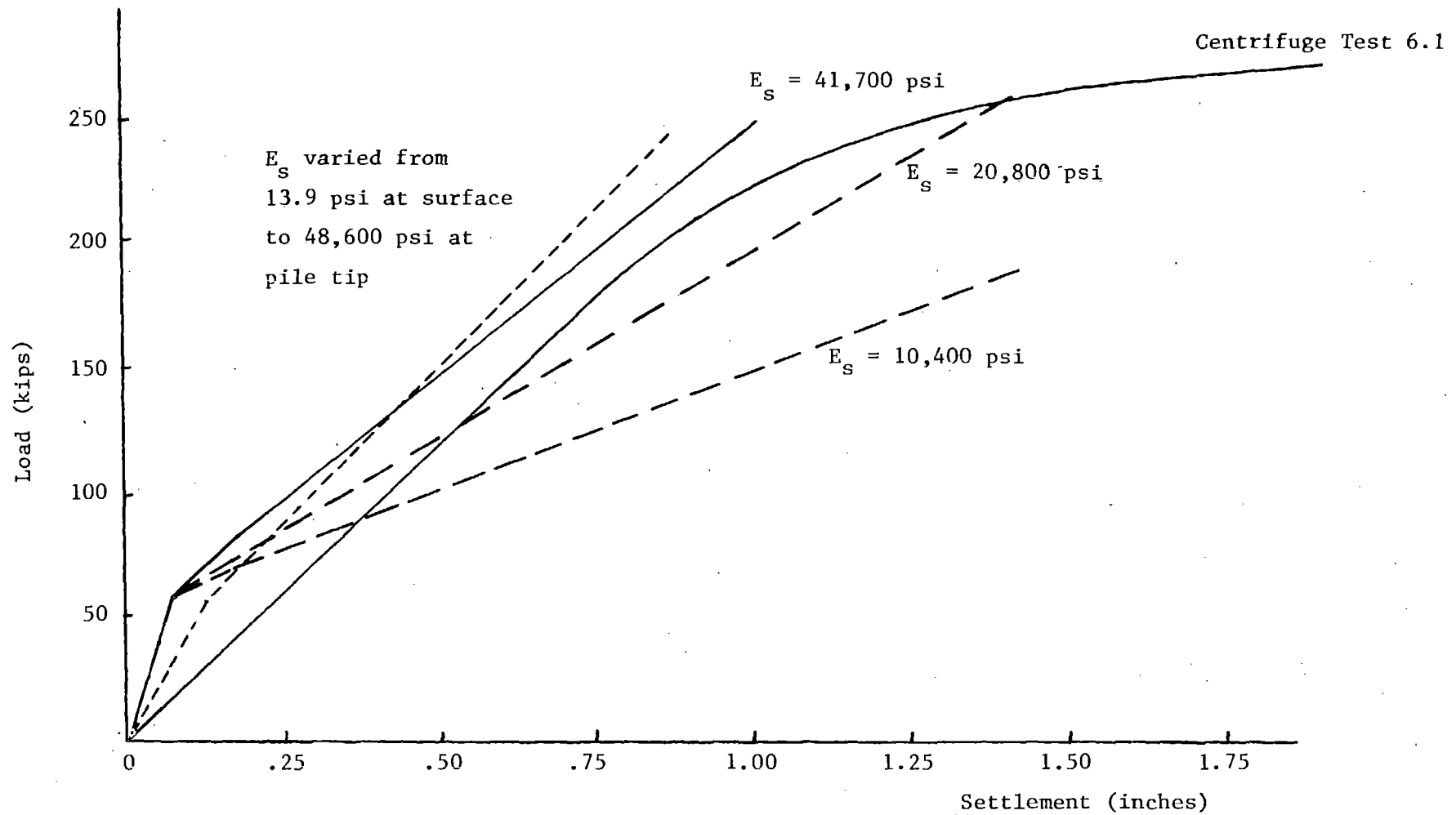


Figure 44. Elasticity-based predictions vs centrifuge data, floating tip (prototype scale).
(1 in = 2.54 cm, 1 kip = 4.45 kN, 1 psi = 6.895 kN/m²)

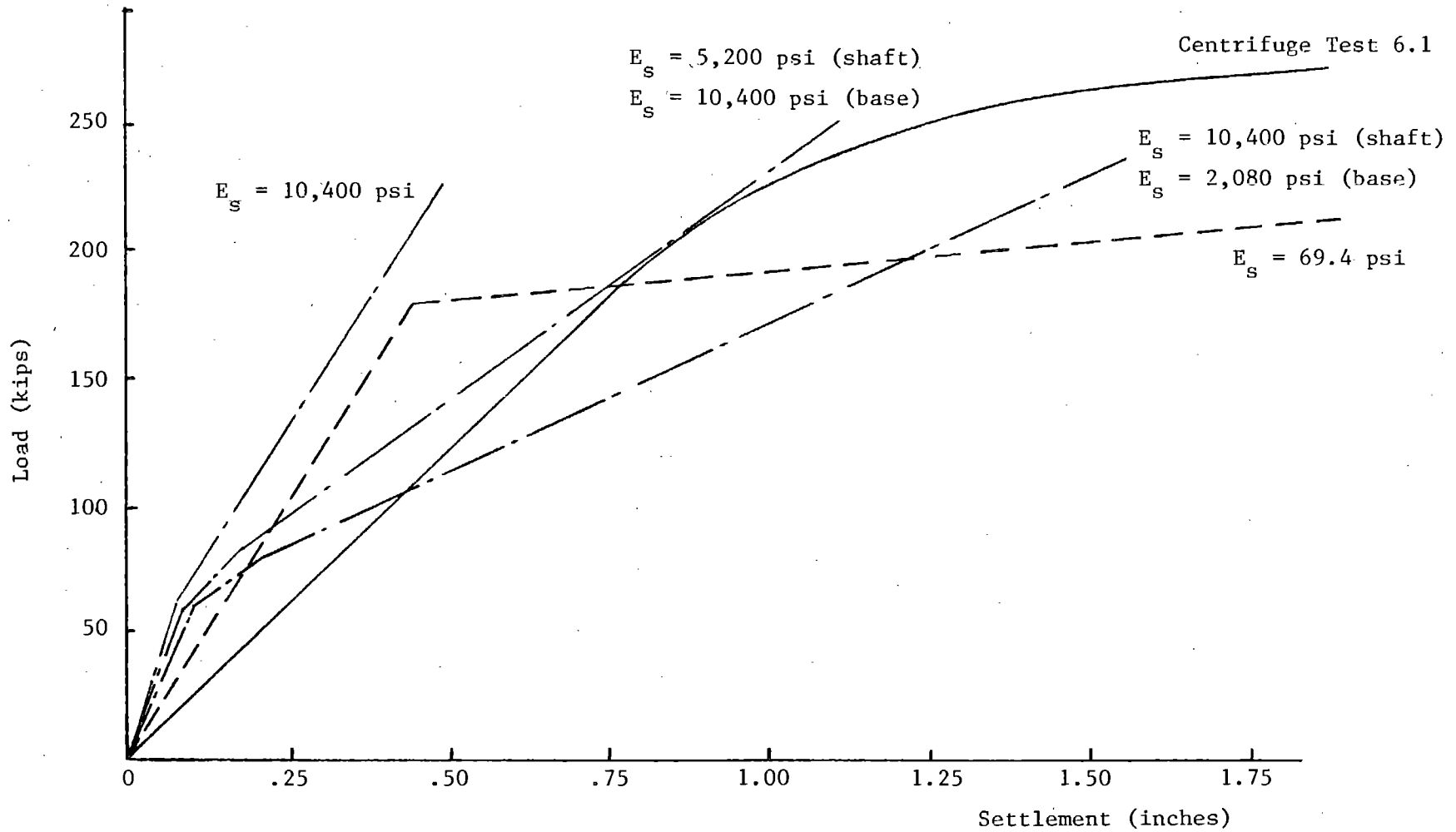


Figure 45. Elasticity-based predictions vs centrifuge data, end bearing (prototype scale).
 (1 in = 2.54 cm, 1 kip = 4.45 kN, 1 psi = 6.895 kN/m²)

Prior to conducting load tests to failure in the field test program all test piles and piles groups were subjected to a cyclic lateral preloading history. This preloading was performed to simulate the type of cyclic loading such piles would experience from operational activities at a lock and dam installation. All piles were first subjected to an axial load of 30 tons (267 kN) per pile which was maintained constant during the preloading activities. A lateral load of 6 tons (53.4 kN) per pile was applied and held until movement ceased. The lateral load was then reduced to 0.6 tons (5.3 kN) per pile after which the 6-ton load was applied again. This cyclic application of lateral loads was continued until less than 0.01 inch (.025 cm) permanent lateral deflection was measured over five cycles of lateral load. Monolith M-5 was subject to 39 cycles of lateral load and Monolith M-6 had 23 cycles applied.

The two monoliths under consideration in this report were part of a program to study the factors affecting the response of axially and laterally loaded piles to driving operations on nearby piles. The monolith was first loaded to its planned level and then a series of piles were driven at successively closer locations to the monolith. Both incremental and cumulative horizontal and vertical displacements were recorded on the loaded monoliths as the adjacent piles were driven. For example, Monolith M-6 had a total cumulative horizontal displacement of 1.99 inch (5.05 cm) and settlement of 1.48 inch (7.48 cm) as the result of driving a total of 14 adjacent piles at horizontal distances ranging from 50 feet (15.2 m) to 10.4 feet (3.2 m).

6.5.2 Comparison to Monolith M-6, Single Pile Field Test

The field tests were conducted under saturated soil conditions with the water table held within a foot of grade. Most of the centrifuge tests were conducted in dry sands. Test 7.2 from the centrifuge, however, provides information on the effect of saturated soil on model pile response. Results from this test (Figure 28) conducted on a sand having a friction angle of 41.85 degrees show that the ratio of load-dry to load-saturated is a constant value of 1.61 throughout most of the settlement range.

Assuming that this ratio of dry to saturated strength will apply to other tests from the centrifuge, the load-settlement curves from tests 4.1, 4.2, and 4.4 were adjusted by the 1.61 factor to obtain their assumed saturated response. The

load-settlement curve from saturated test 7.2 and the adjusted curves from tests 4.1, 4.2, and 4.4 are plotted in Figure 46 at prototype scale together with the results of the single pile field test on Monolith M-6.

The field test curve in Figure 46 continues to pick up additional load at large settlement values whereas the centrifuge curves generally have reached constant values of load at much smaller settlement values. It is seen that the results from test 4.2 ($\phi = 40.7^\circ$) provide a good match to the field test data up to approximately 70 percent of the field test ultimate load value. Test 4.4 ($\phi = 41.35^\circ$), however, provides the best match to the field test at ultimate load.

The initial load-settlement response from the field test is seen to be slightly stiffer than results from the model tests. This could easily reflect the soil densification around the field test pile resulting from the cyclic lateral testing and the effects of driving the 14 adjacent piles near Monolith M-6.

The extreme sensitivity of the model test capacities to the angle of internal friction of the sand is well-illustrated in Figure 46. An increase in friction angle of 1.40 degrees from 40.45 degrees to 41.85 degrees is seen to increase the ultimate load capacity by a factor of 2.5. This sensitivity requires that meticulous care be taken in preparing the model soil and in conducting the model tests. The correct characterization of the soil profile at a field site is also seen to be essential. The centrifuge data shows that a friction value of 40.7 degrees provides the best prediction of the field test data over 70 percent of the load range where as a friction value of 40.0 degrees had been assumed to represent the average field angle of friction. As illustrated in Figure 1a the angle of internal friction shows considerable variation at a given depth depending on the method used to estimate friction angle and also shows variation vertically due to changes in the soil profile. These variations reflect the variation to be expected in any natural deposit as well as difficulties inherent in determining insitu properties at a site.

The field test site friction angle estimated from pressure meter results ranged from 38 to 42 degrees over the depth of the pile while that estimated from cone penetration was lower than this range for the upper 12 feet of the pile and averaged 40 degrees below this level. Considering the measured range and accuracy of determining the friction angle in the field, the good correlation obtained with

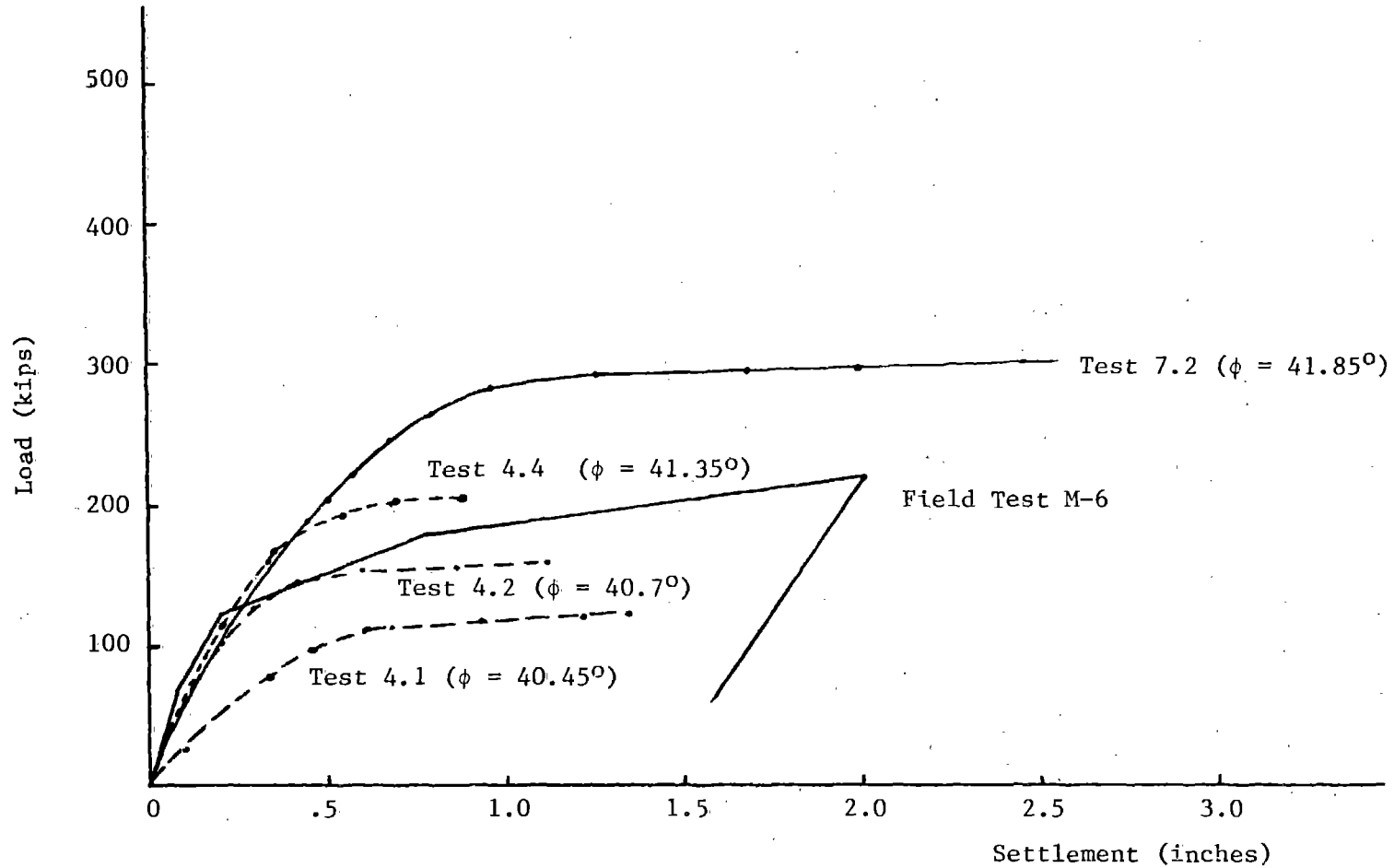


Figure 46. Comparison of single pile field test M-6 to centrifuge results
(1 in = 2.54 cm, 1 kip = 4.45 kN)

centrifuge test 4.2 having an angle of 40.7 degrees is seen to be well within the likely range of field values.

6.5.3 Comparison to Monolith M-5, 2x4 Group Field Test

Monolith M-5 was a 2x4 group test that was loaded in the field to axial failure. The load-settlement curve from the field test is shown in Figure 47. At failure the pile cap had rotated with a settlement of 3.2 inches (8.1 cm) at the south end and 2.3 inches (5.8 cm) at the north end. The settlement plotted for M-5 in Figure 47 is the average of measured settlements at the north and south ends.

Also shown in Figure 47 are the load-settlement curves from the four group tests (5.1 to 5.4) conducted in the centrifuge. The plotted loads have been reduced by the 1.61 factor determined from the dry versus saturated test conducted on the single pile (Test 7.2).

The comparison between the field test on the pile group and scaled centrifuge results is poorer than experienced with the single pile comparison. The group field test curve falls below the lowest density centrifuge test which had a friction angle of 40.8 degrees. In the working load range only the highest density centrifuge test (No. 5.4) with a friction angle of 42.5 degrees is close to the field curve with the other centrifuge curves predicting less settlement.

The poorer comparison between field and centrifuge results for the group test M-5 as compared to the single pile test M-6 is difficult to explain. Both M-5 and M-6 monoliths were installed using the jetting and then driving procedures previously described. Both were subjected to the cyclic lateral preloading tests and to the effects of having adjacent piles driven close-by.

The differential settlement observed on M-5 at failure suggests either a variability in soil properties across the width of the pile cap or significant differences arising possibly from the jetting and driving operation.

Another explanation is that the average strength properties varied sufficiently over the 115 foot (35 m) horizontal distance between monoliths M-5 and M-6. The effective strength properties at M-6 may have been closer to 41 degrees as suggested by Figure 46 whereas as at the M-5 location the effective strength properties may have been closer to the 40 degrees assumed for the field site. This one degree variation is within the variability present in the field soils data. From Figure 47

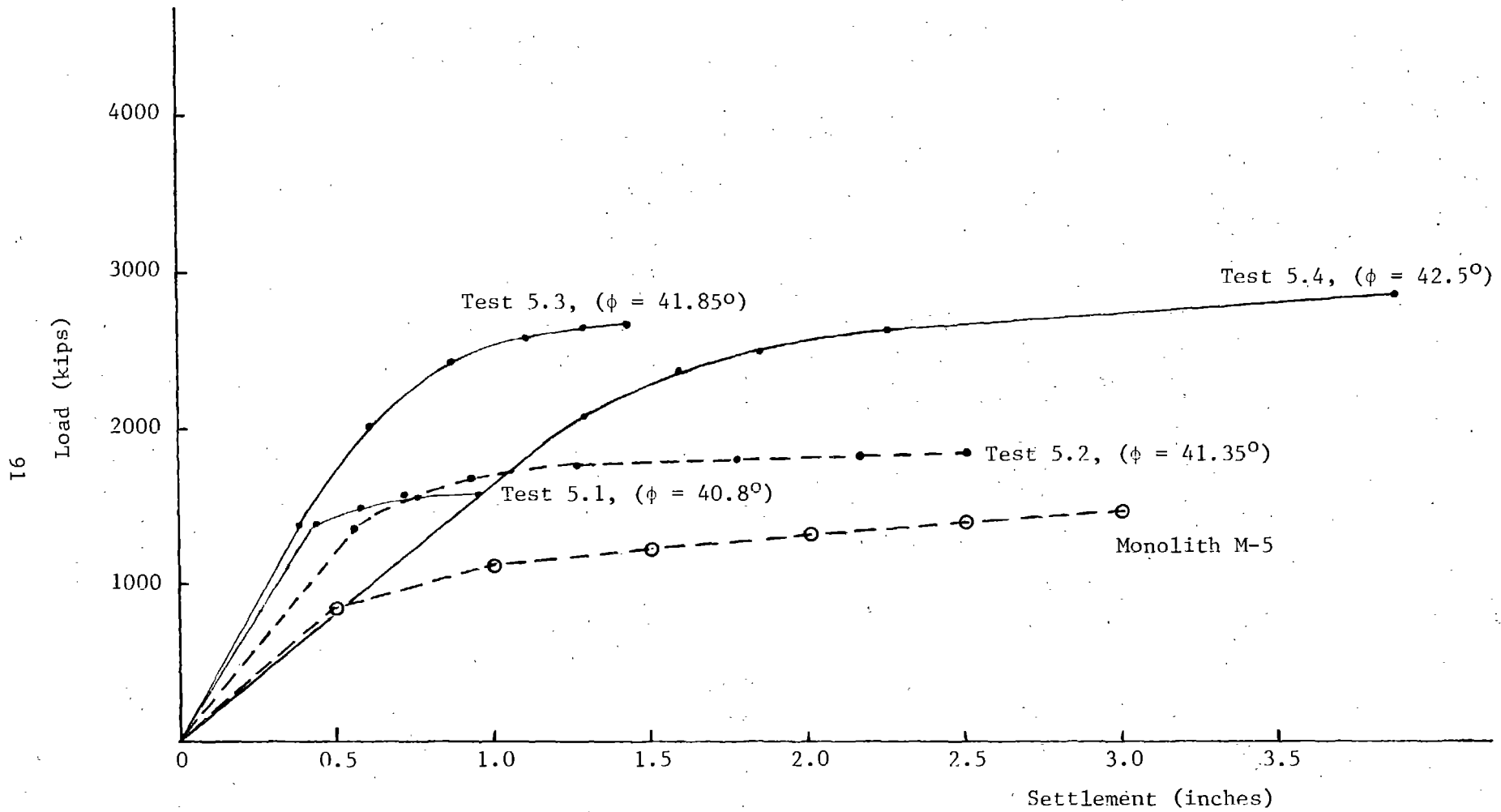


Figure 47. Comparison field group test to scaled centrifuge tests (prototype scale).
 (1 in = 2.54 cm, 1 kip = 4.45 kN)

it can be projected that results on a centrifuge group test in a 40-degree soil would give a closer match to at least the ultimate loads measured in the field test. Again the sensitivity of the centrifuge results to the soil friction angle is evident.

6.5.4 Comparison to Monolith M-6, Single Pile Lateral Test

The results of the lateral test on Monolith M-6 are presented in Figure 48. This test was conducted after the axial test to failure and was conducted with an axial load of 60 kips. The field test shows a significantly stiffer response than the centrifuge test. The history of the field pile which includes the 23 cycles of cyclic lateral loading, the pile driving effects tests, the axial load test to failure and the applied 60 kip axial load likely account for the observed differences.

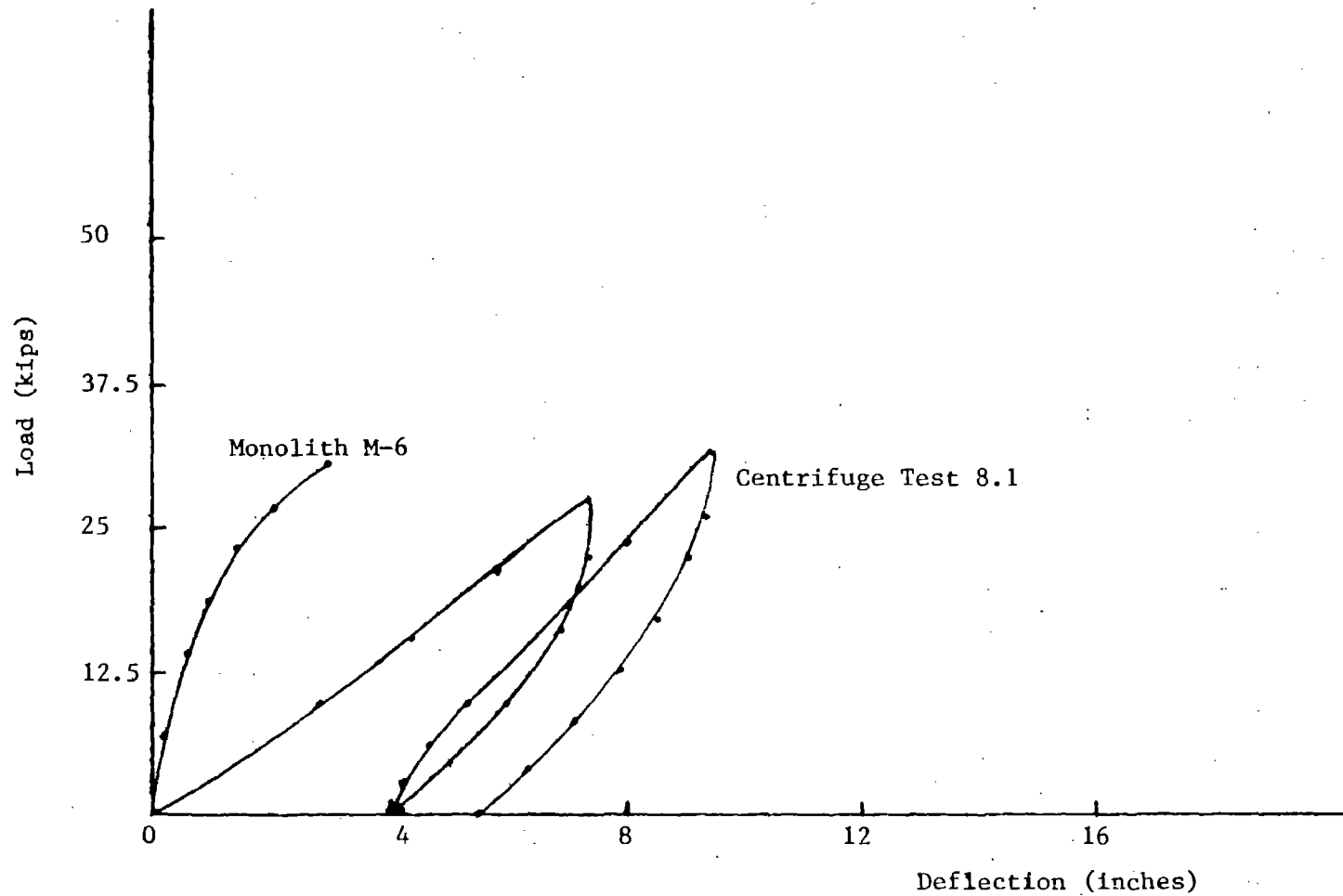


Figure 48. Comparison field lateral load test to centrifuge test, single pile (prototype scale). (1 in = 2.54 cm, 1 kip = 4.45 kN)

CHAPTER 7. SUMMARY, CONCLUSIONS, RECOMMENDATIONS

7.1 Summary

The results of a research program to study the feasibility of conducting model tests on single piles and pile groups in sand in a geotechnical centrifuge are presented in this report. The study required development of consistent soil preparation techniques, fabrication and instrumentation of model piles at various scale factors, and development of experimental techniques including pile installation under high gravity conditions.

A comprehensive test program conducted in the centrifuge investigated the following items:

- Effect of inflight pile installation
- Effect of centrifuge stoppage
- Effect of model scale
- Parametric study of the influence of soil density
- Pile group tests
- Tapered vs straight pile capacity
- Effect of soil saturation on pile performance
- Lateral load tests
- Load transfer in sand from side shear and tip loads

The experimental program conducted in the centrifuge was designed to model single pile and pile group tests conducted at the Locks and Dam No. 26 field test site on the Mississippi River. Modeling aspects included the soil, the type, size and shape of the piles, and test conditions.

7.2 Conclusions

Conclusions drawn from the results of this study are grouped into three specific categories.

7.2.1 Experimental Technique

- Careful soil preparation is necessary to achieve the uniform soil properties required for successful centrifuge tests.
- In-flight installation of model piles is essential for proper modeling.
- The instrumentation developed in this study provided good data on pile response.

7.2.2 Centrifuge Test Results on Model Piles

- The good agreement obtained in the 'modeling of models' study verified the similitude theory assumed and the experimental techniques employed over 1/50, 1/70, and 1/100 model scales.
- Results from both single pile and pile group tests revealed the very strong dependence of ultimate pile capacity on the density of the sand soil. The initial slope of the load-settlement curve, however, had little or no dependence on density.
- Individual pile driving records for piles in a group clearly show the influence of driving sequence.
- The pile shape, e.g., tapered vs straight, had a significant effect on ultimate capacity and slope of the load-settlement curve.

7.2.3 Comparison to Field Test Data

- Centrifuge model test results for both single pile and pile group tests can be said to fall within the range of field test data if the variability of site soil properties are taken into account.
- The average friction angle determined is influenced by the natural variability of the soil deposit at the site and by the accuracy of determining in situ soil properties. The sensitivity of centrifuge results to friction angle combined with the lack of precision in specifying the field friction angle makes the exact modeling of field conditions difficult. The load history experienced by the field test piles including the cyclic preloading and driving effects of adjacent piles resulted in additional and unknown effects on ultimate field behavior.

7.2.4 General Conclusions

- This study has proven the internal consistency of the results of centrifugal model testing of piles in cohesionless soil. Using the observed internal consistency as a verification of the approach, the various studies in this program into areas as the effects of pile taper, driving sequence, saturation and group effects, show that the method of centrifugal testing of piles can provide insight into the effect of these variables on pile performance. Centrifugal testing on these variables as well as many others that influence pile response can greatly increase the understanding of pile behavior.

- Centrifuge modeling of specific field pile foundation designs can, at present, provide only an approximate estimate of actual load-settlement and ultimate load response. The accuracy in precisely determining field soil properties is felt to be the major limitation. Centrifuge testing of proposed field construction projects can, however, provide useful and cost effective information on the influence of design parameter such as pile size and shape, driving sequence, pile patterns, etc. on pile response.

7.3 Recommendations

This study has proven the effectiveness of the geotechnical centrifuge for studying in a cost-effective and accurate manner the influence of various parameters affecting pile response. Among the items that should receive additional study are:

- The effect of pile design and shape over a considerable range should be studied. Variables could include shape (straight, step-taper, tapered), length/diameter ratios, and pile type.
- Additional studies are needed to determine effects of pile behavior in saturated and partially saturated soils.
- The load-transfer curves for side shear stress ($f-z$) and tip load bearing ($Q-z$) need to be determined.
- The influence of the method of pile installation (jetting, jacking or driving) and the effect of driving adjacent piles on ultimate pile response should be investigated.
- The effect of pile driving sequence on pile group response in soils of various densities should be studied.
- Studies should be conducted in soils having both cohesion and frictional strength.

REFERENCES

- Bucky, P.B. (1931), "The Use of Models for Study of Mining Problems," Transactions of the American Institute of Mining Engineers, n. 96.
- Cargill, K.W. (1980), "Centrifugal Modeling of Transient Water Flow in Earth Embankments," M.S. Thesis University of Colorado.
- Coyle, H.M, and L.C. Reese (1966), "Load Transfer for Axially Loaded Piles in Clay," J. Soil Mech. Found. Div. ASCE, Vol. 92, SM2, pp. 1-26.
- Coyle, H.M., and T. Sulaiman (1967), "Skin Friction for Steel Piles in Sand," J. Soil Mech. Found. Div. ASCE, Vol. 93, no. SM6.
- Ha, H.B., and M.W. O'Neill (1981), "Field Study of Pile Group Action," Report No. FHWA/RD-81/003.
- Hougnon, J.H. (1980), "Centrifugal Modeling of Axially Loaded Piles," M.S. Thesis, Department of Civil Engineering, University of Colorado, Boulder, Colorado.
- Ladd, R.S. (1978), "Preparing Test Specimens Using Undercompaction," Geotechnical Testing Journal, GTJODJ, Vol 1, No. 1, March, pp. 16-23.
- Meyerhof, G.G. (1959), "Compaction of Sands and Bearing Capacity of Piles," J.S.M.F.D., ASCE, Vol. 85: SM6, 1-29.
- Mikasa, M. and Takada, N. (1973), "Significance of Centrifugal Model Test in Soil Mechanics," 8th Internal Conference on Soil Mechanics and Foundation Engineering, Vol. 1, pp. 273-278.
- Pokorovsky, G.I. and I.S. Fedorov (1936), "Studies of Soil Pressure and Soil Deformations by Means of a Centrifuge," Proc. First Int'l. Conf. on Soil Mech. and Fndn. Engr.
- Poulos, H.G. (1968), "Analysis of the Settlement of Pile Groups," Geotechnique, Vol. 18, No. 4, pp. 449-471.
- Poulos, H.G., and E.H. Davis (1968), "The Settlement Behavior of Axially-Loaded Incompressible Piles and Piers," Geotechnique, Vol. 18, pp. 351-371.
- Poulos, H.G. (1978), Users Guide, AXPIL5 Program, University of Sydney, Sydney.
- Poulos, H.G., and E.H. Davis (1980), "Pile Foundation Analysis and Design Series in Geotechnical Engineering," John Wiley and Sons, Inc.
- Reese and Awoshika (1980), "Class Notes" CE 583, Foundation Design.
- Rocha, M. (1957), "The Possibility of Solving Soil Mechanics Problems by the Use of Models," Proc. Fourth Int'l Conf. on Soil Mech. and Fndn. Engr., Vol. 1, pp. 183-188.

REFERENCES (continued)

- Roscoe, K.H. (1968), "Soils and Model Tests," *Journal of Strain Analysis*, 3, pp. 57-64.
- Salas, J.A.J., and J.A. Belzunce (1965), "Resolution theorique de al distribution des forces dans less Pieux," *Proc. 6th Int. Conf. on Soil Mech. Found. Eng.*, Vol. 2, pp. 309-313.
- Scott, R.F. (1979), "Centrifuge Studies of Cyclic Lateral Load-Displacement Behavior of Single Piles," Report to American Petroleum Institute, OSAPR Project 8.
- Seed, H.B., and L.C. Reese (1957), "The Action of Soft Clay Along Friction Piles," *Trans. ASCE*, Vol. 122.
- Vesic, A.S. (1967), "A Study of Bearing Capacity of Deep Foundations," Final Rep., Proj. B-189, School of Civil Eng., Georgia Inst. Tech., Atlanta, GA.
- Vesic, A.S. (1977), "Design of Pile Foundations," National Cooperative Highway Research Program, Synthesis of Highway Practice Report No. 42, Transportation Research Board, 68 pp.
- Woodward-Clyde Consultants (1979), "Phase IV Report Volume III and IIIA, Results and Interpretation of Pile Driving Effects Test Program," Prepared for United States Army Corps of Engineers Contract No. DACW43-78-C-0005.

☆ U.S. GOVERNMENT PRINTING OFFICE: 1985-461-816/10276